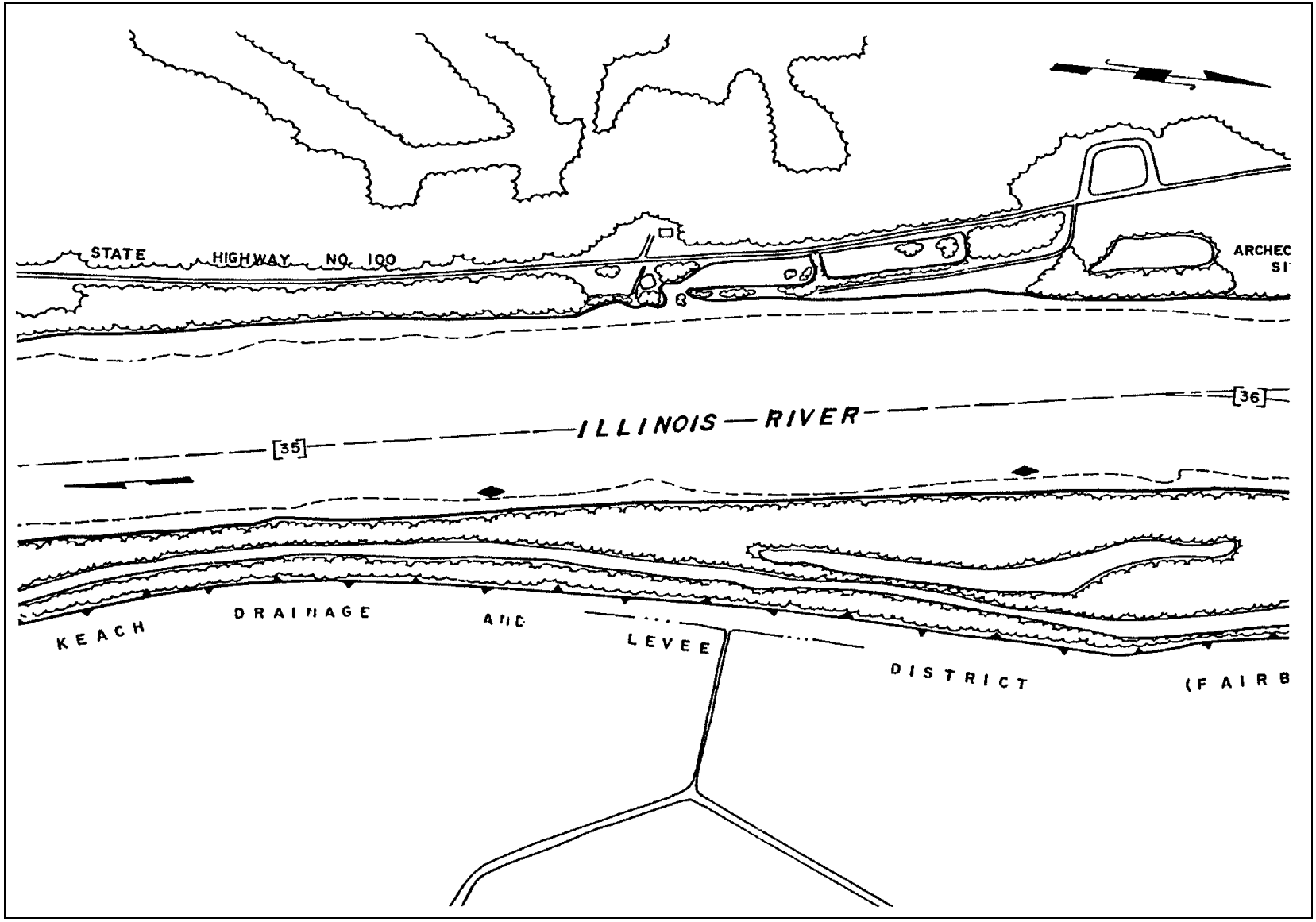

Figure 1. Kampsville site on the Illinois River, RM 35.2

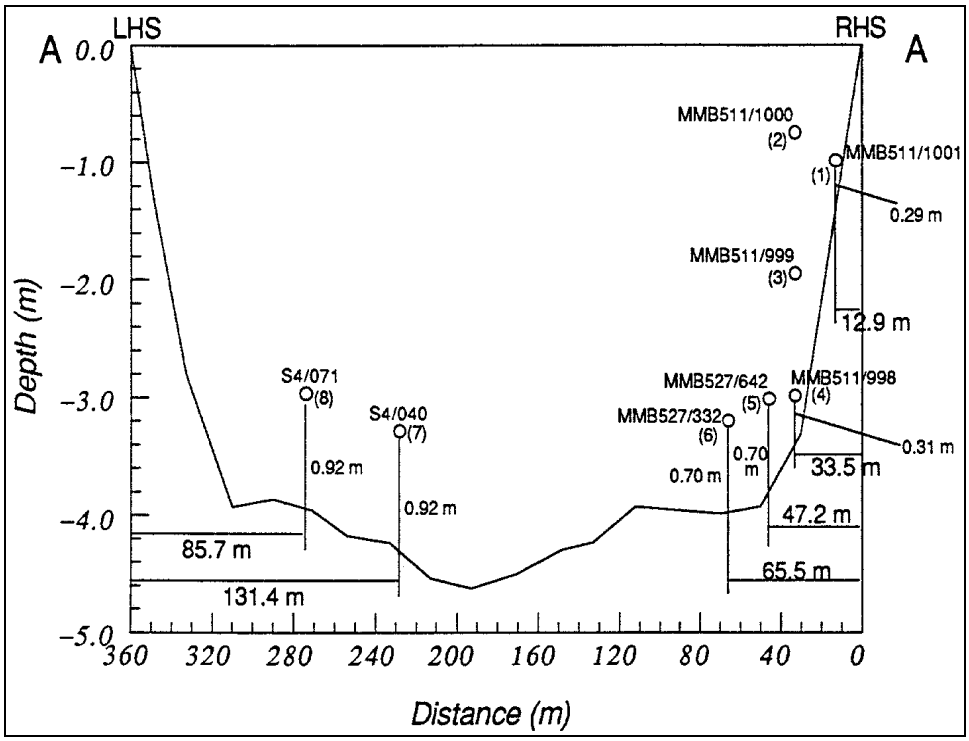

Figure 2. Cross section of the Illinois River at the Kampsville site for trip 1

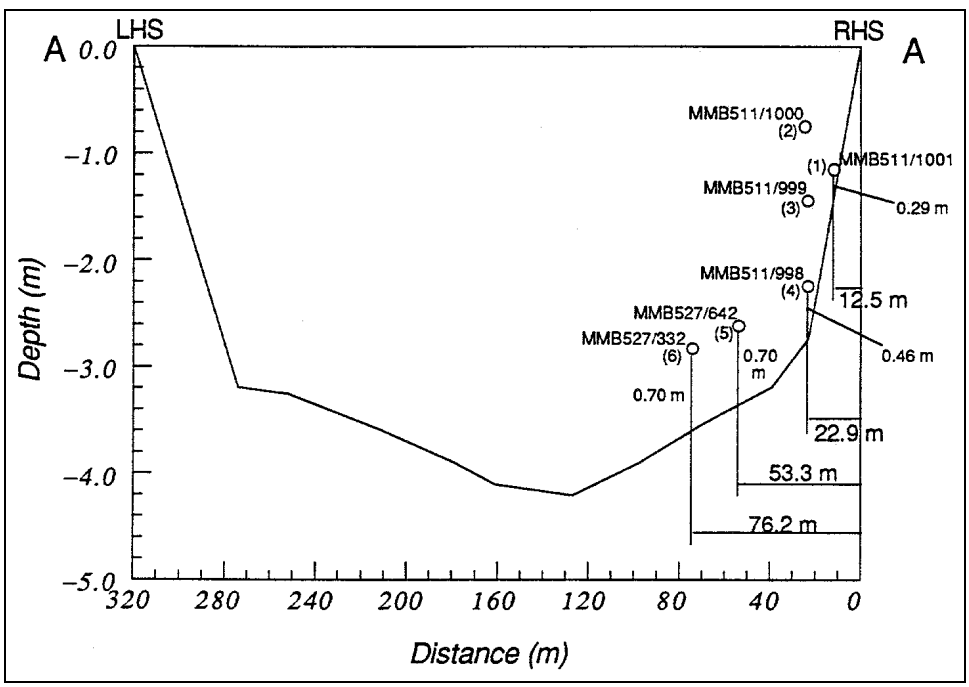

Figure 3. Cross section of the Illinios River at the Kampsville site for trip 2

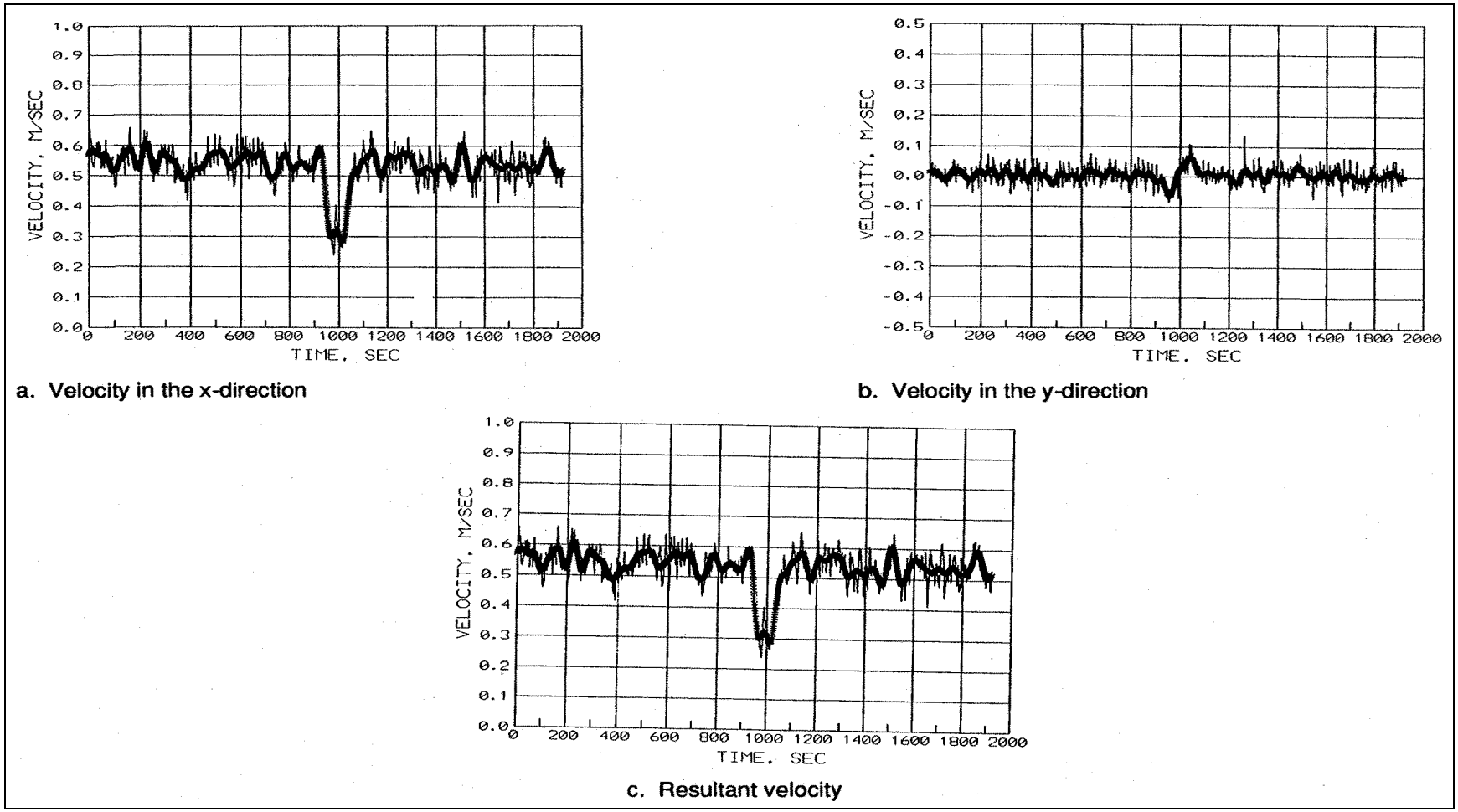

Figure 4. Prototype data, *William C. Norman*, meter MMB527/332

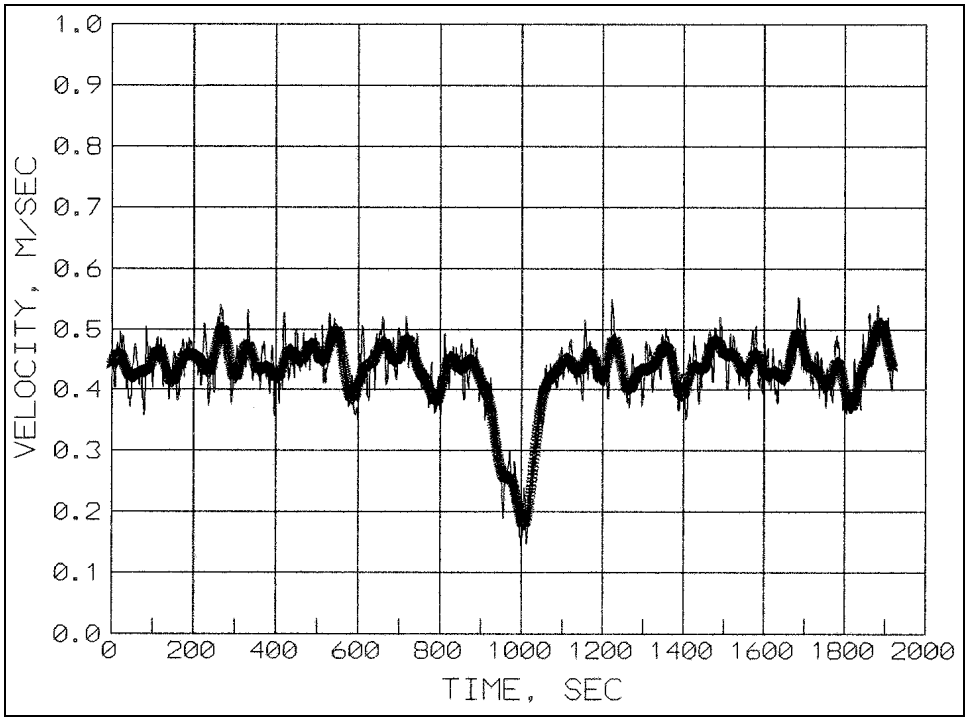

a. Velocity in the x-direction

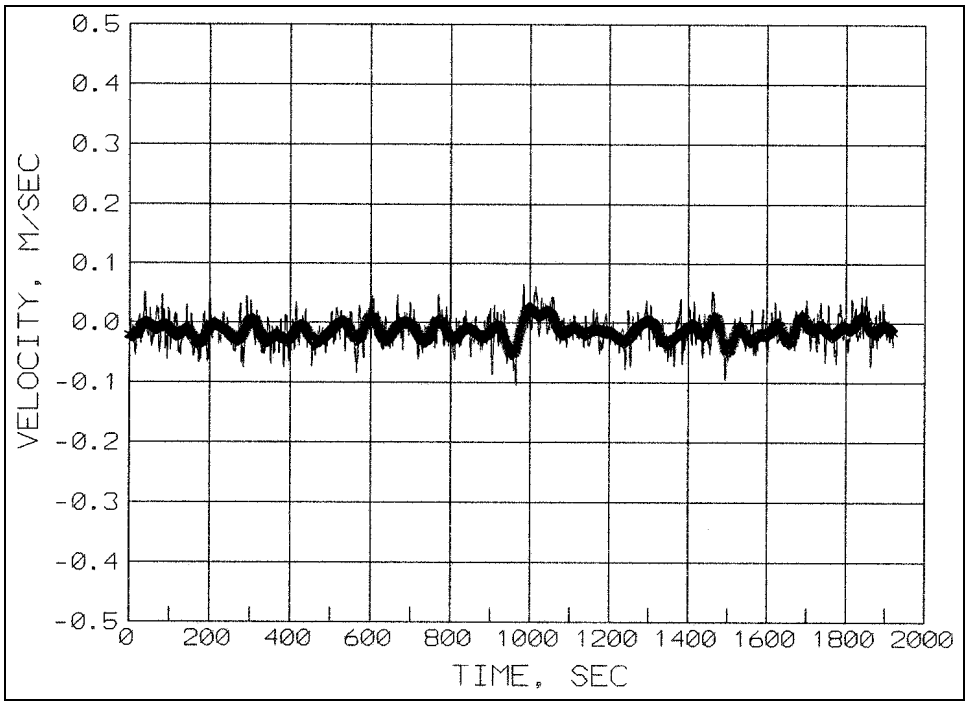

b. Velocity in the y-direction

Figure 5. Prototype data, *Wiliiam C. Norman*, meter MMB527/642

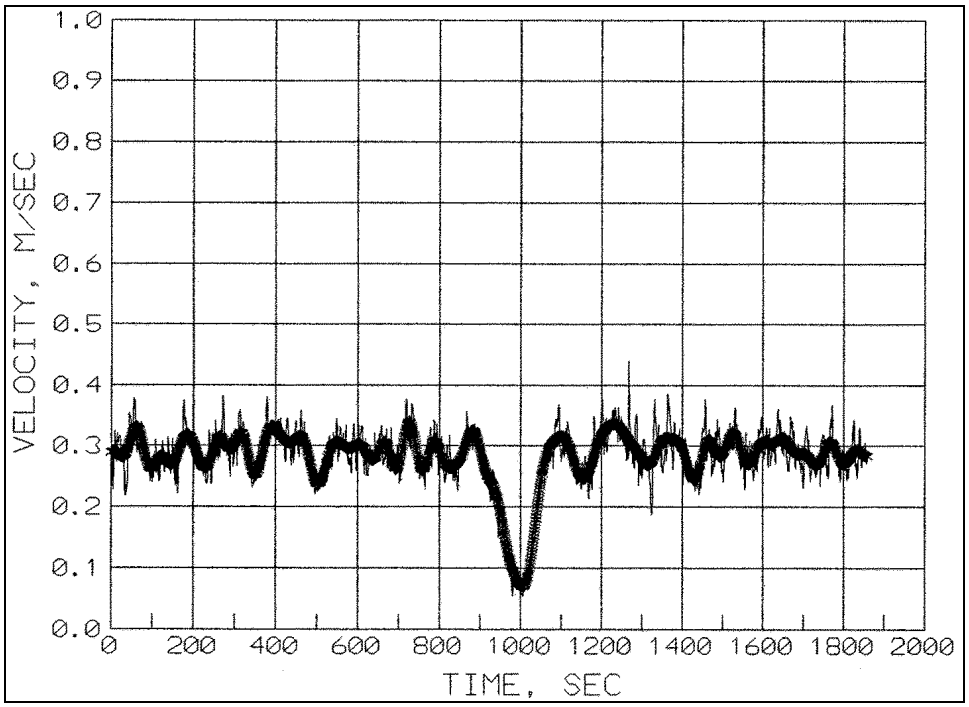

a. Velocity in the x-direction

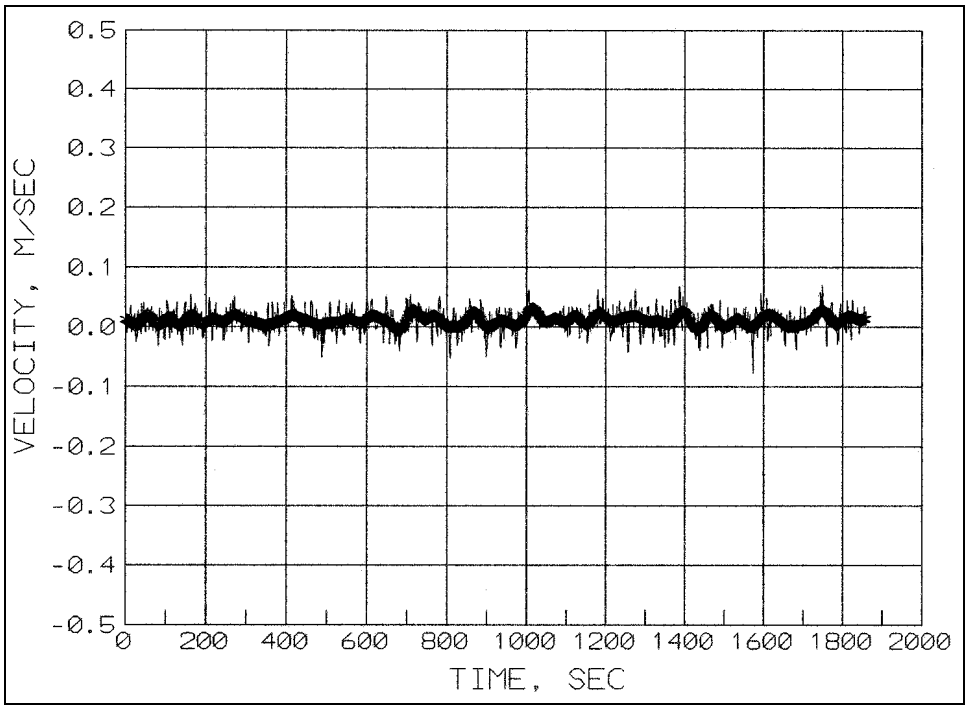

b. Velocity in the y-dirction

Figure 6. Prototype data, *William C. Norman*, meter MMB511/998

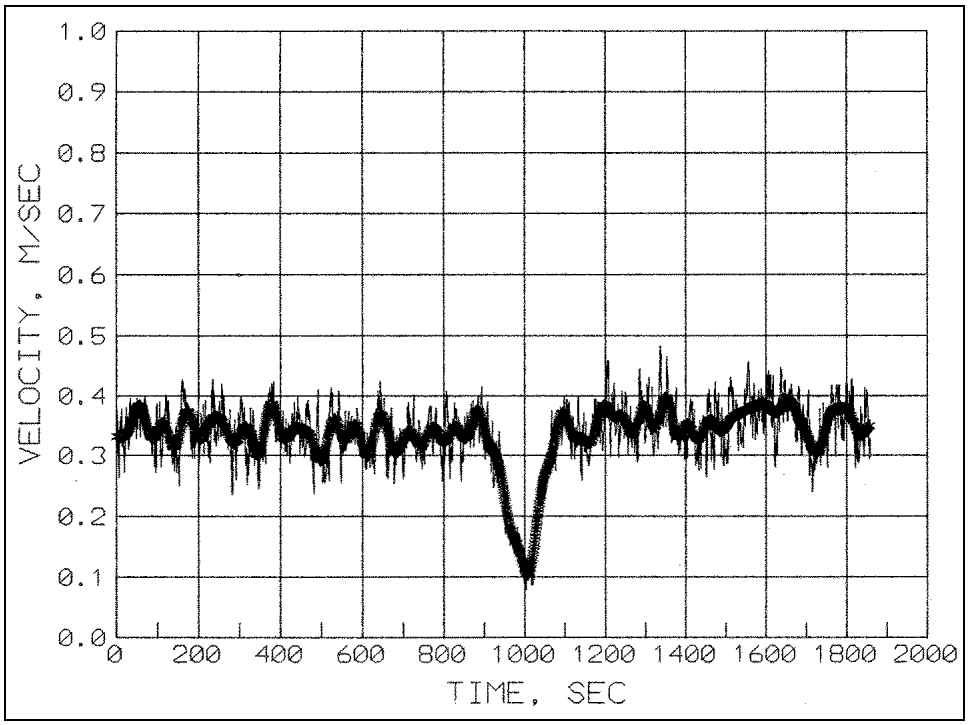

a. Velocity in the x-direction

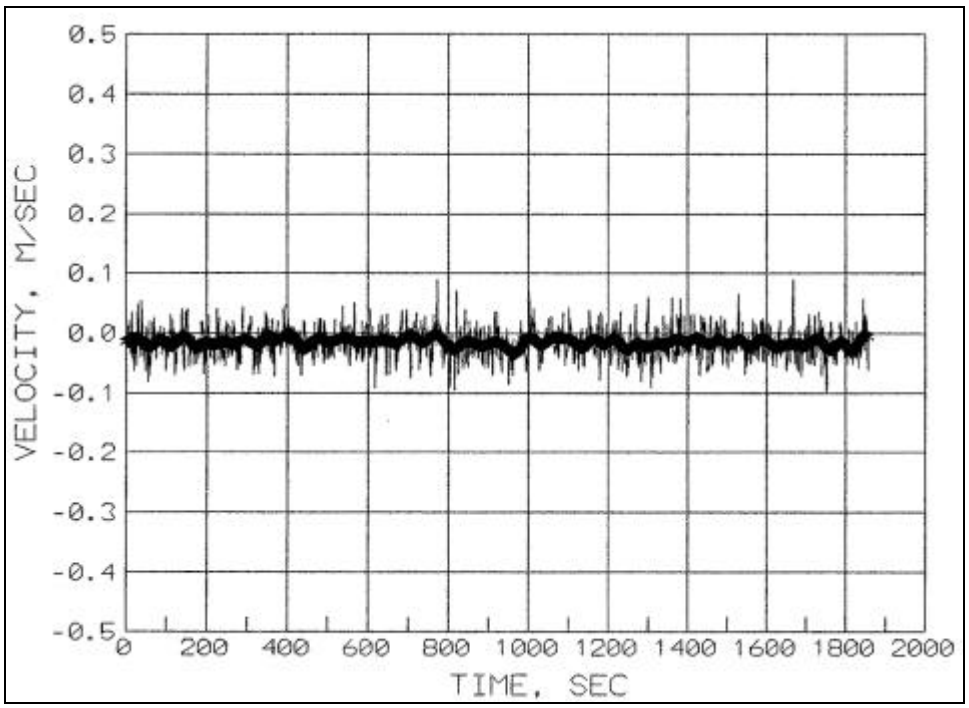

b. Velocity in the y-direction

Figure 7. Prototype data, *William C. Norman*, meter MMB511/999

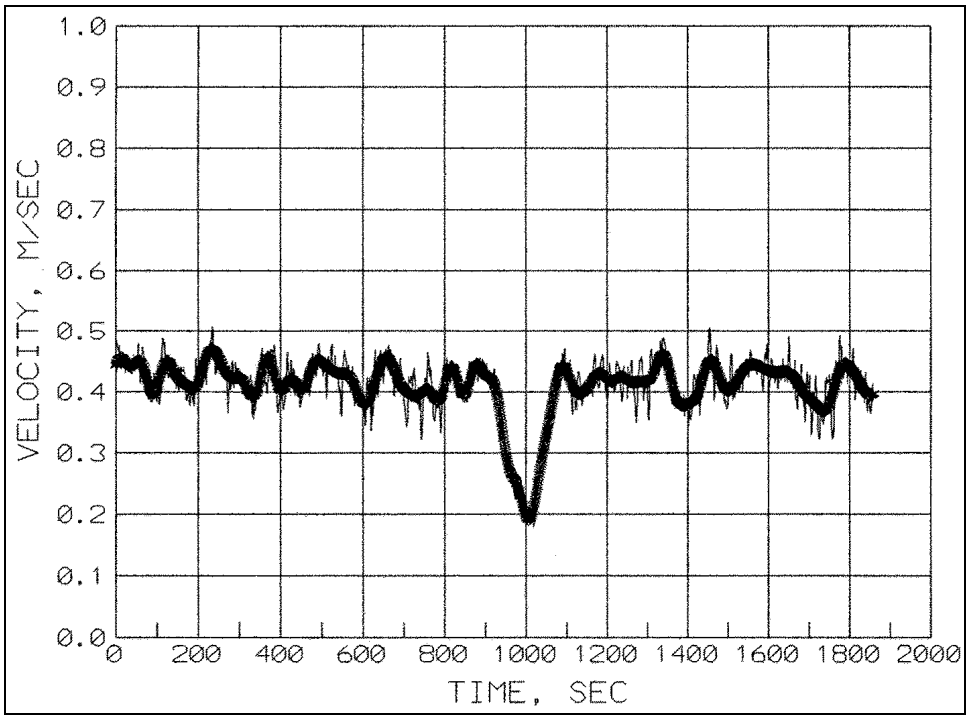

a. Velocity in the x-direction

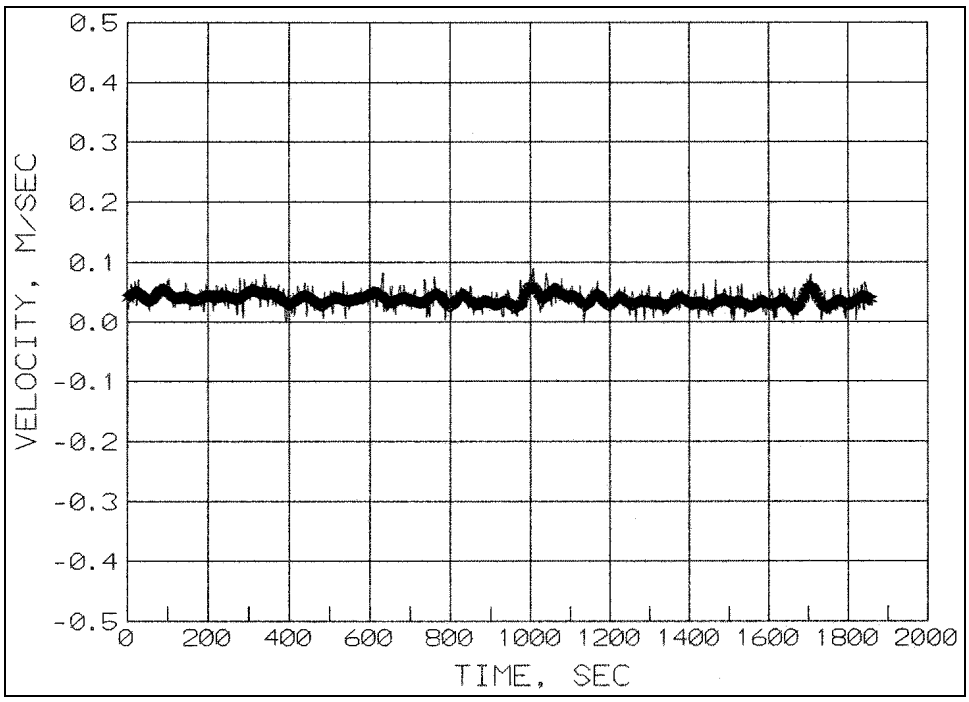

b. Velocity in the y-direction

Figure 8. Prototype data, *William C. Norman*, meter MMB511/1000

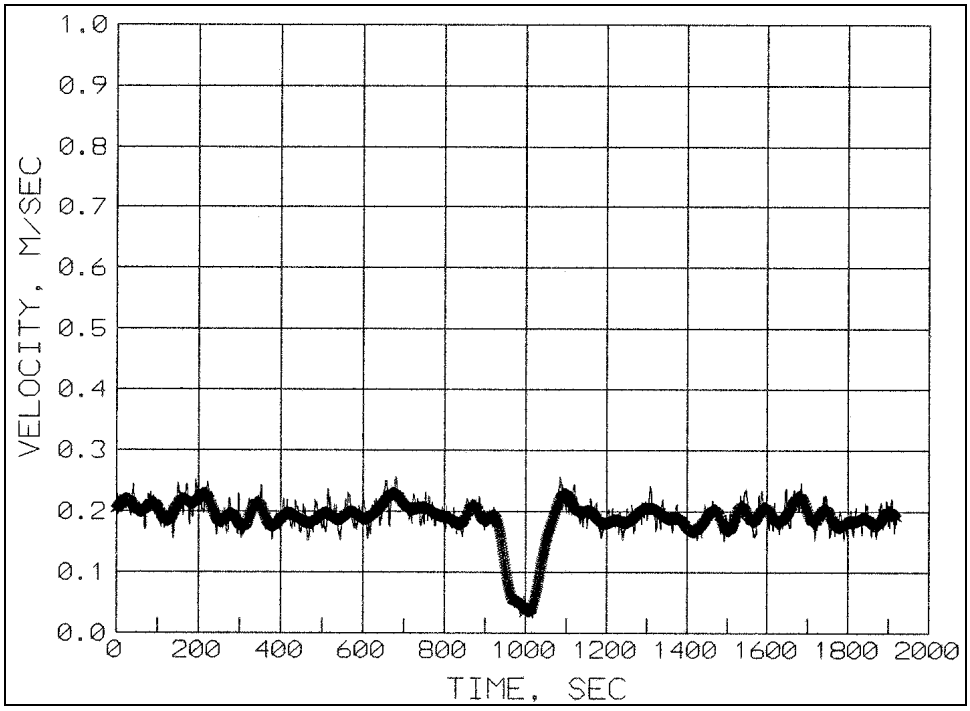

a. Velocity in the x-direction

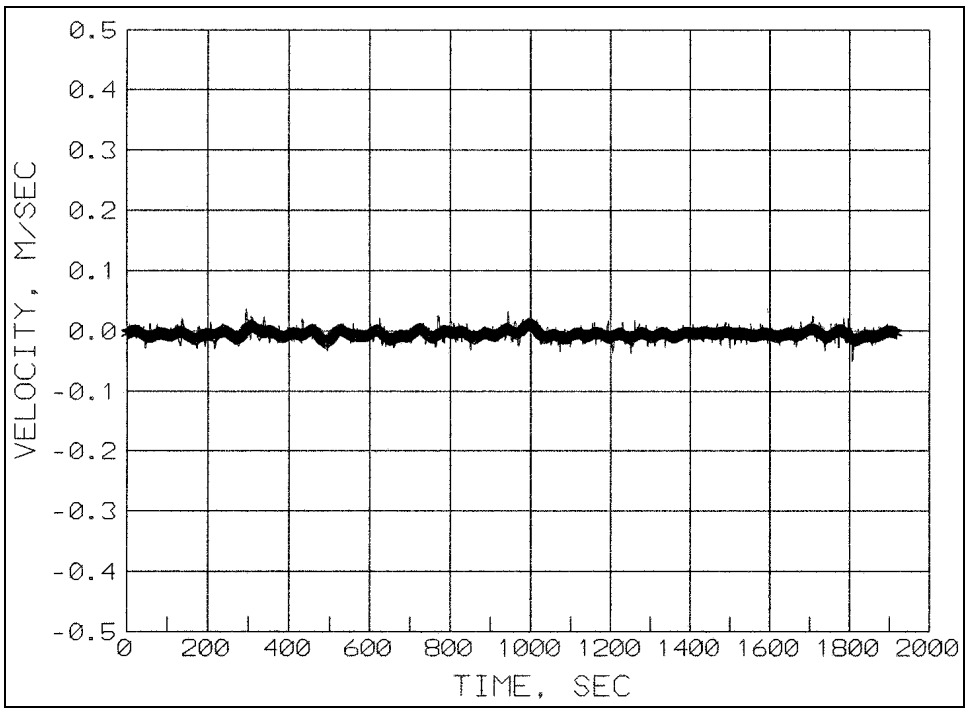

b. Velocity in the y-direction

Figure 9. Prototype data, *William C. Norman*, meter MMB511/1001

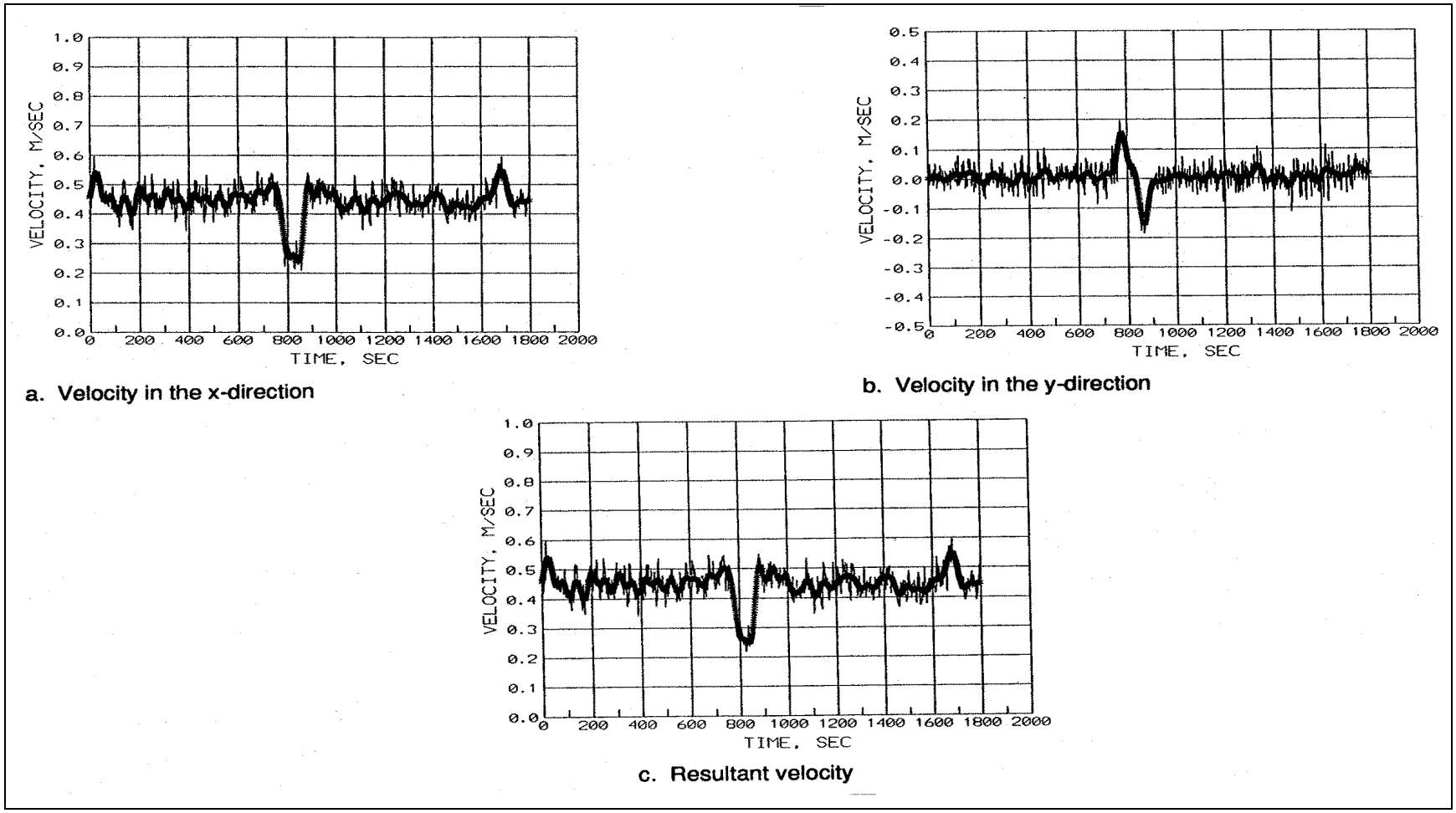

Figure 10. Prototype data, *William C. Norman*, meter S4/040

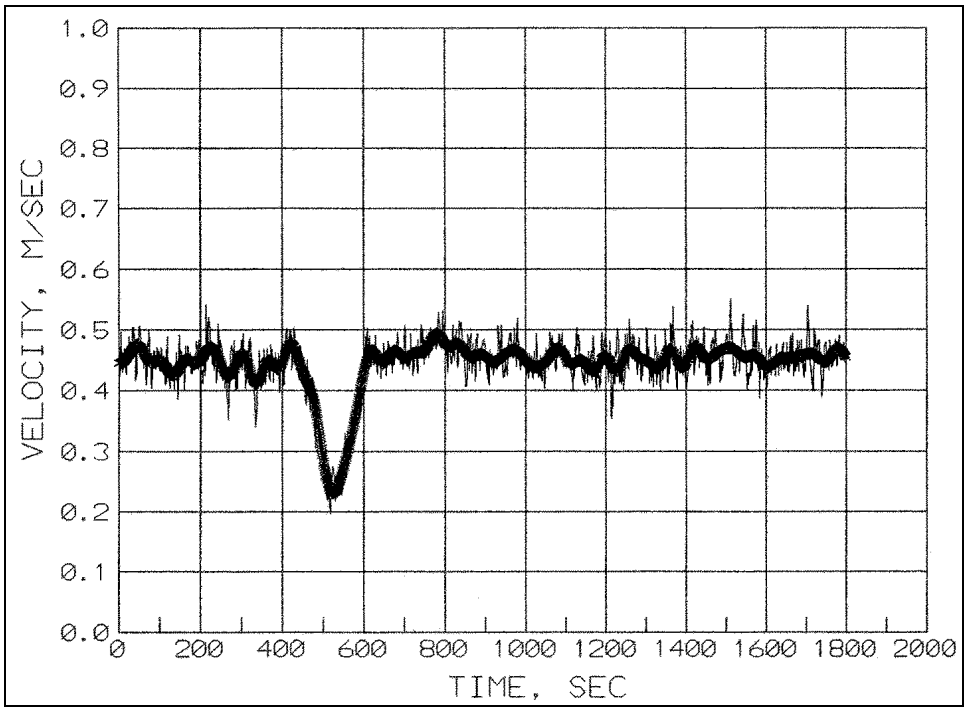

a. Velocity in the x-direction

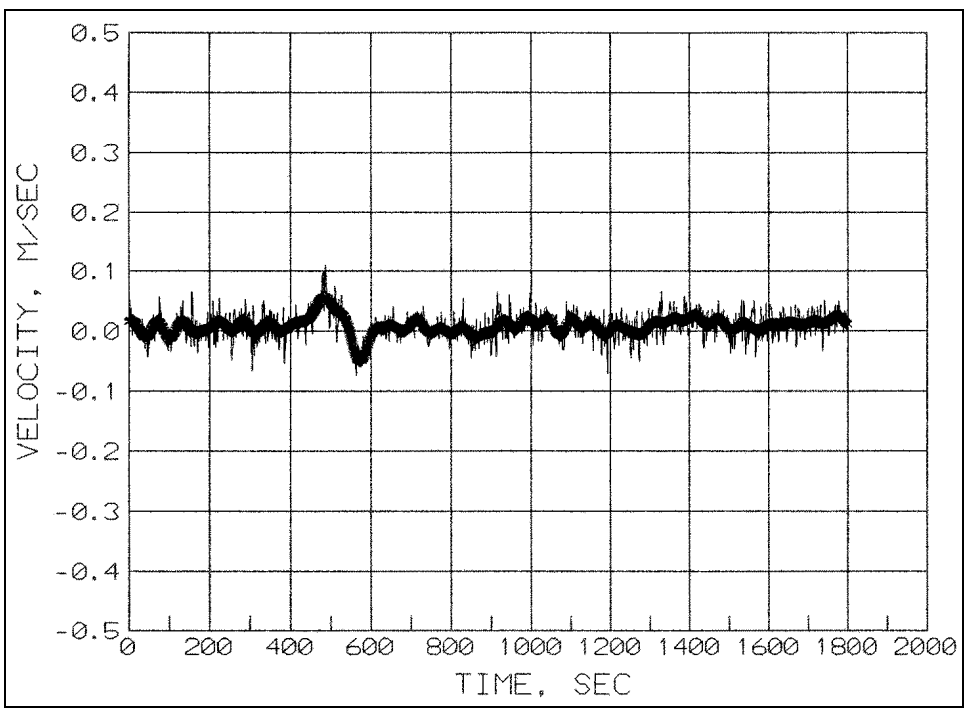

b. Velocity in the y-direction

Figure 11. Prototype data, *William C. Norman*, meter S4/071

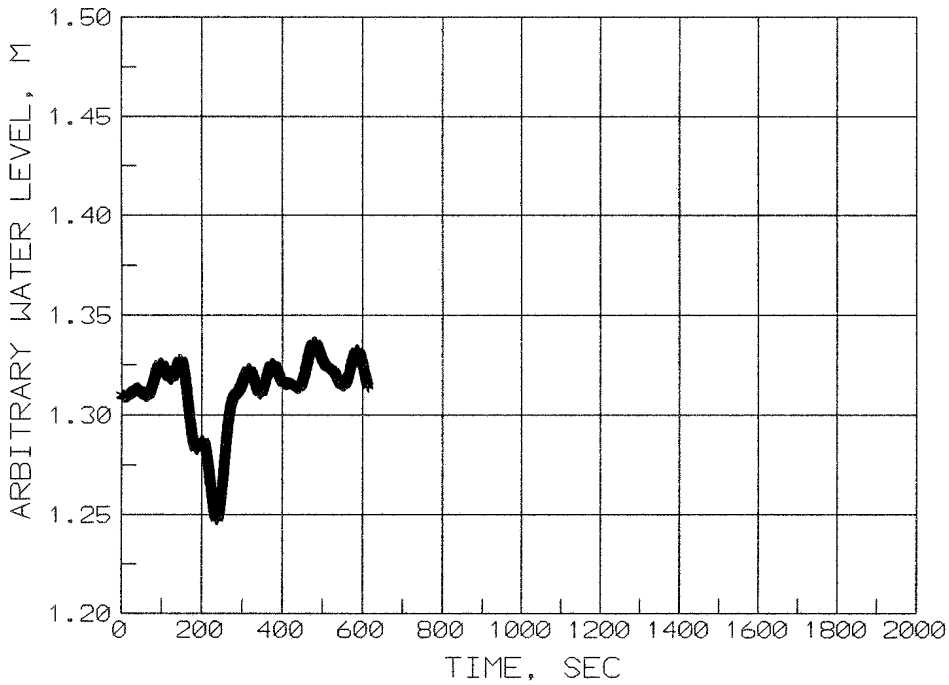

Figure 12. Prototype data, *William C. Norman*, wave gauge

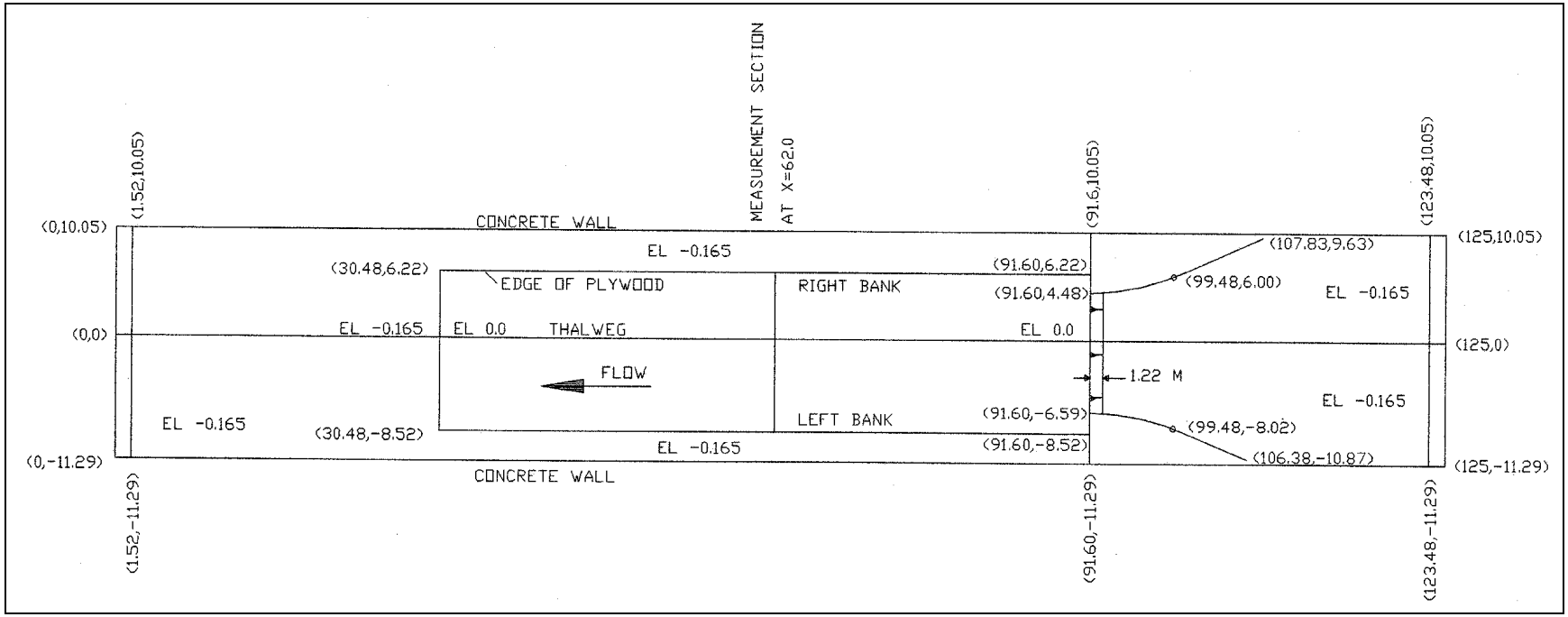

a. Flume dimensions

Figure 13. Dimensions and schematic of Kampsville Reach in navigation effects flume (Continued)

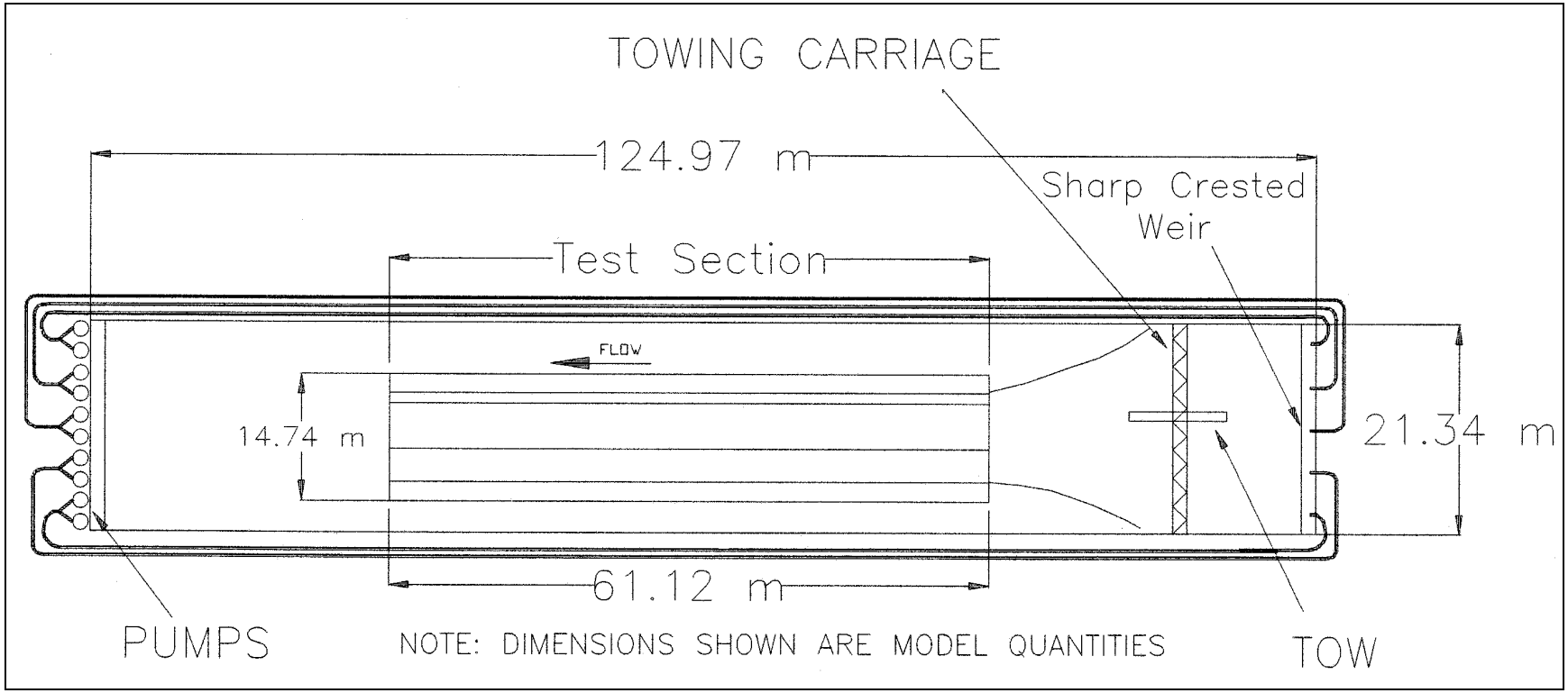

b. Details of discharge system

Figure 13. (Concluded)

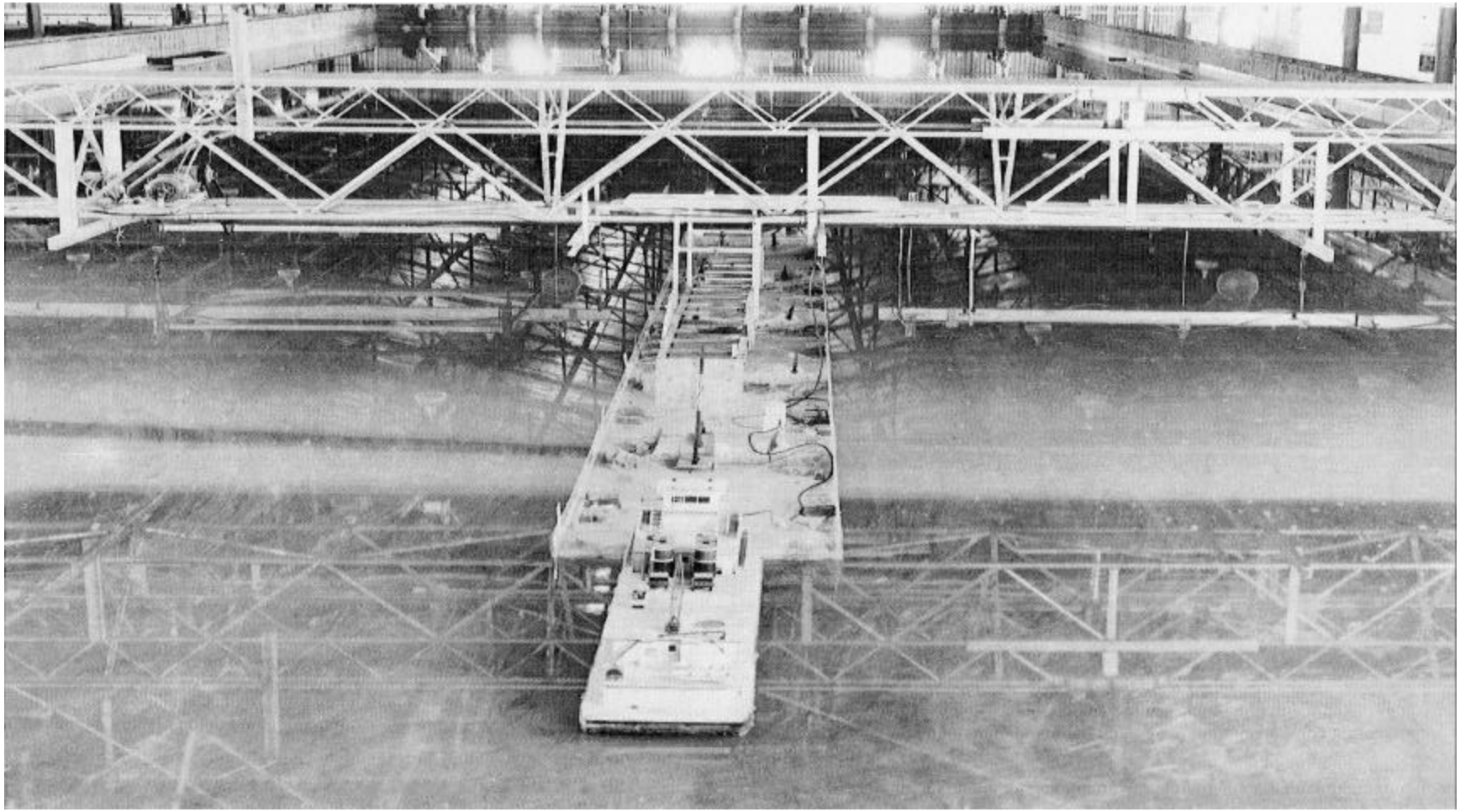

Figure 14. Navigation effects flume (looking downstream)

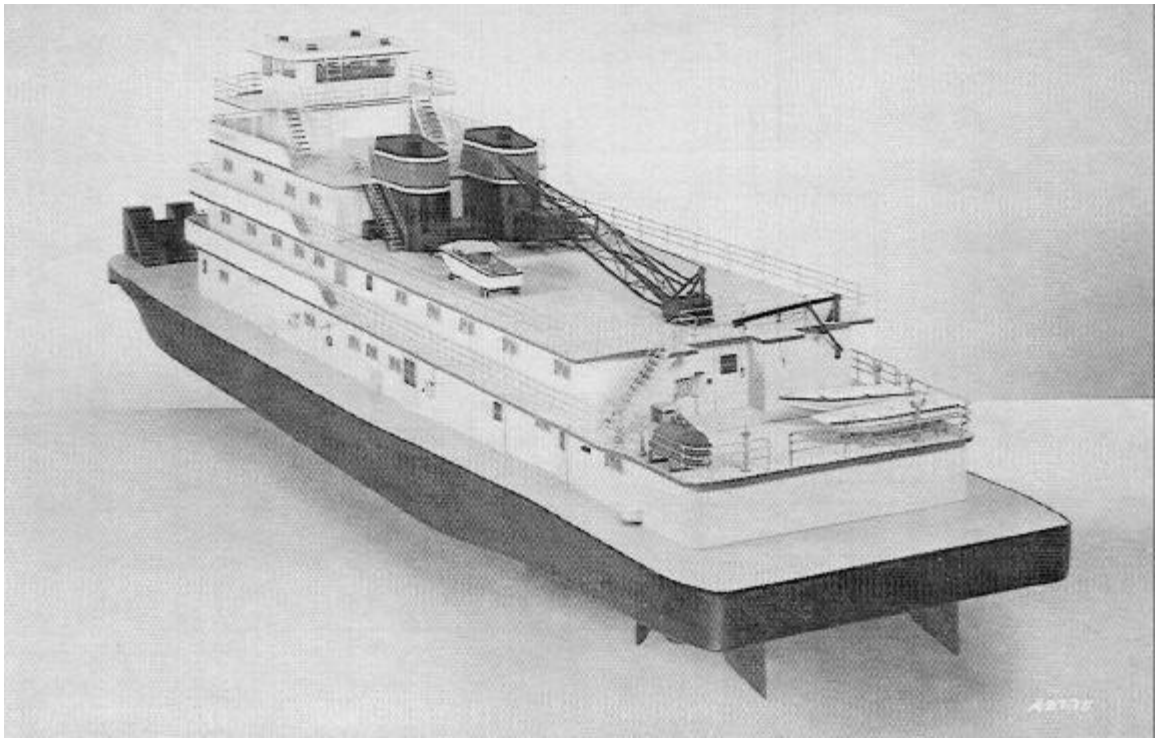

Figure 15. 1:25-scale towboat *MV Benyaurd*

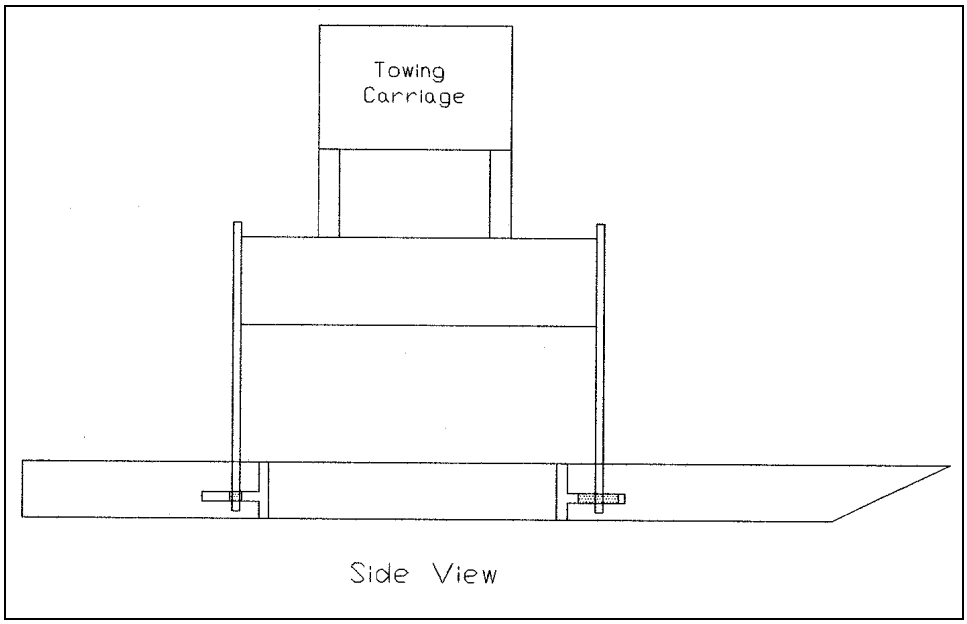

a. Side view

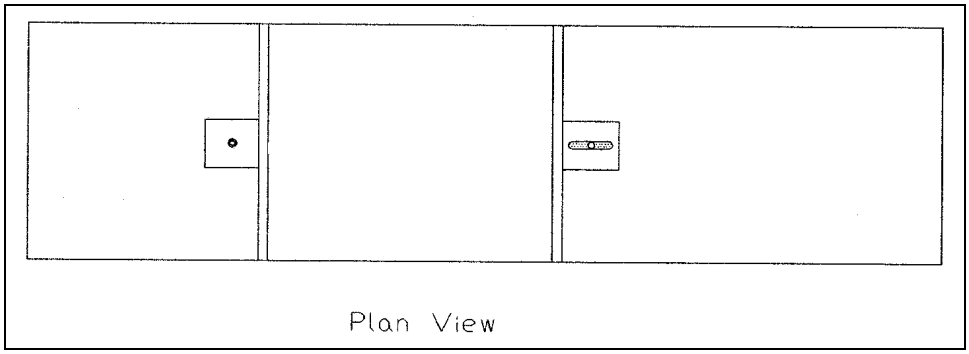

b. Plan view

Figure 16. Connection between tow and towing carriage

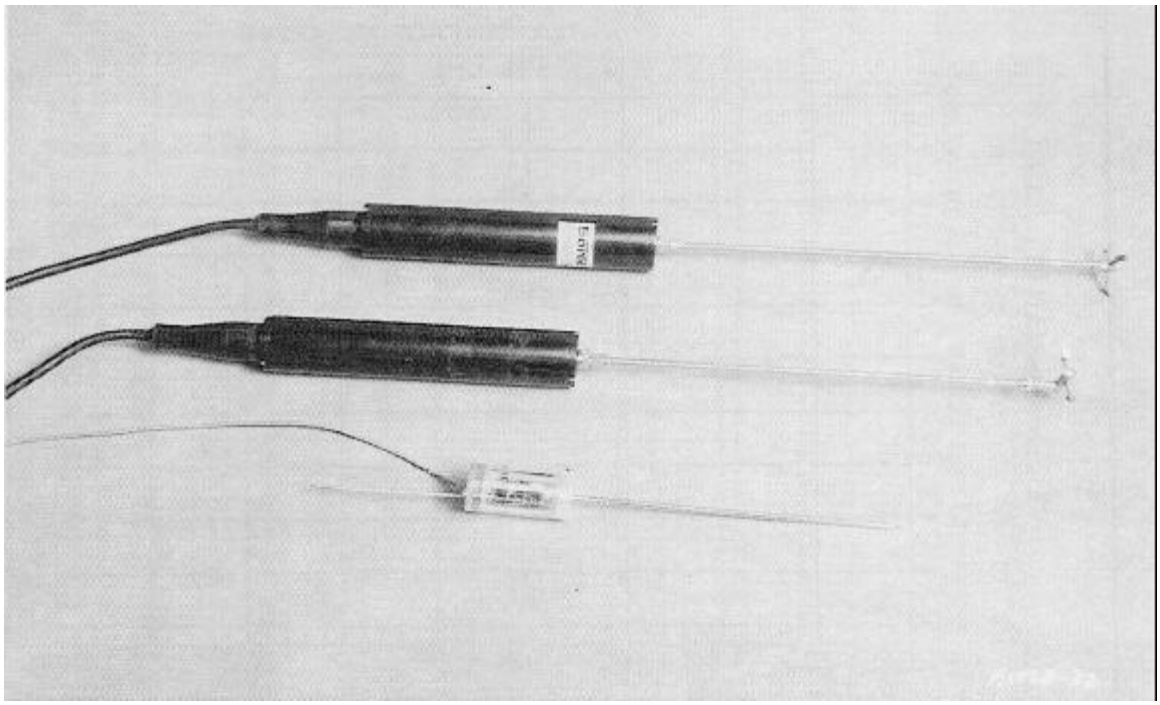

Figure 17. 2-D and 3-D ADV's and wave gauge

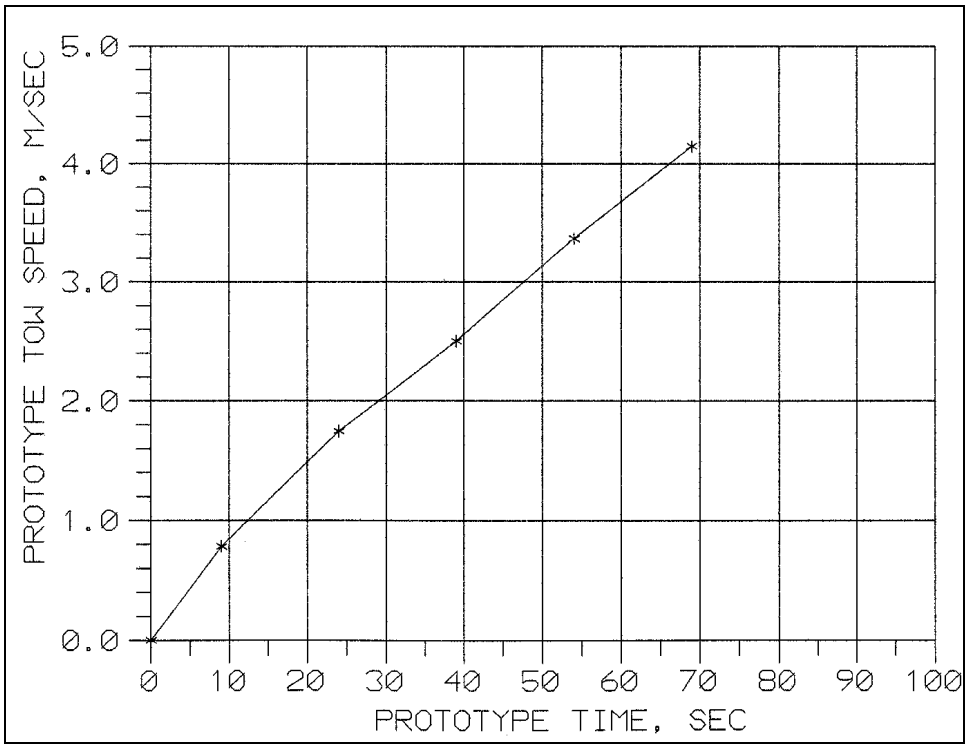

Figure 18. Acceleration of model tow

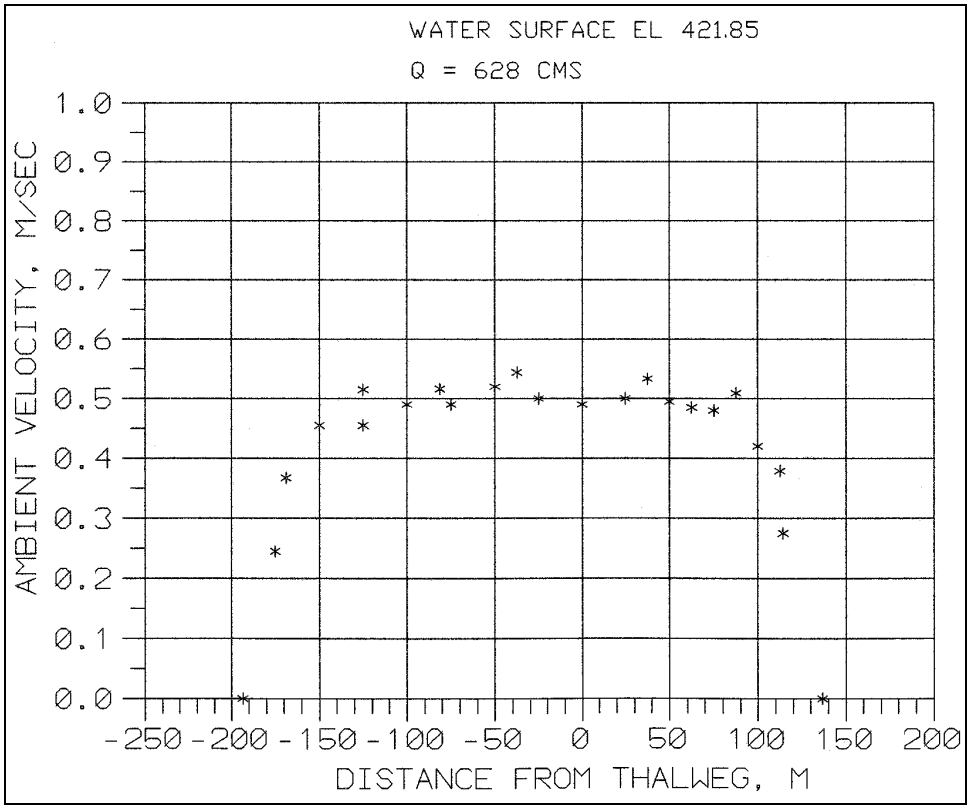

Figure 19. Ambient velocity distribution for *William C. Norman* test condition

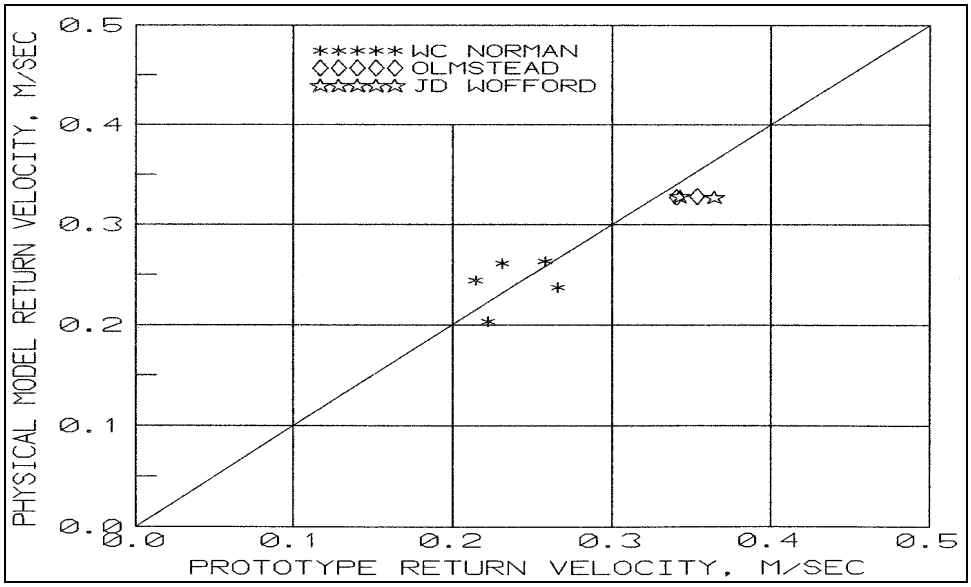

Figure 20. Physical model return velocity versus prototype return velocity, verification runs for vessels *William C. Norman*, *Olmstead*, and *Jack D. Wofford* with 2.28-m draft

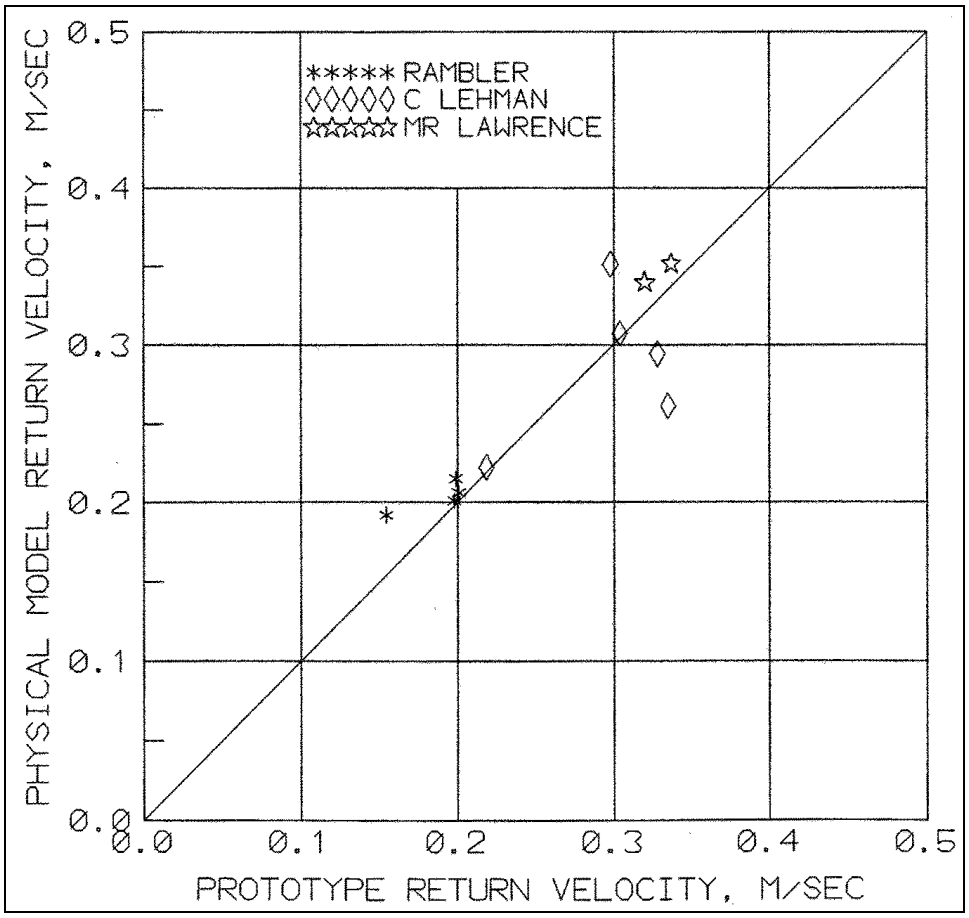

Figure 21. Physical model return velocity versus prototype return velocity, verification runs for vessels *Rambler*, *Charles Lehman*, and *Mr. Lawrence* with 2.28-m draft

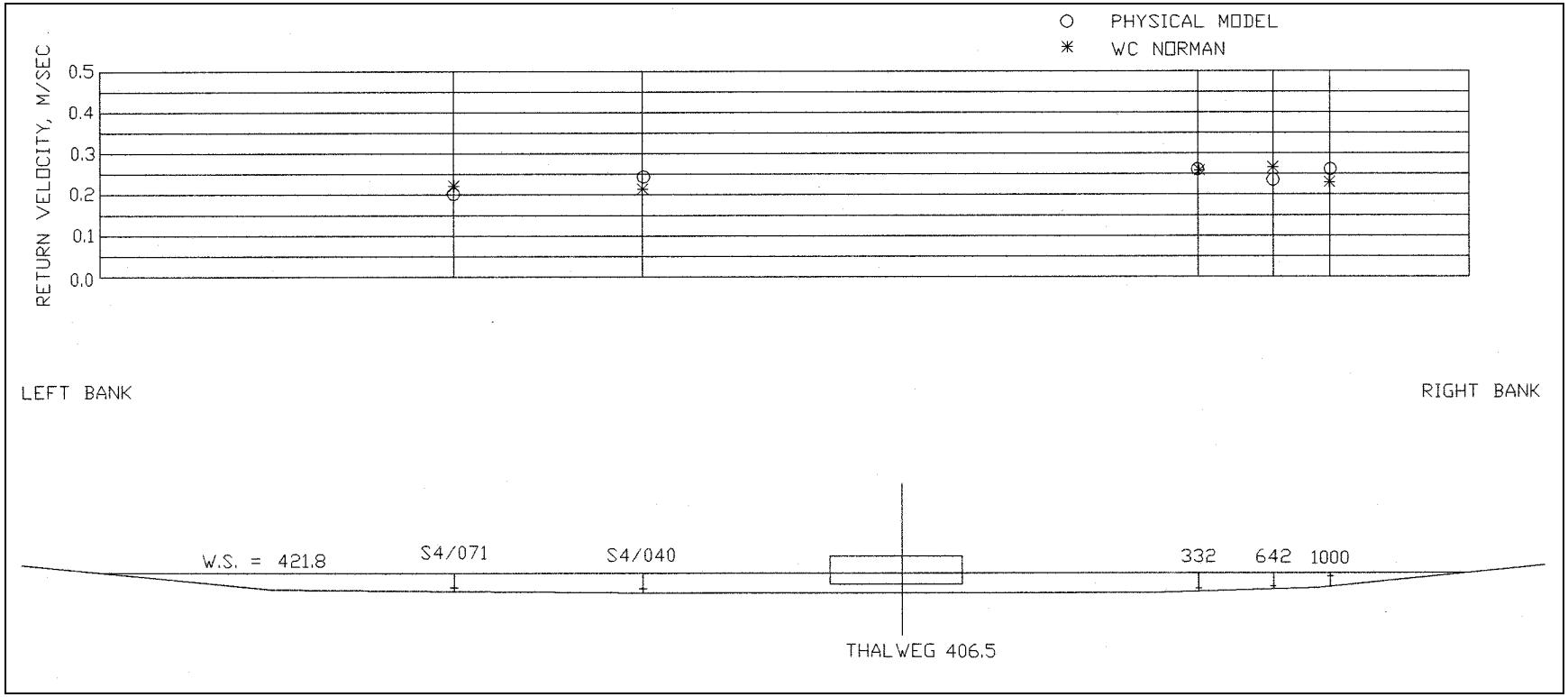

Figure 22. Physical model return velocity versus prototype for *William C. Norman*

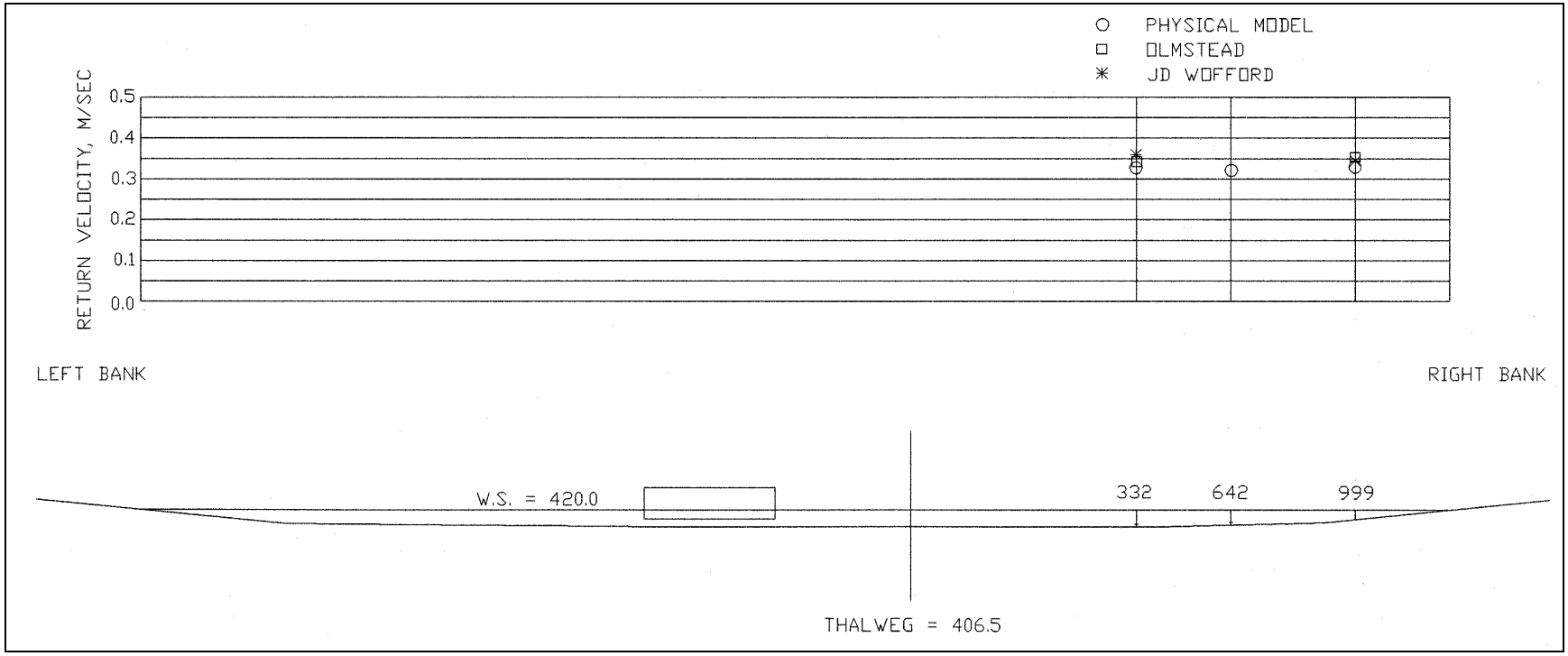

Figure 23. Physical model return velocity versus prototype return velocity for *Olmstead* and *Jack D. Wofford*

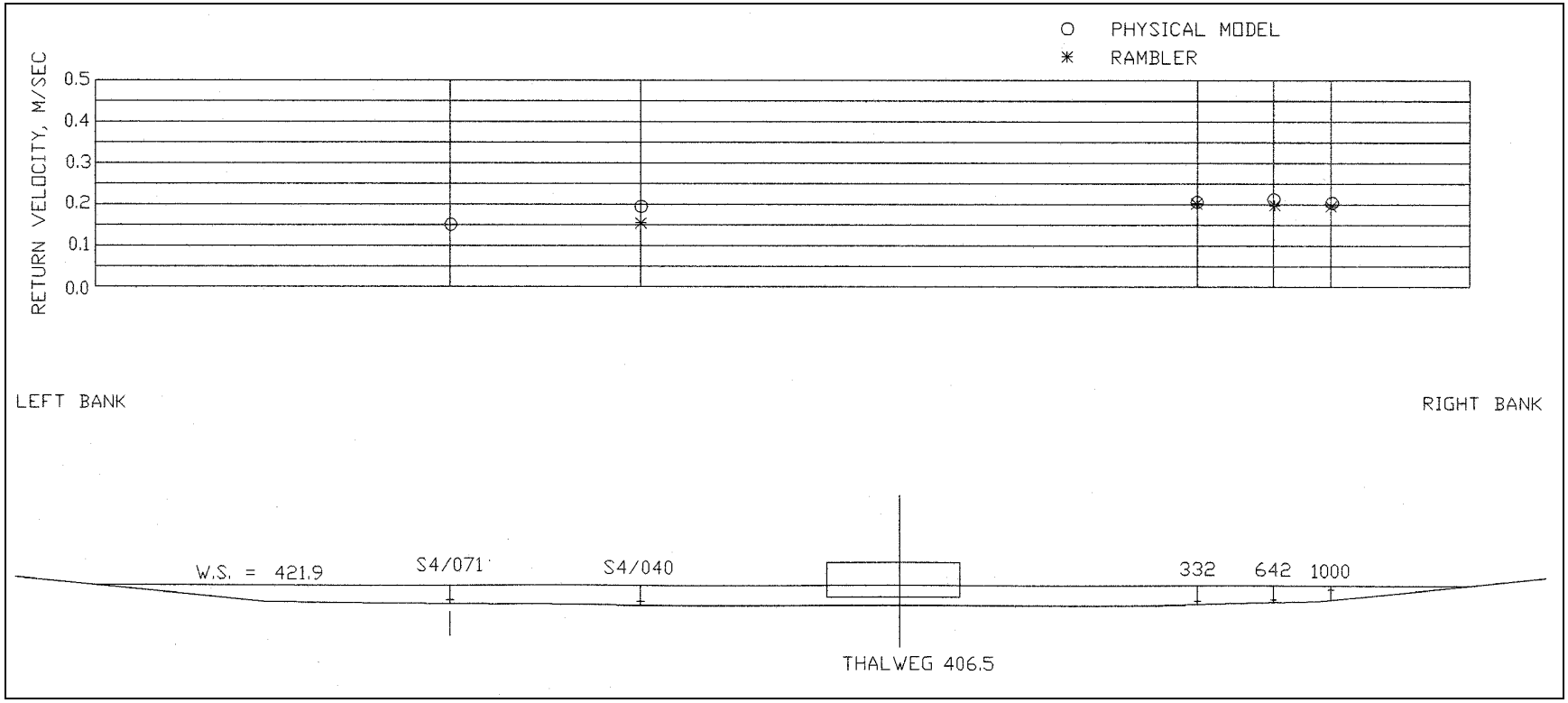

Figure 24. Physical model return velocity versus prototype return velocity for *Rambler*

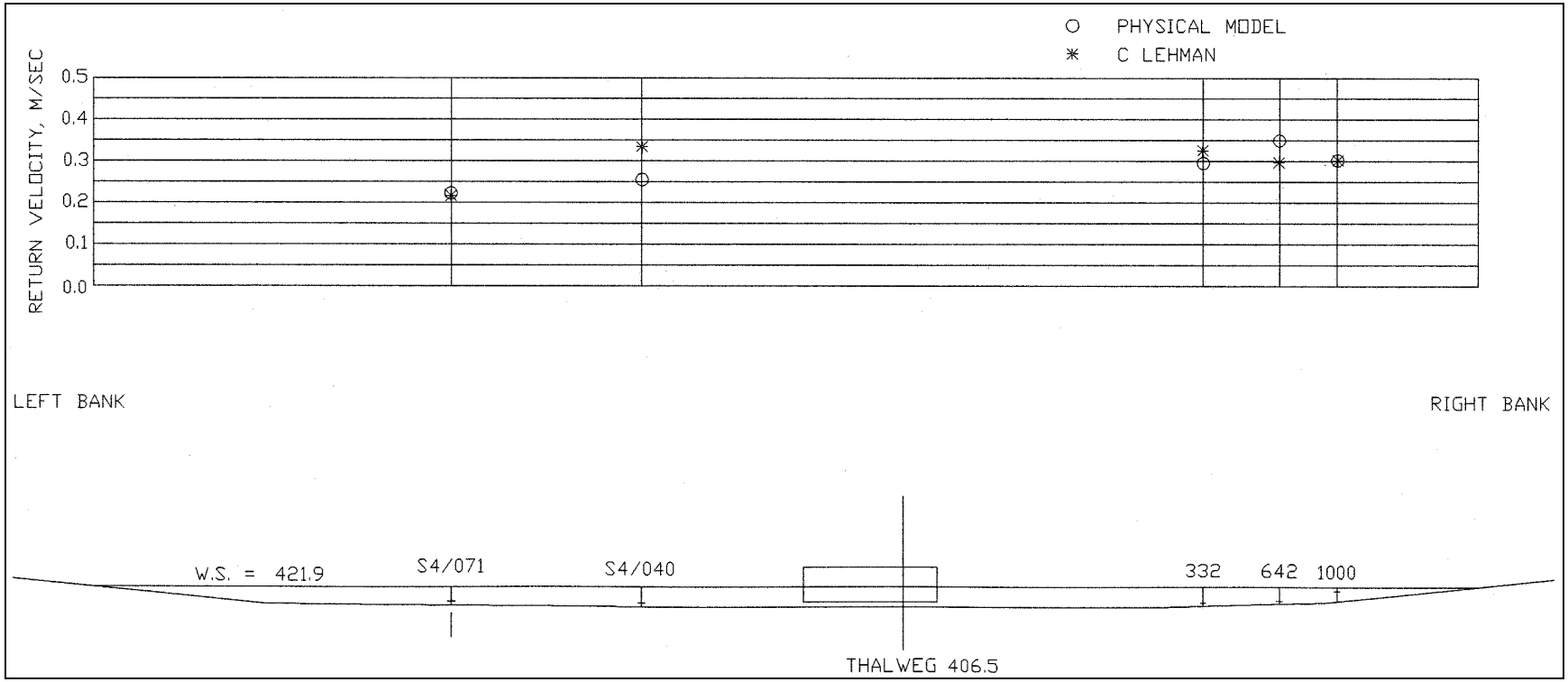

Figure 25. Physical model return velocity versus prototype return velocity for *Charles Lehman*

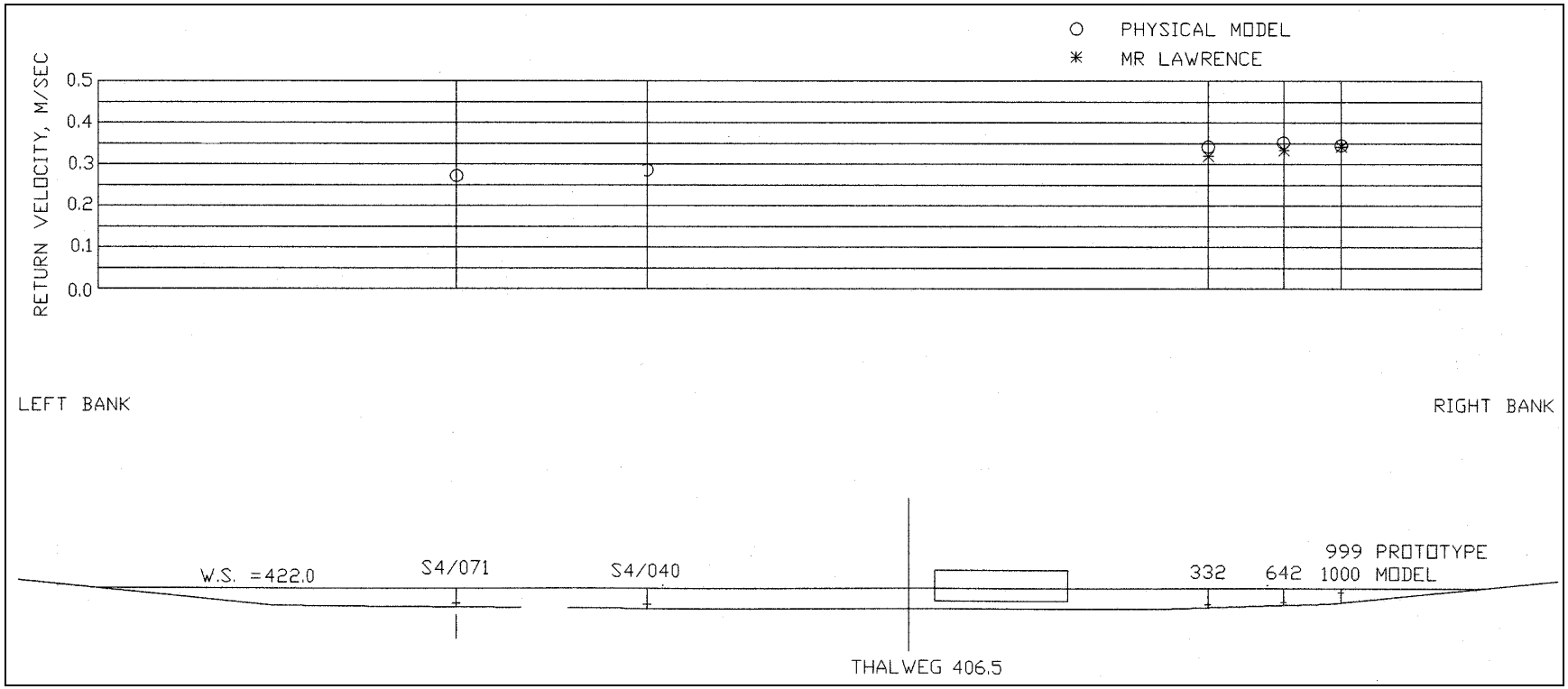

Figure 26. Physical model return velocity versus prorotype return velocity for *Mr. Lawrence*

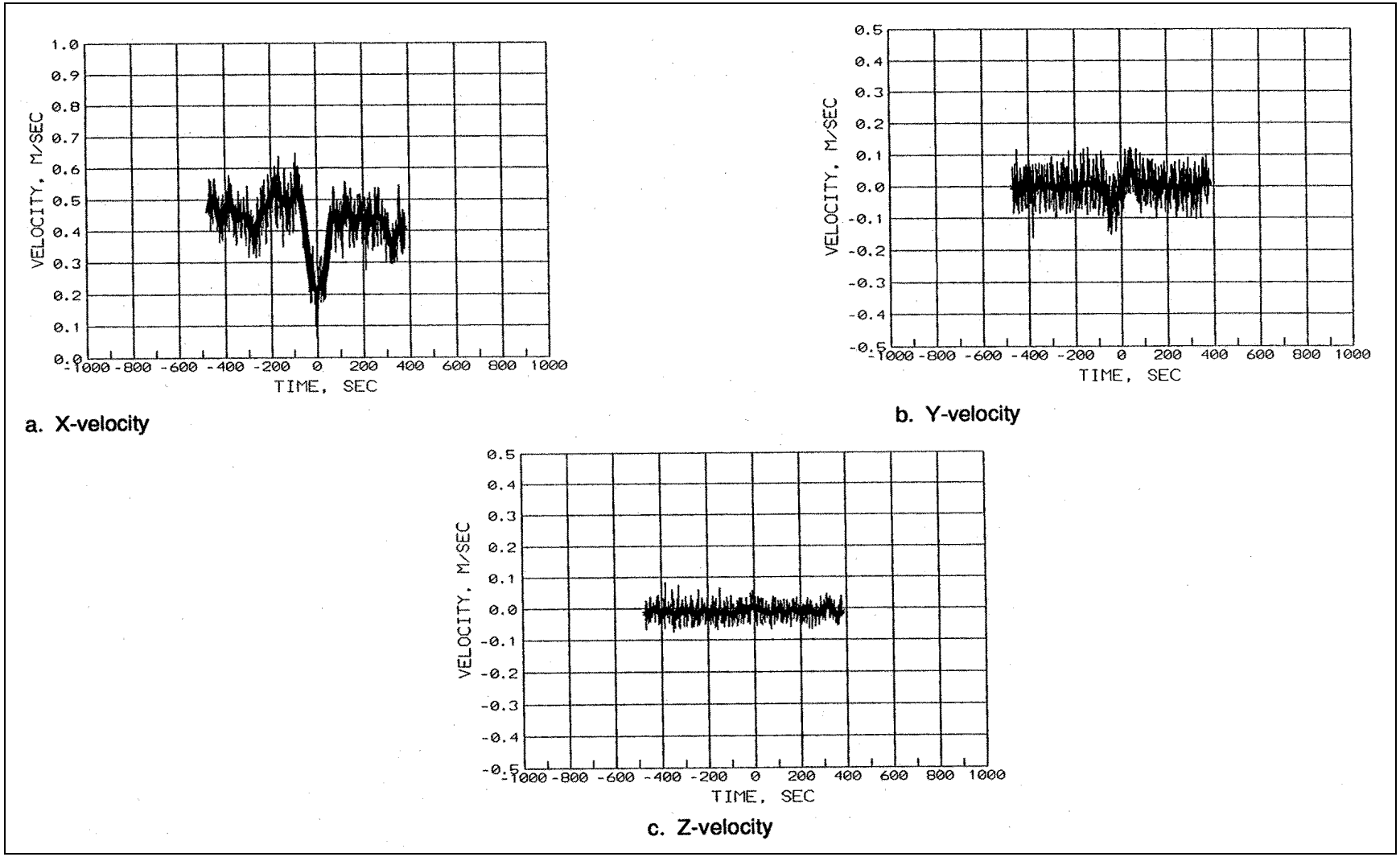

Figure 27. Physical model data, *William C. Norman*, meter at location of MMB527/332

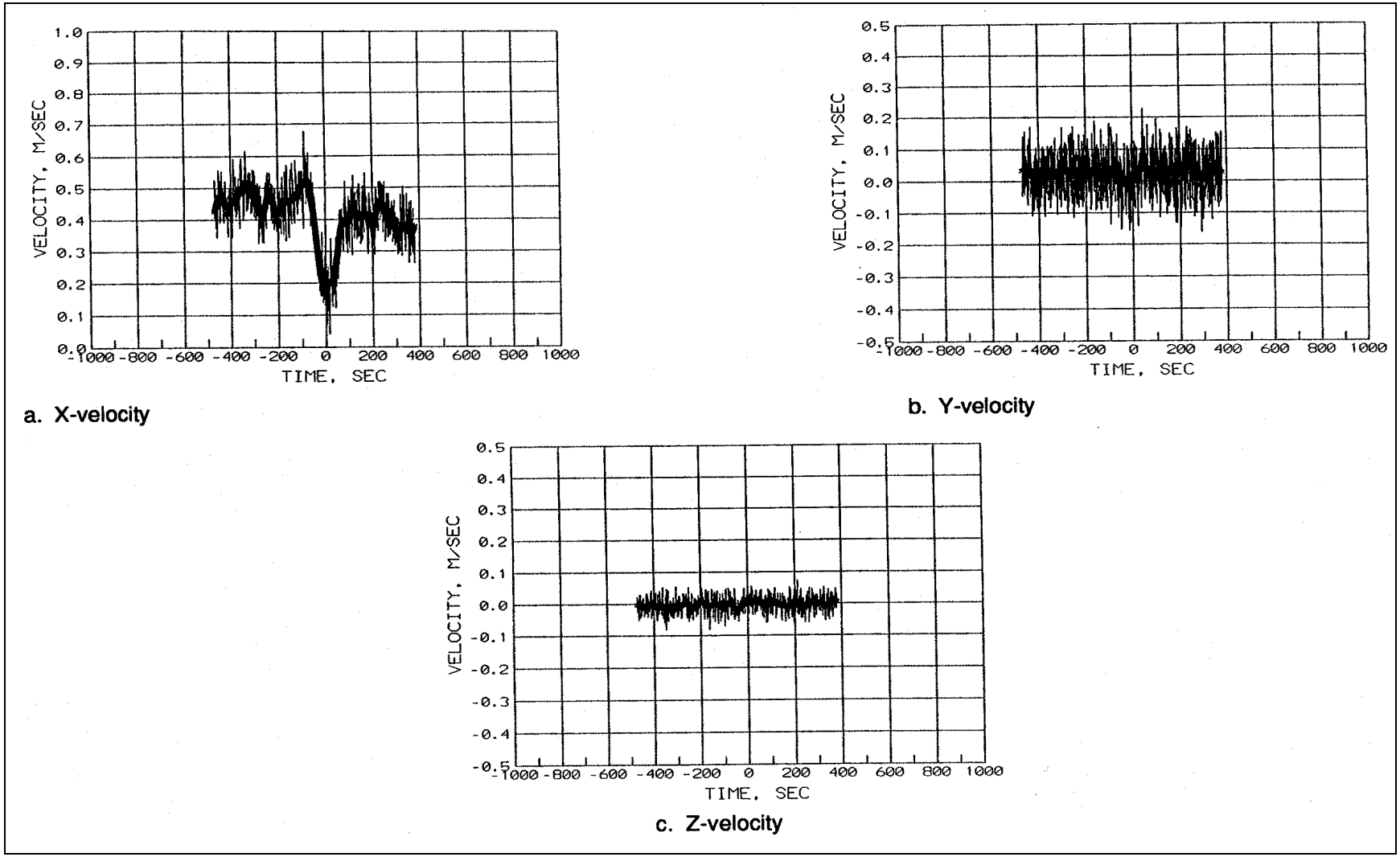

Figure 28. Physical model data, *William C. Norman*, meter at location of MMB527/642

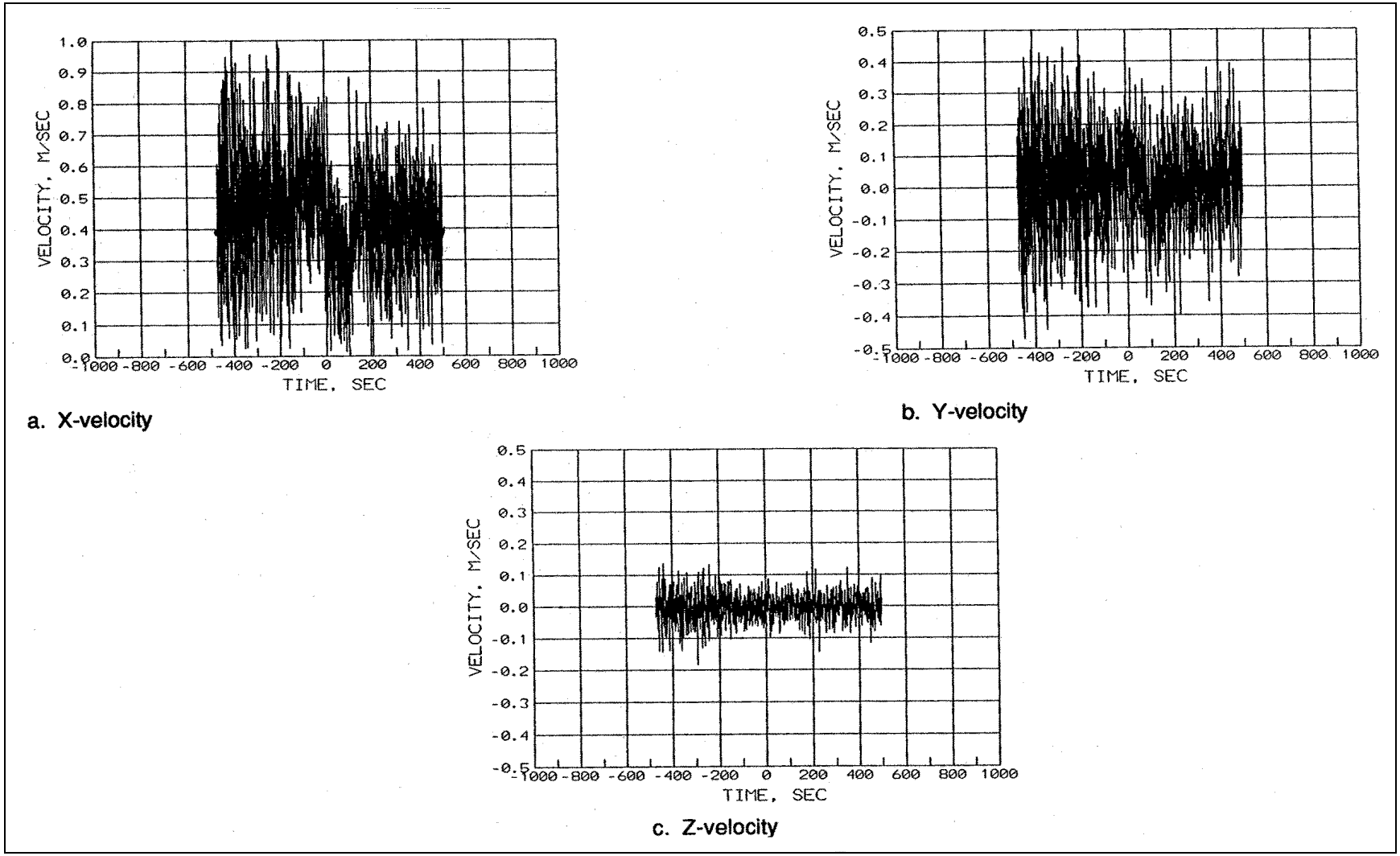

Figure 29. Physical model data, *William C. Norman*, meter at location of S4/040

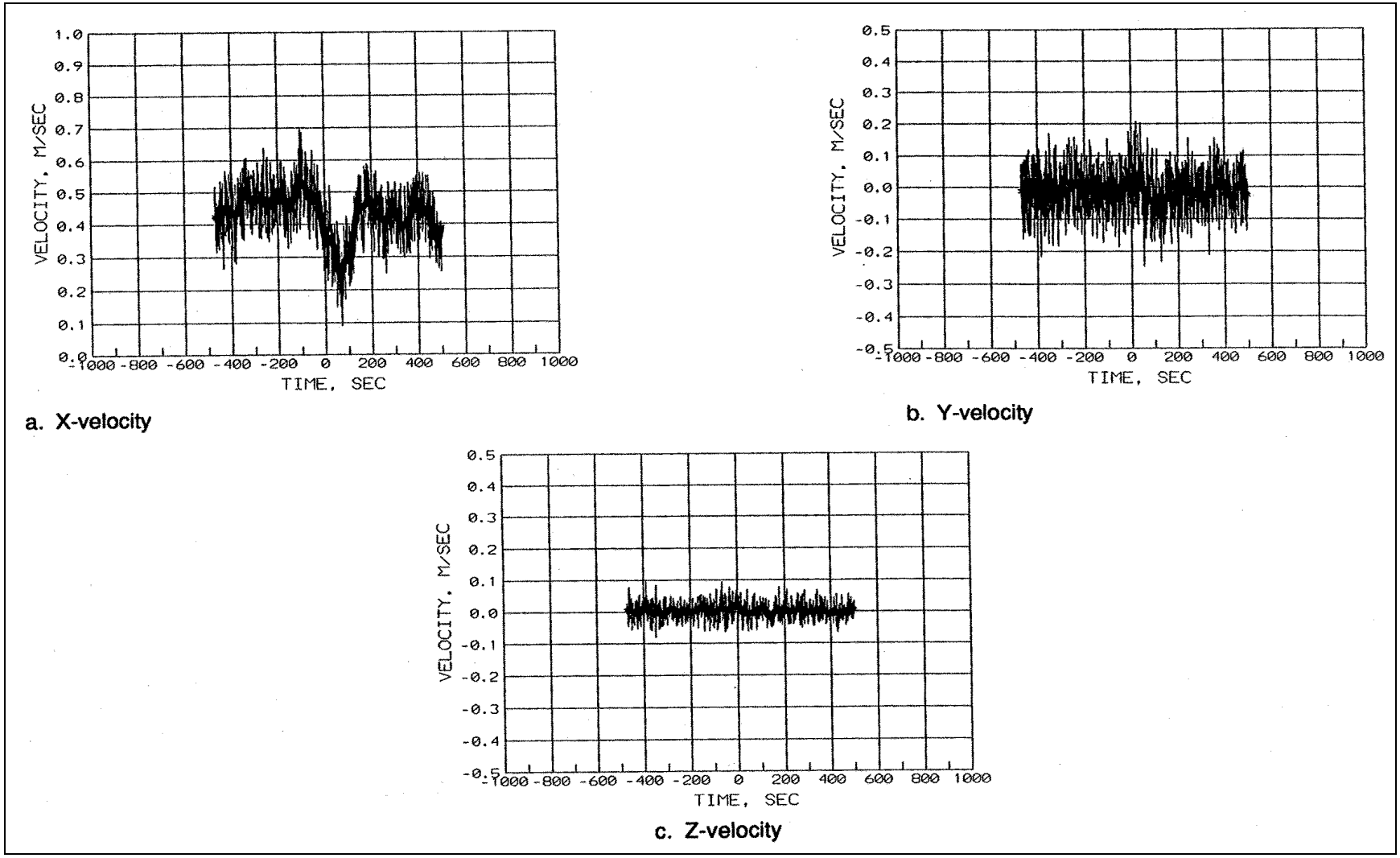

Figure 30. Physical model data, *William C. Norman*, meter at location of S4/071

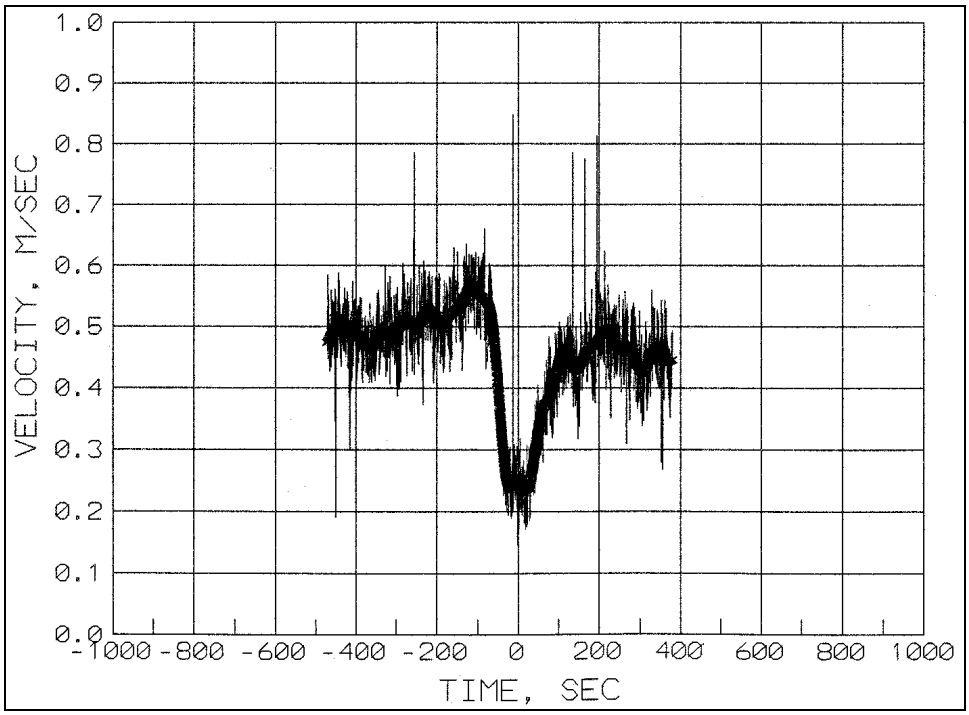

a. X-velocity

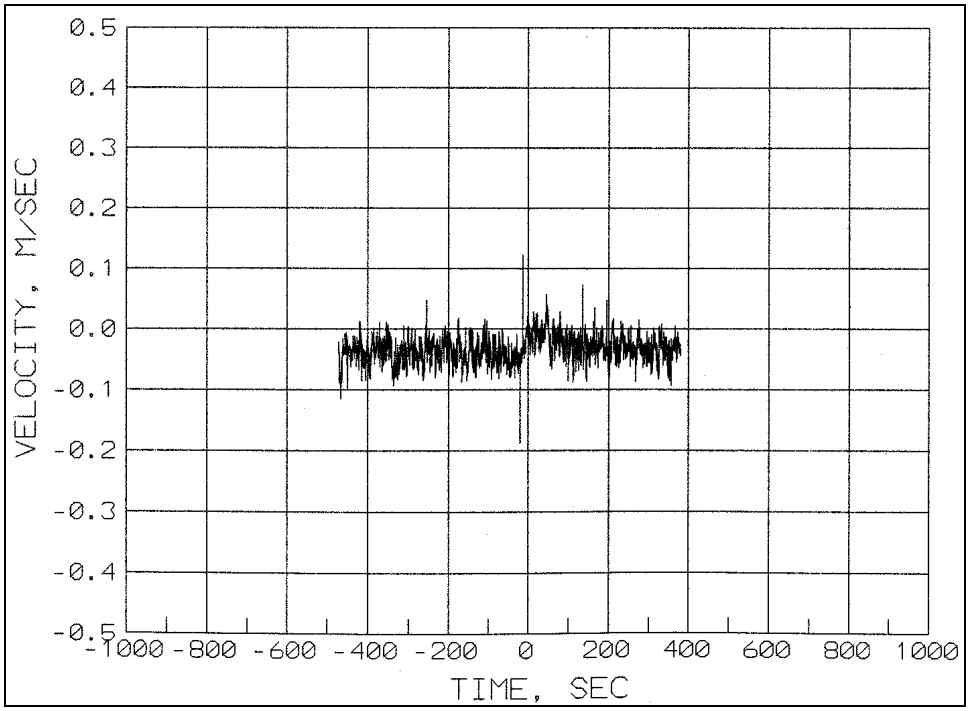

b. Y-velocity

Figure 31. Physical model data, *William C. Norma*, meter at location of MMB511/1000

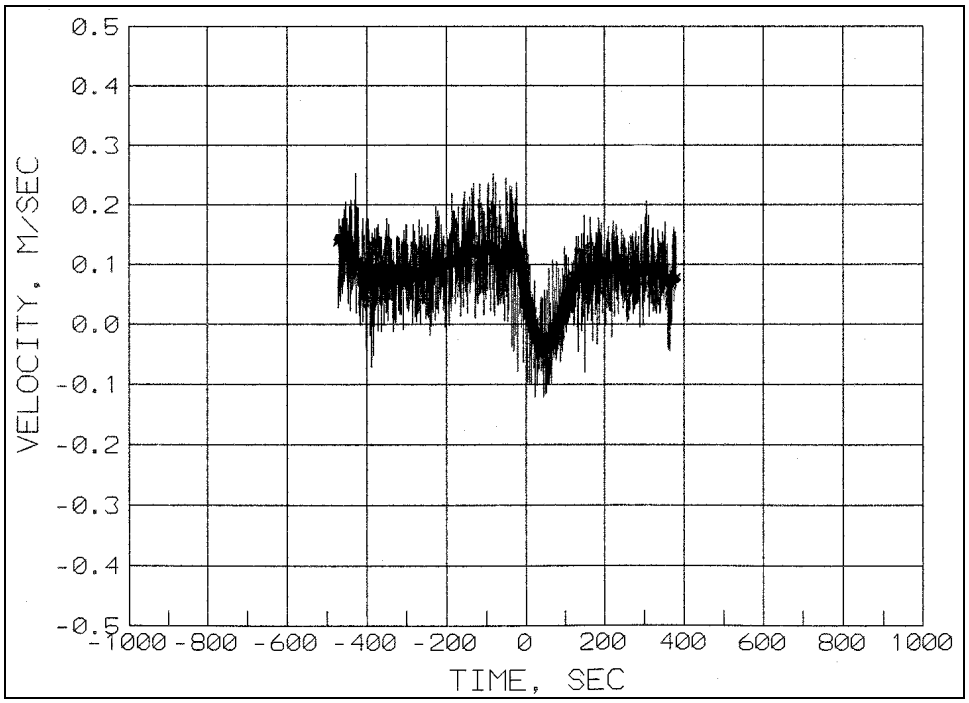

a. X-velocity

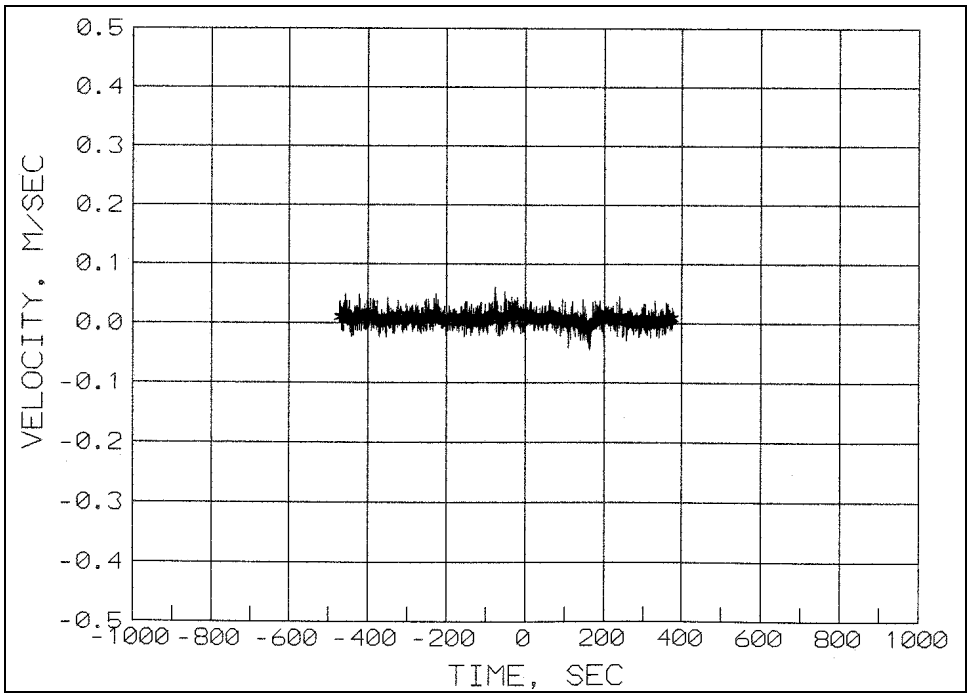

b. Y-velocity

Figure 32. Physical model data, *William C. Norman*, meter at location of MMB511/1001

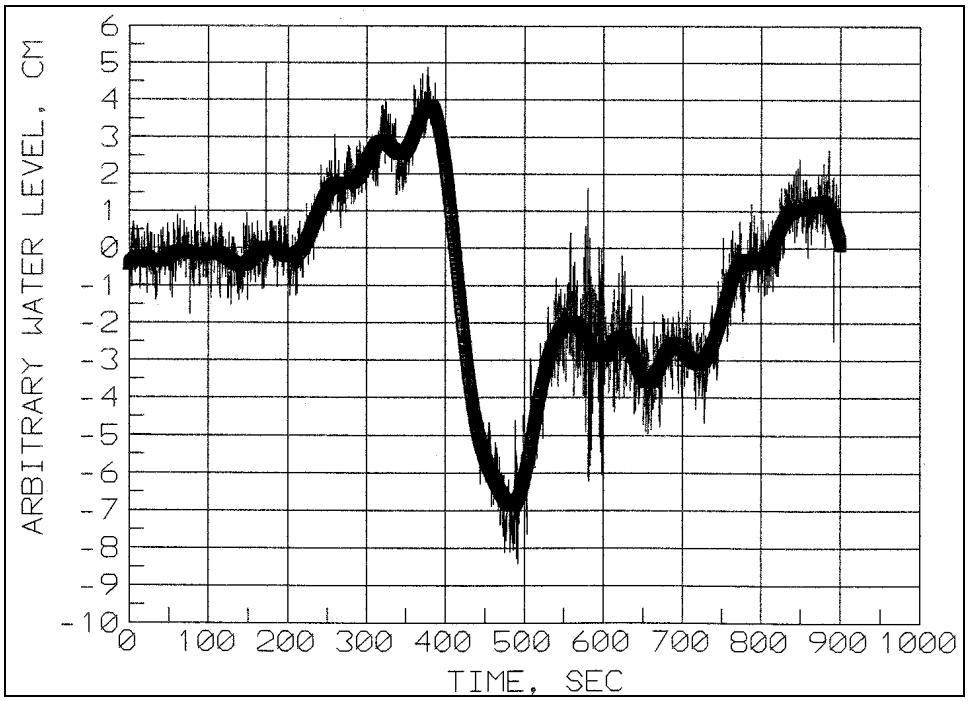

Figure 33. Physical model data, *William C. Norman*, wave gauge

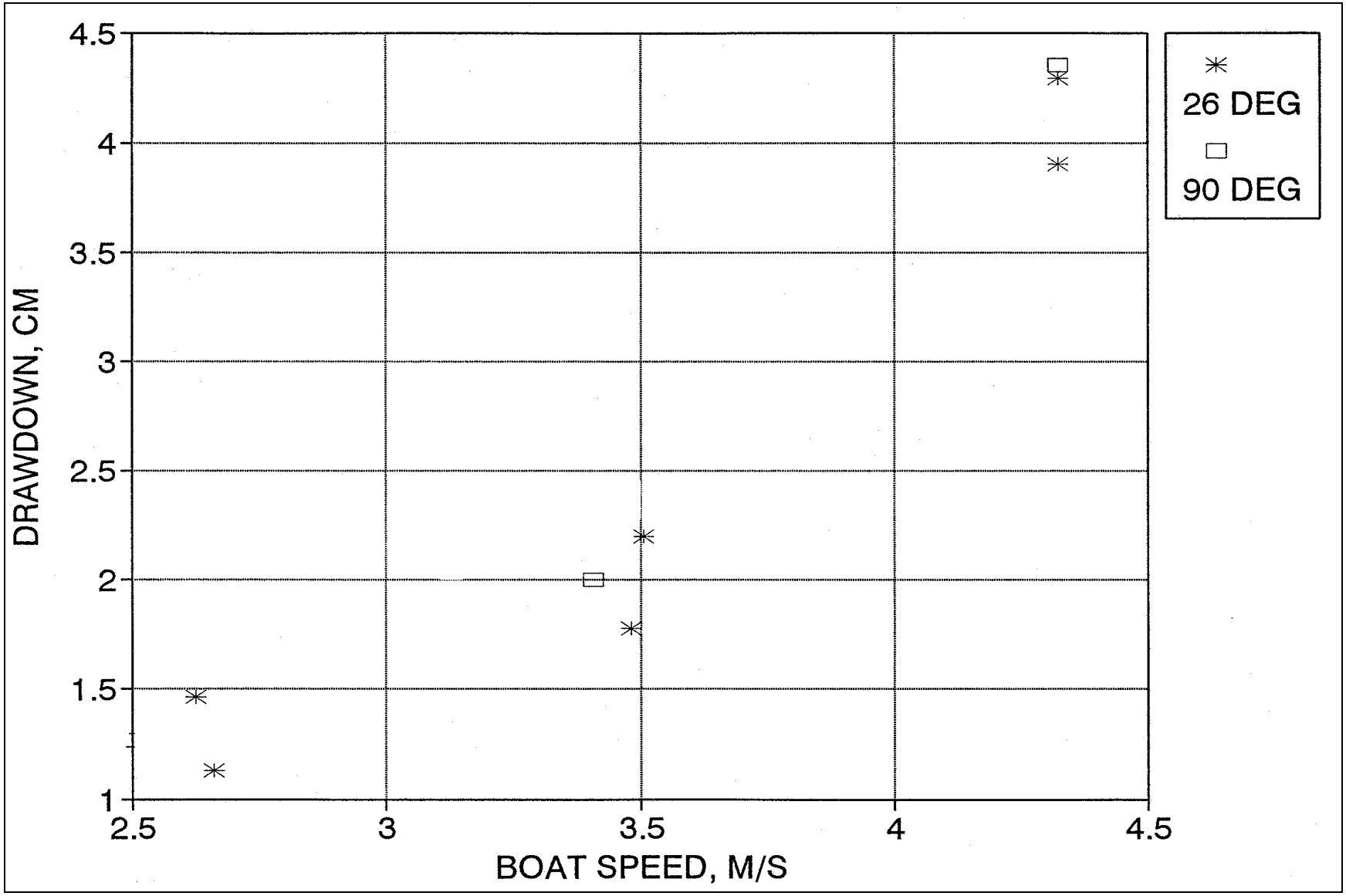

Figure 34. Rake experiments, drawdown, rod 2, 226.5 m from right bank

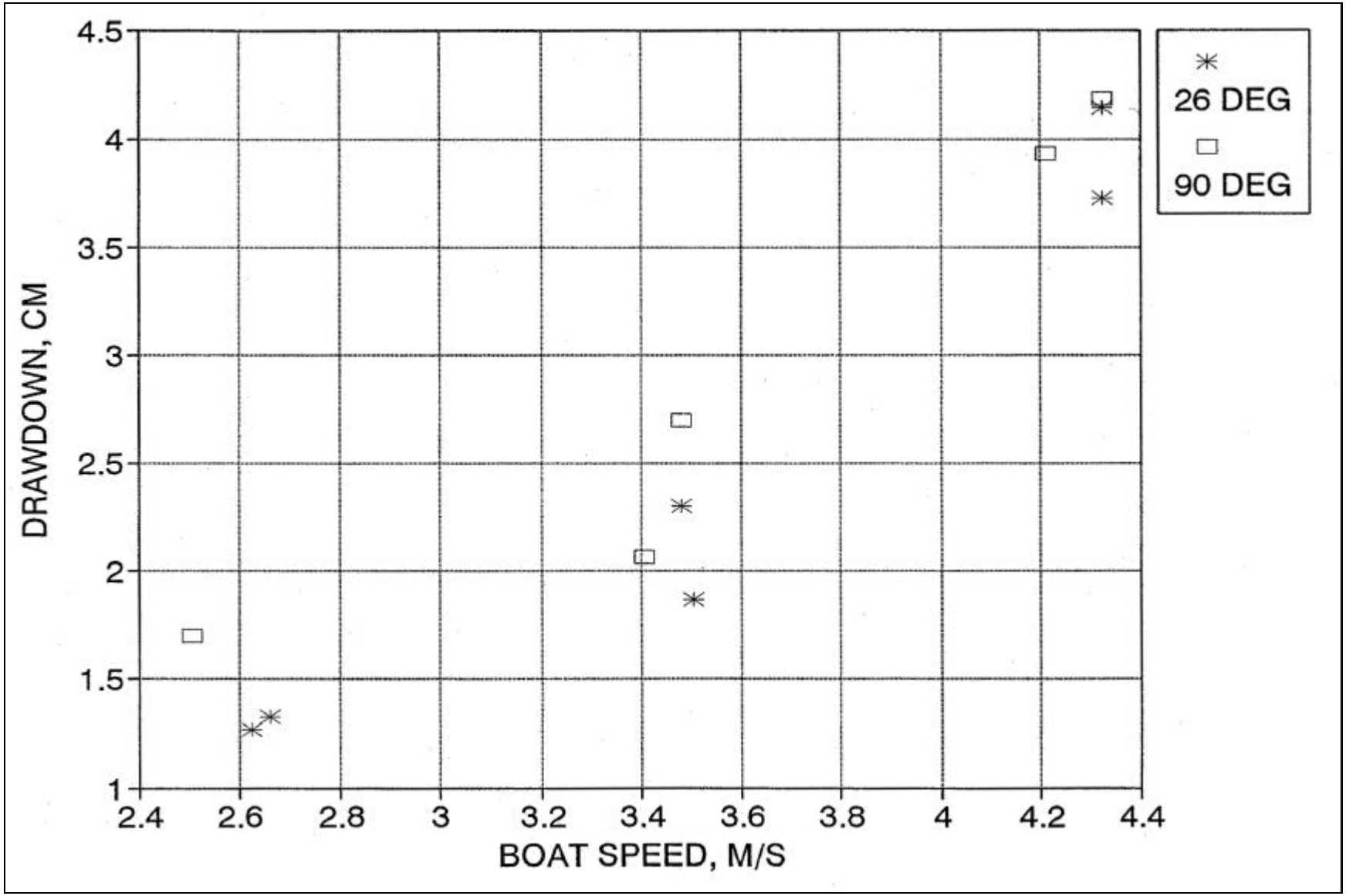

Figure 35. Rake experiments, drawdown, rod 1, 56.5 m from right bank

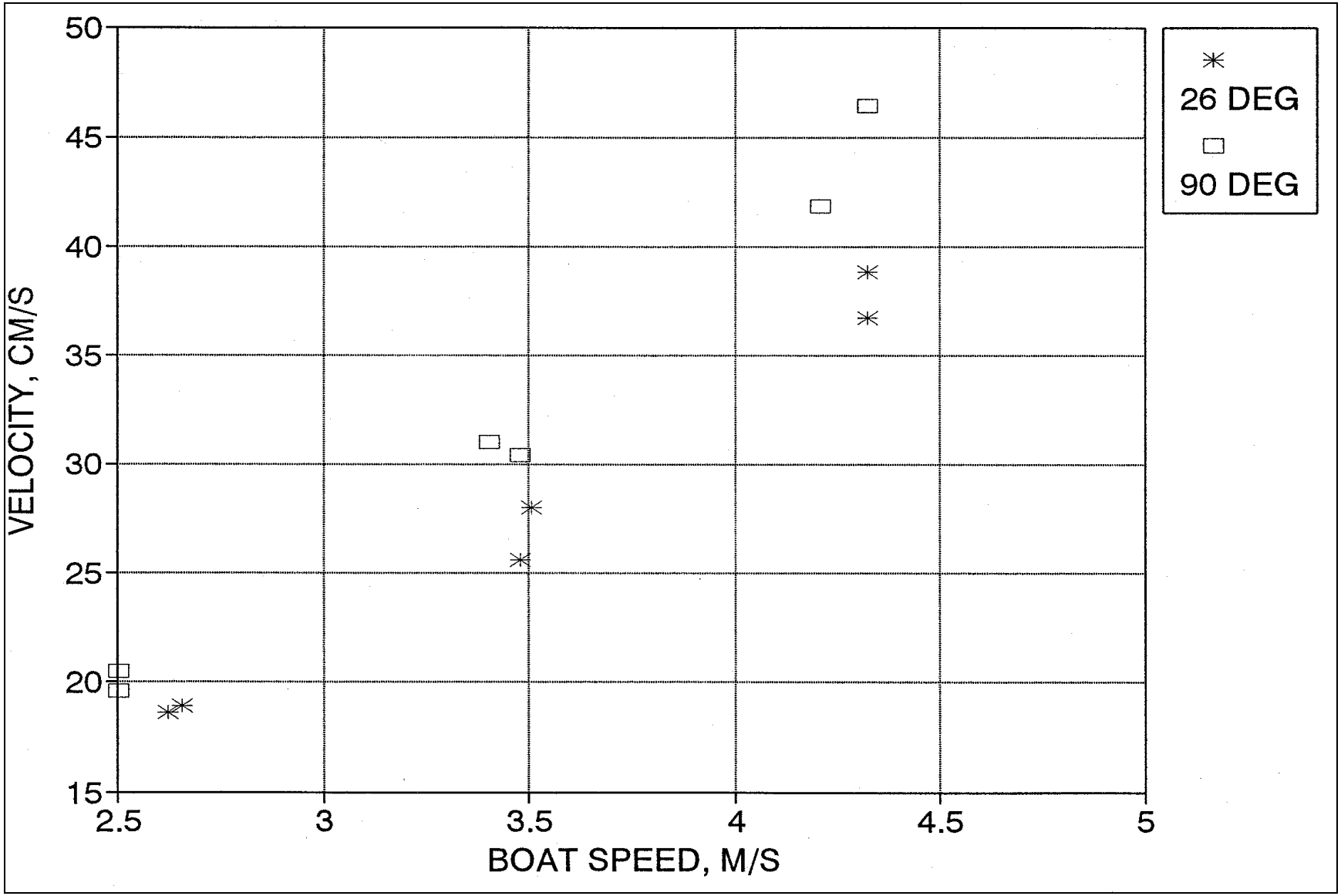

Figure 36. Rake experimetns, return velocity, x velocity, near tow

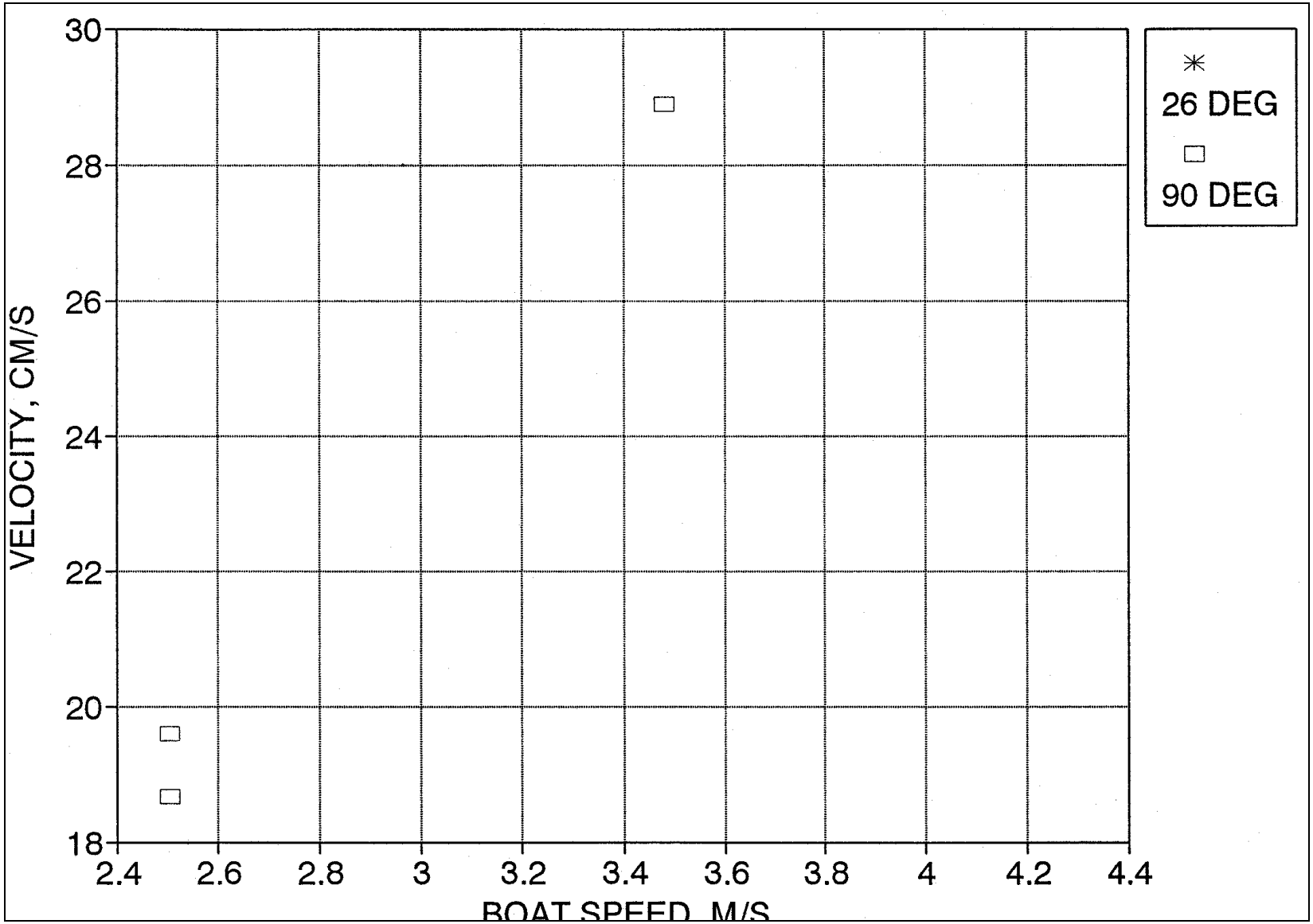

Figure 37. Rake experiments, return velocity, x velocity, midway between tow and bank

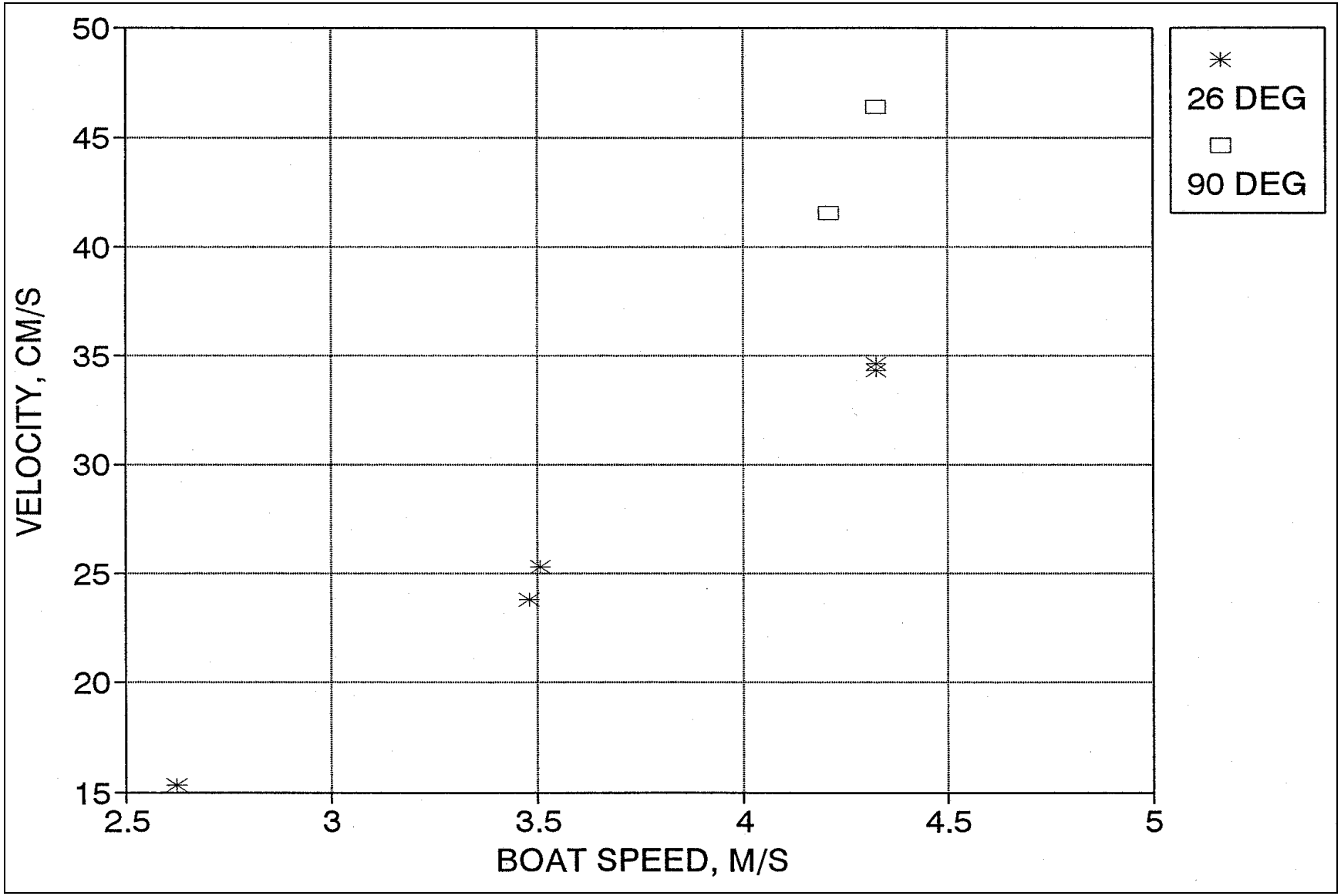

Figure 38. Rake experiments, return velocity, x direction, near bank

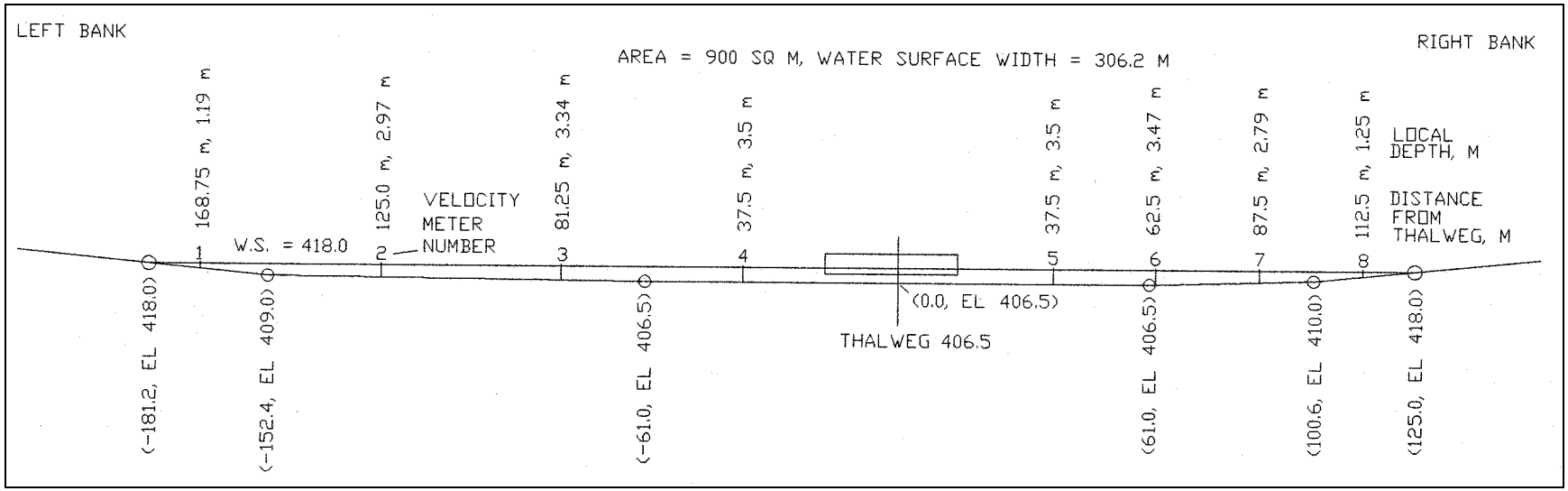

Figure 39. Cross section and meter locations for pool el 418.0 experiments

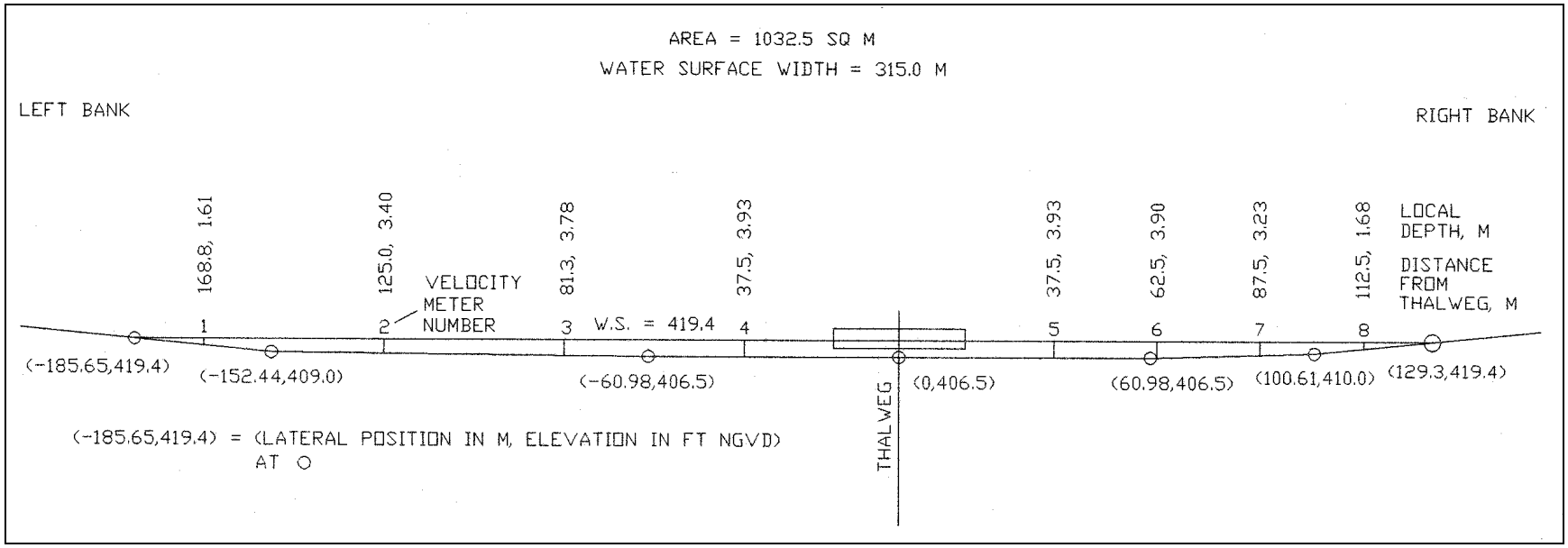

Figure 40. Cross section and meter locations for pool el 419.4 experiments

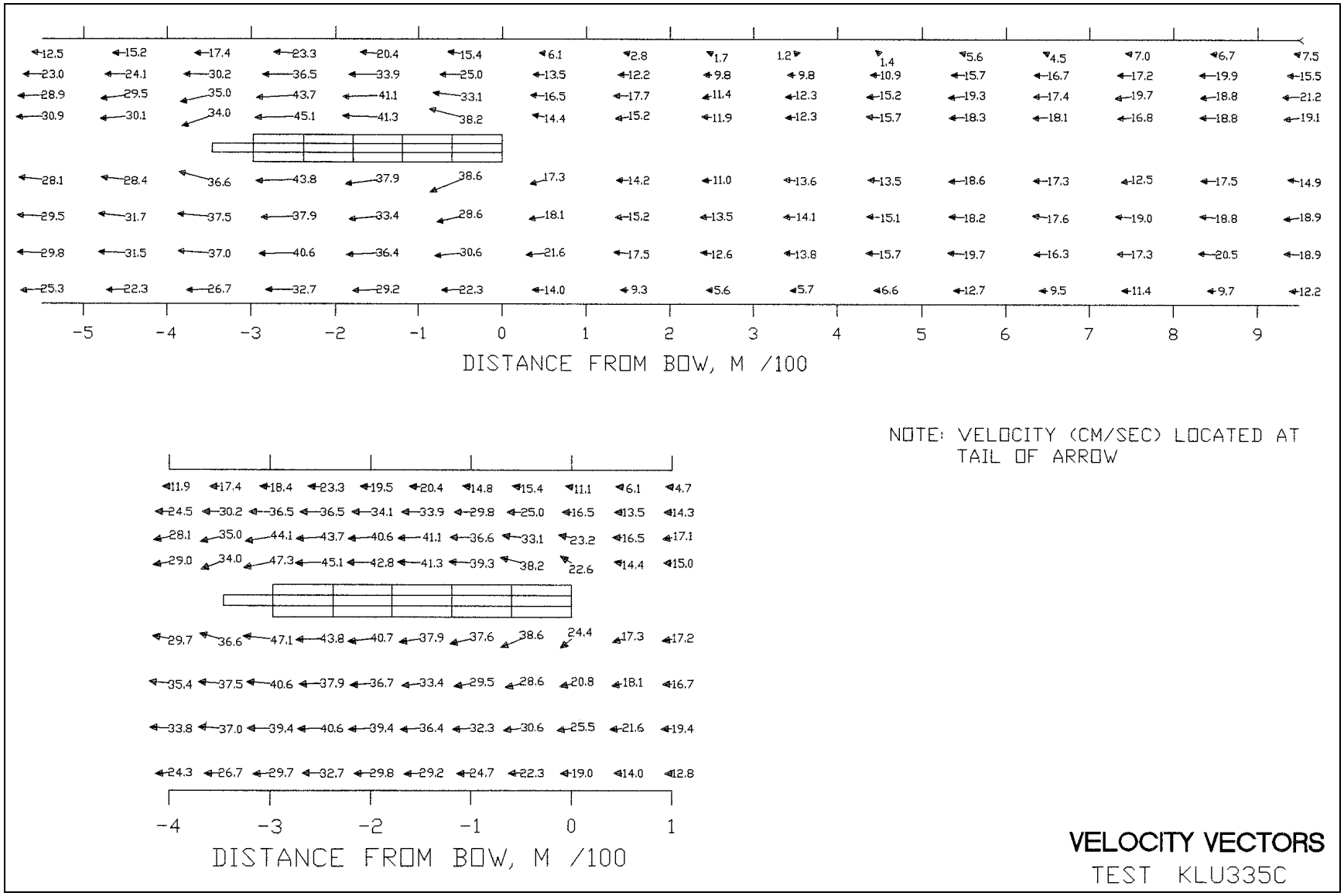

Figure 41. Velocity vectors, experiment KLU335C

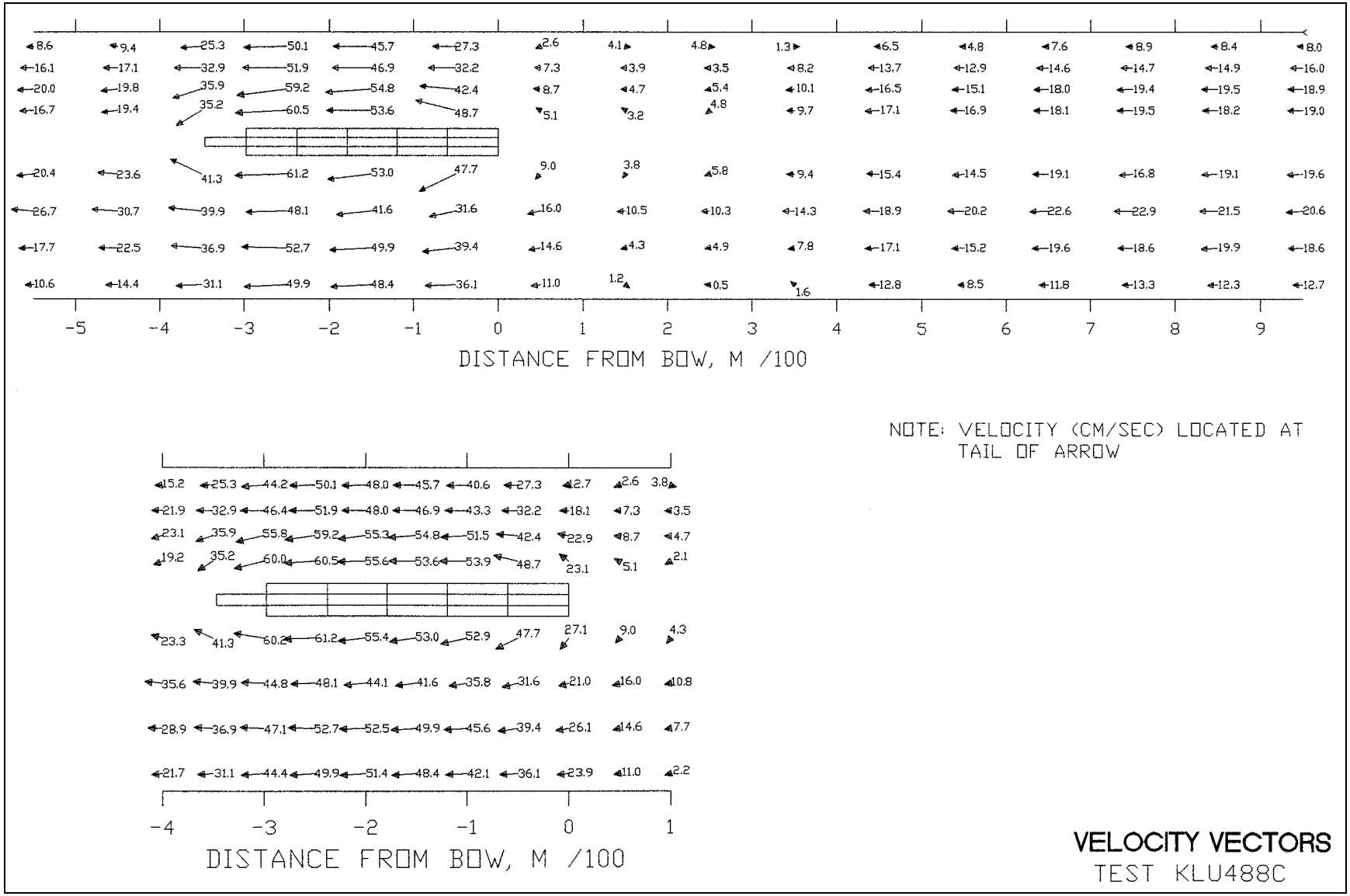

Figure 42. Velocity vectors, experiment KLU488C

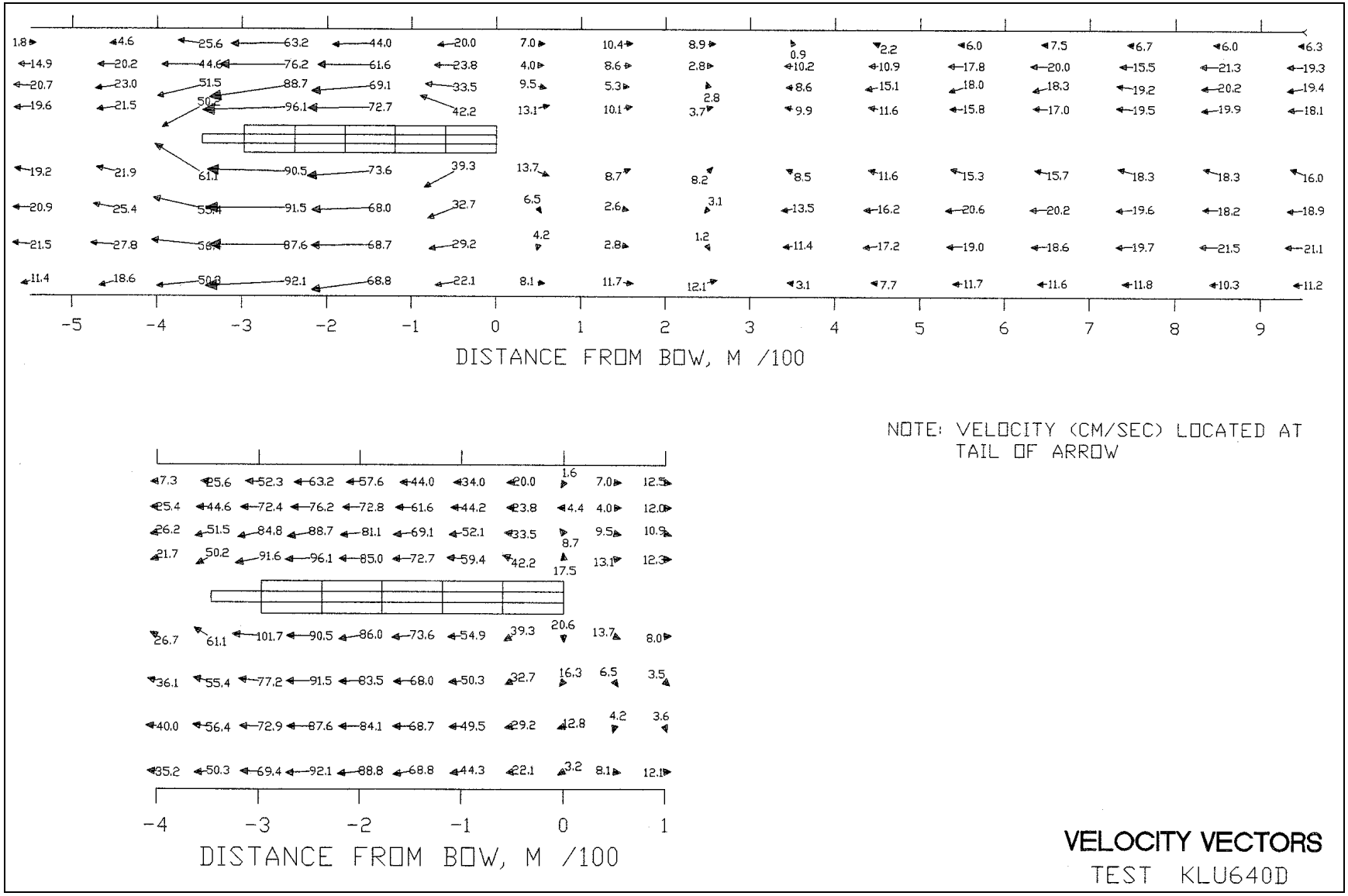

Figure 43. Velocity vectors, experiment KLU640D

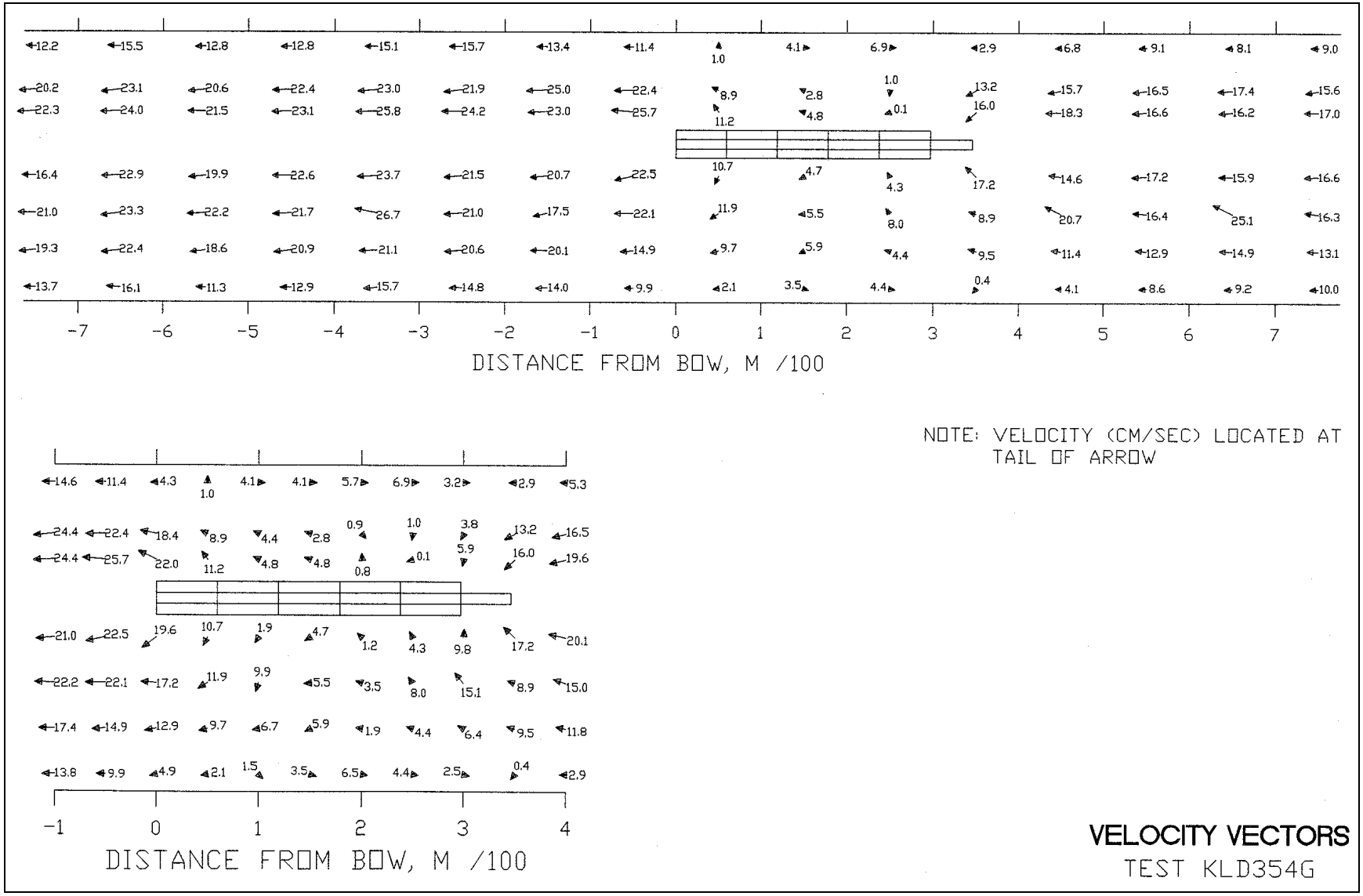

Figure 44. Velocity vectors, experiment KLD354G

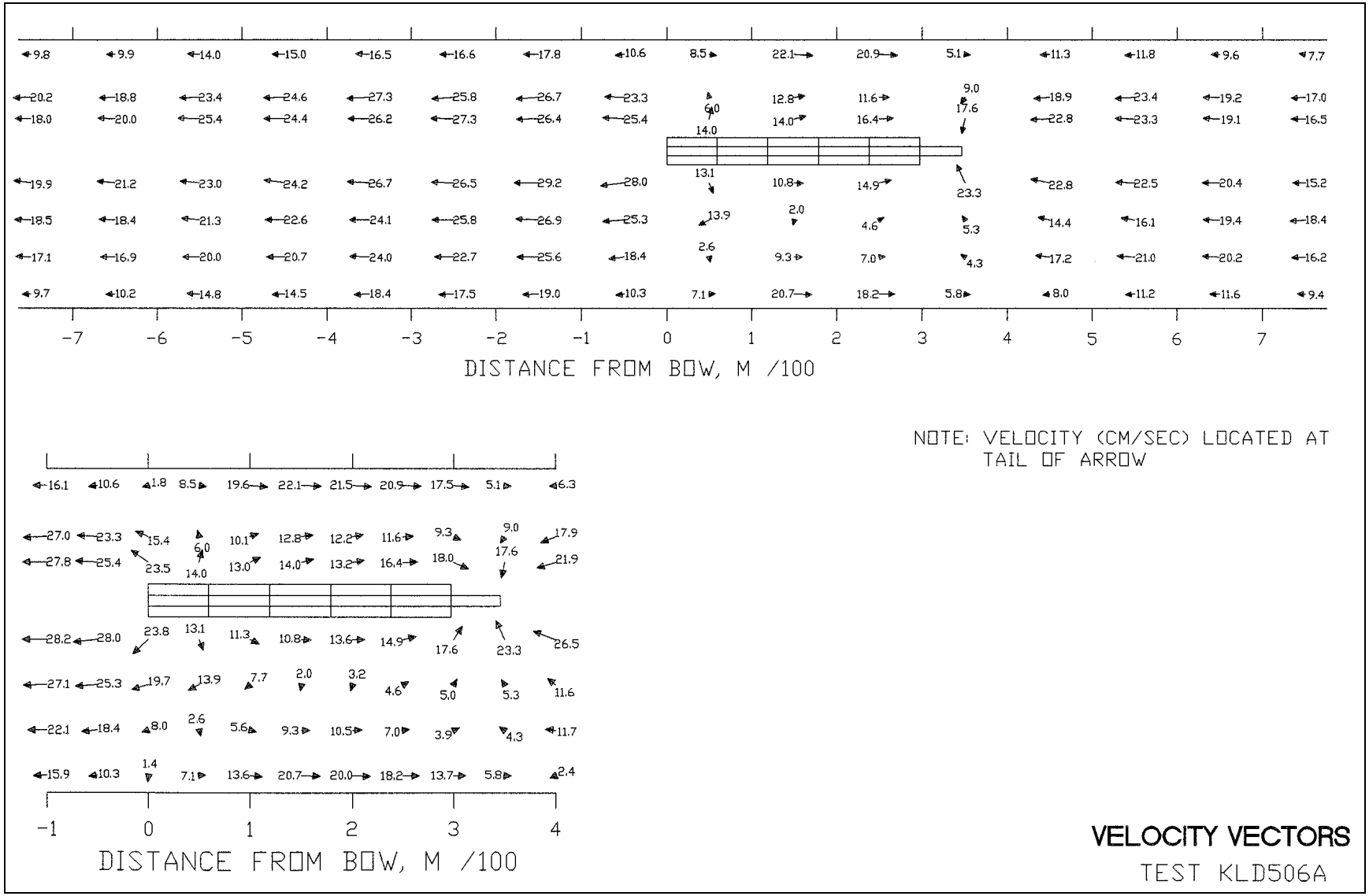

Figure 45. Velocity vectors, experiment KLD506A

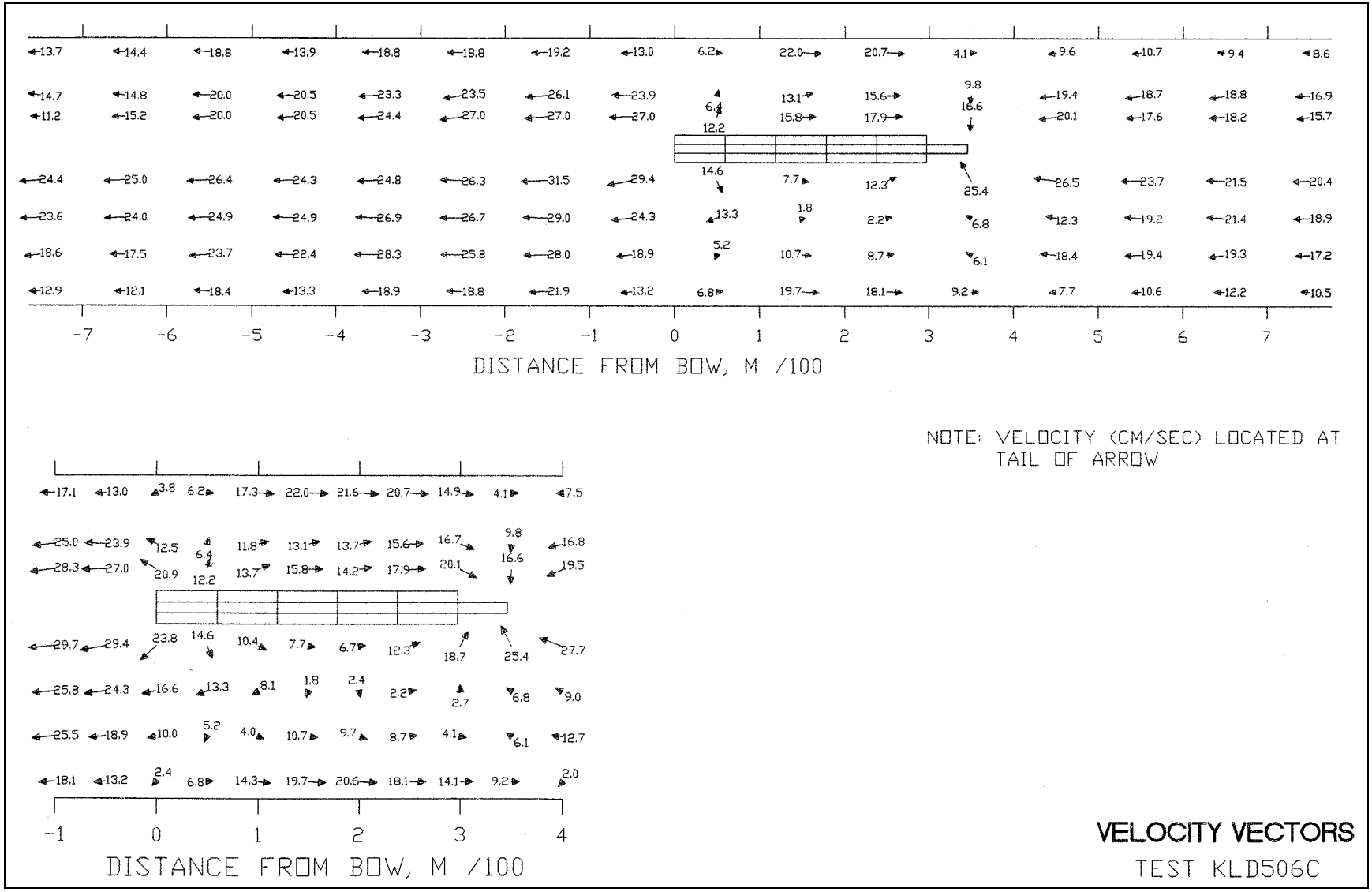

Figure 46. Velocity vectors, experimetn KLD506C

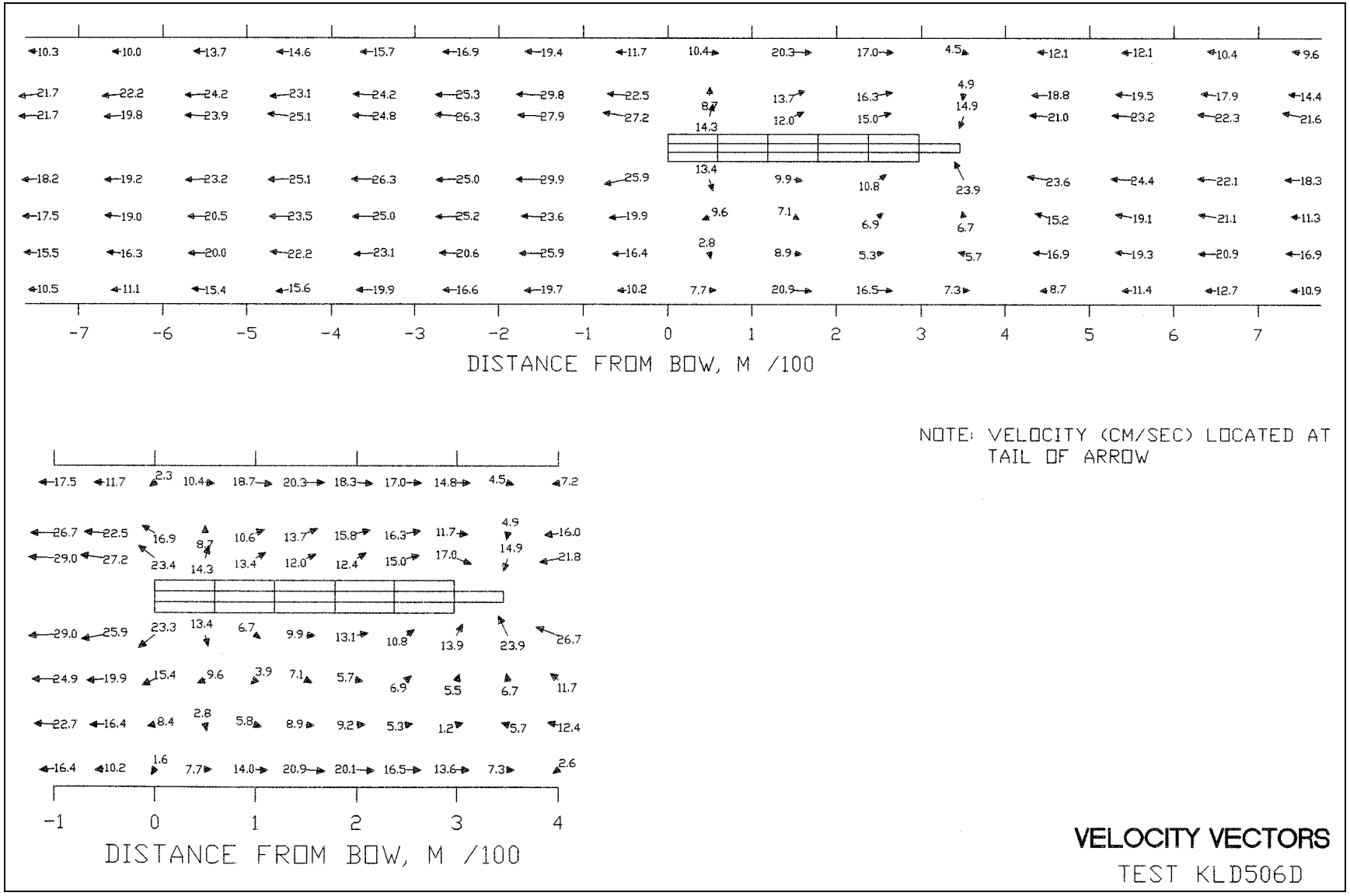

Figure 47. Velocity vectors, experiment KLD506D

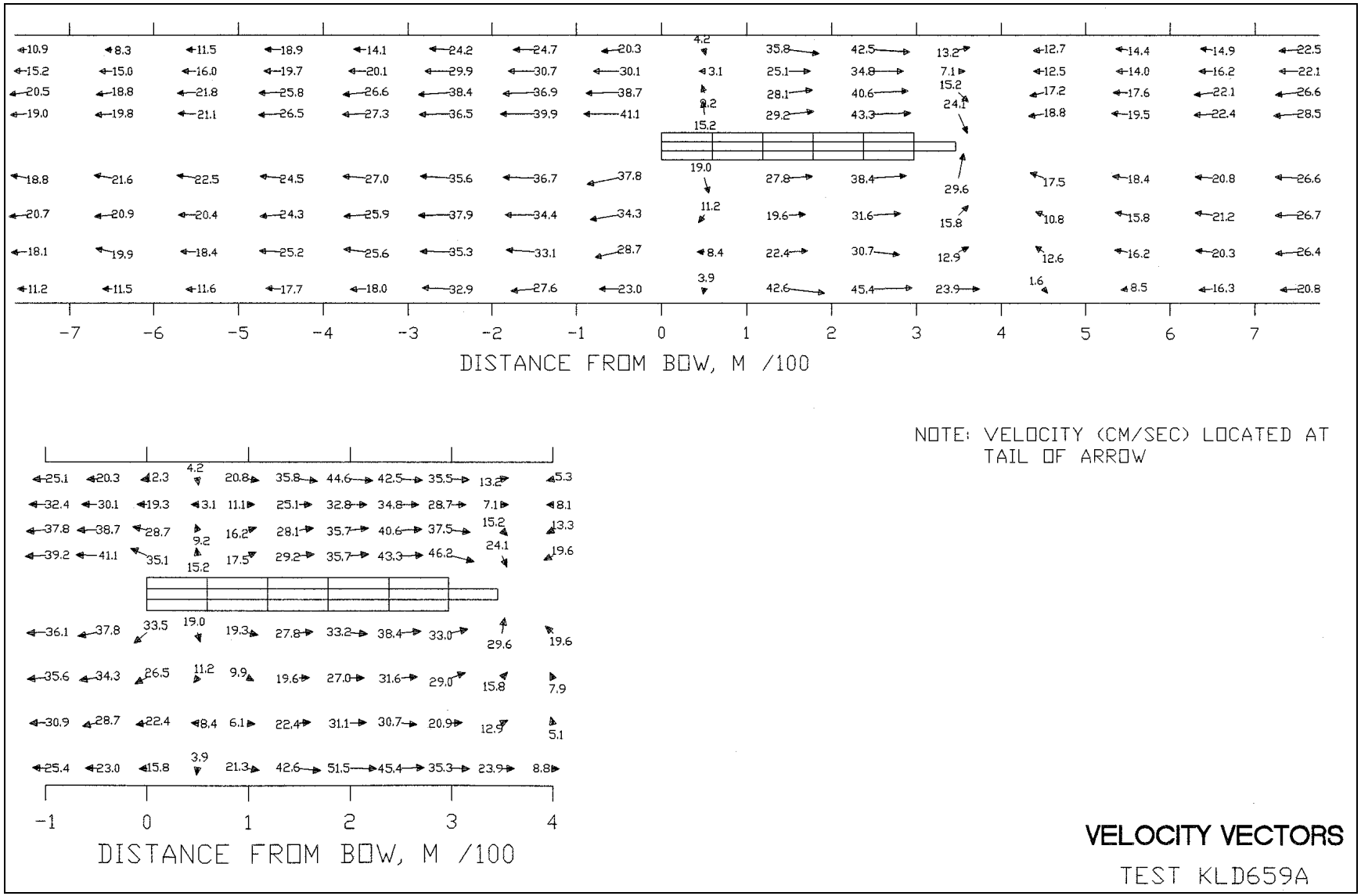

Figure 48. Velocity vectors, experimetn KLD659A

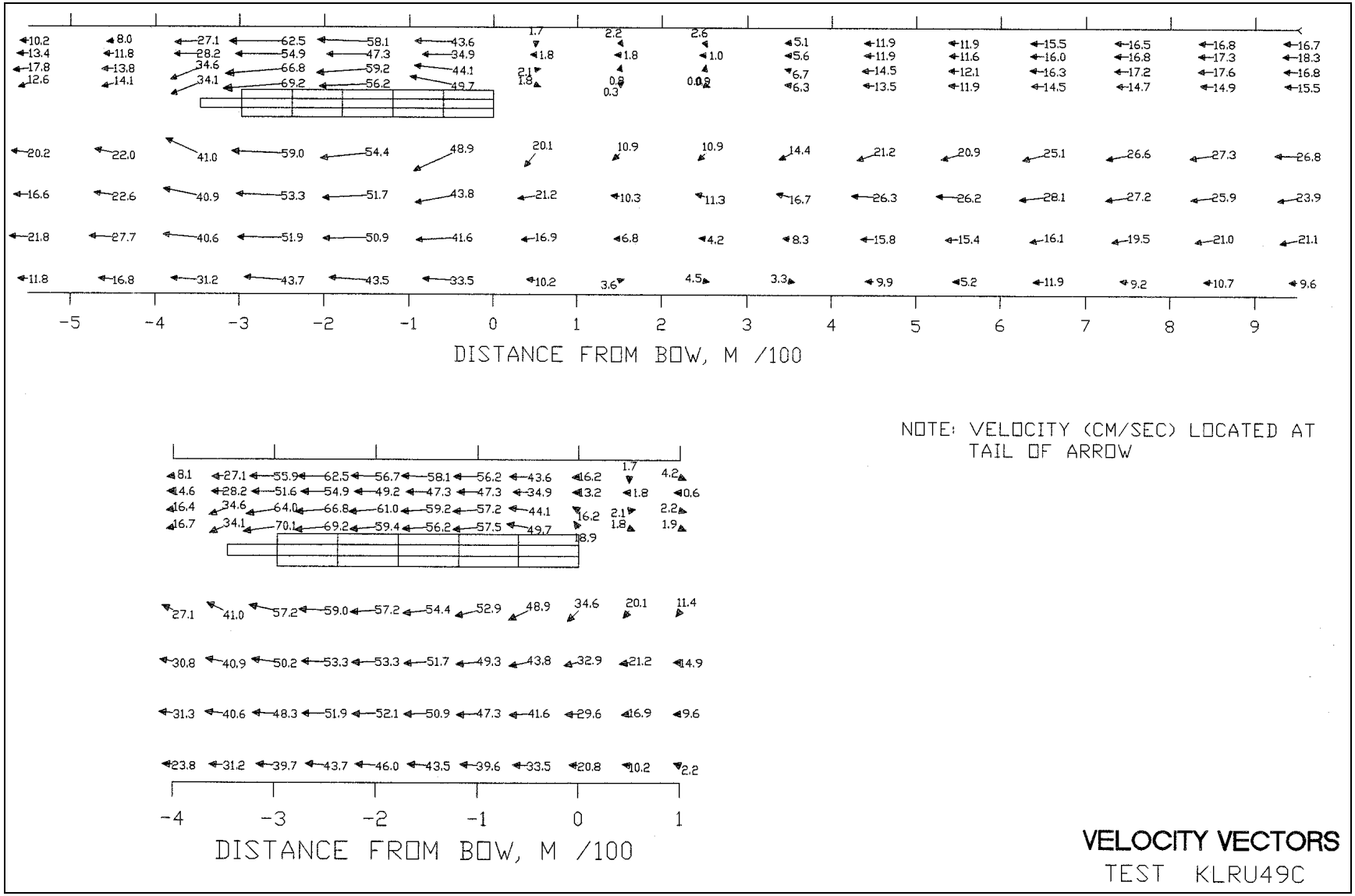

Figure 49. Velocity vectors, experimetn KLRU49C

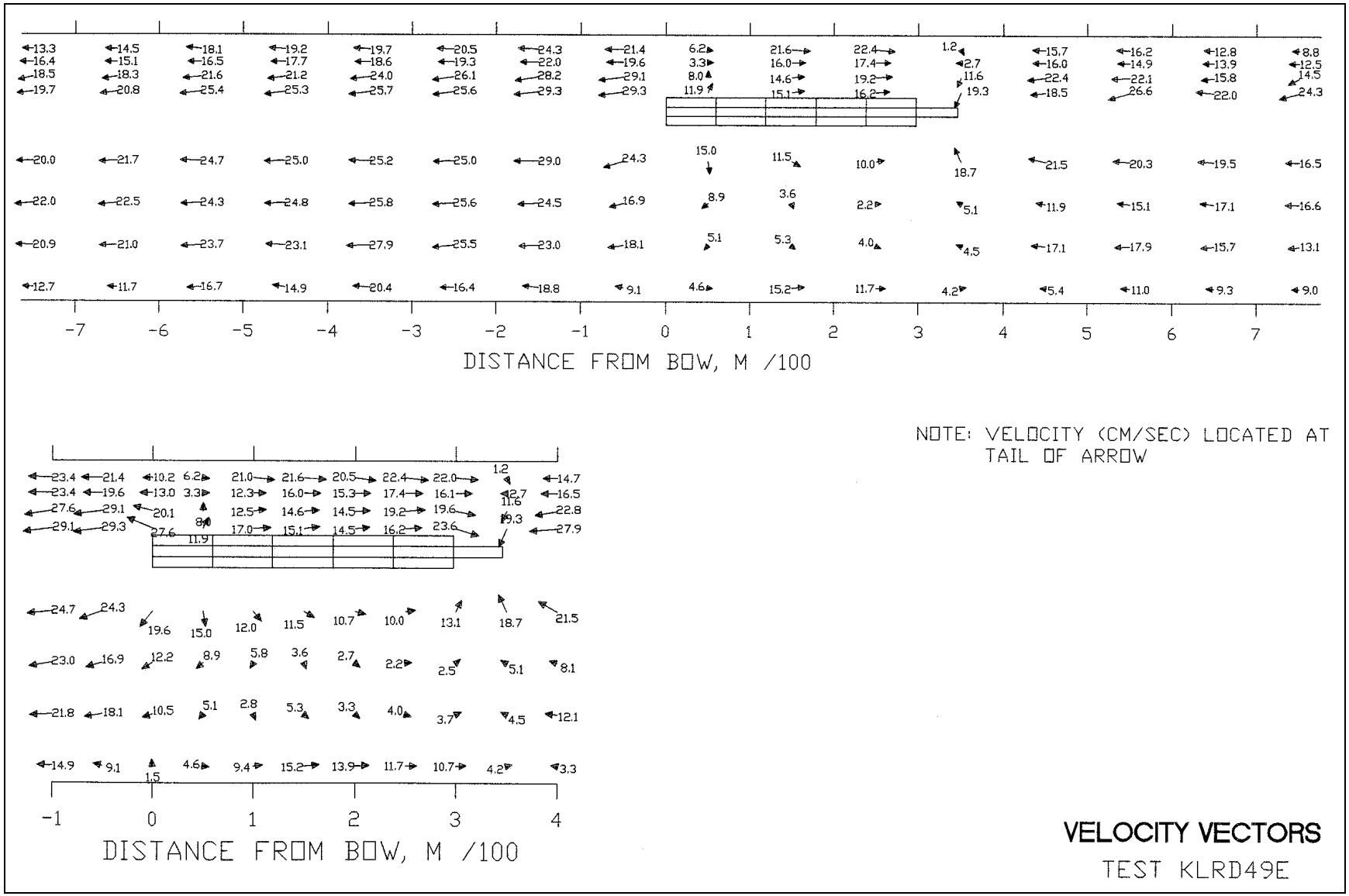

Figure 50. Velocity vectors, experimetn KLRD49E

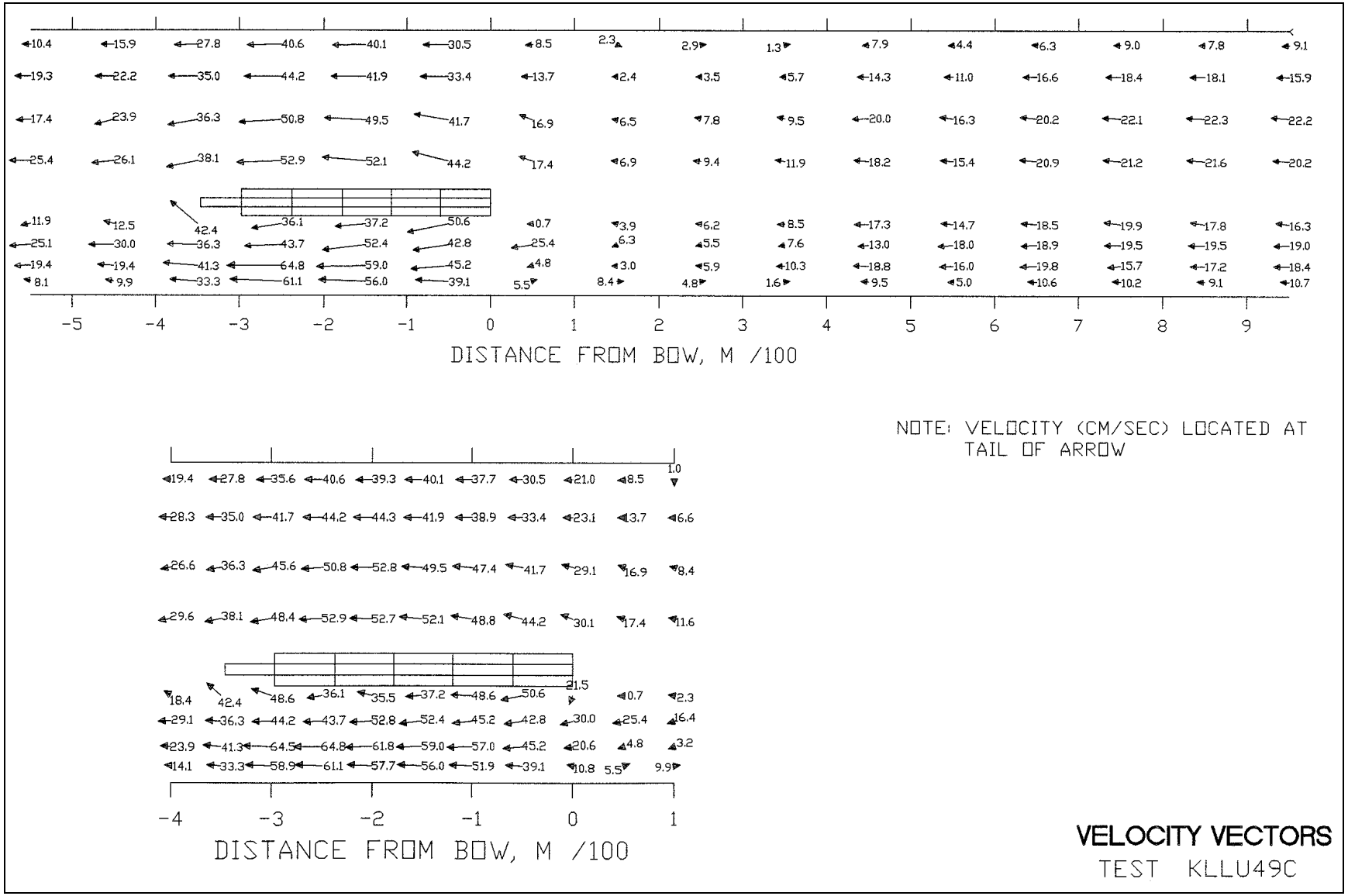

Figure 51. Velocity vectors, experiment KLLU49C

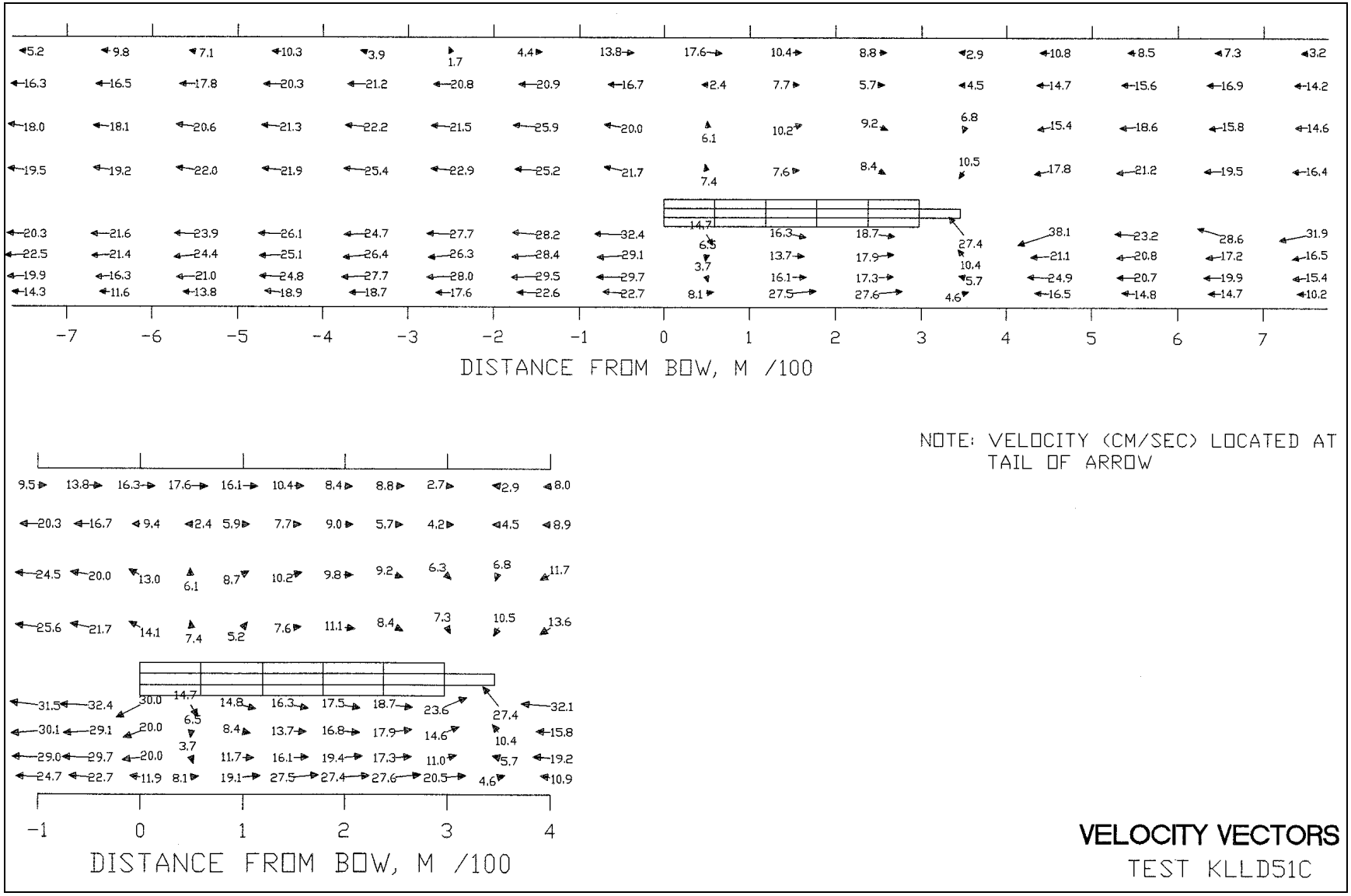

Figure 52. Velocity vectors, expeirment KLLD51C

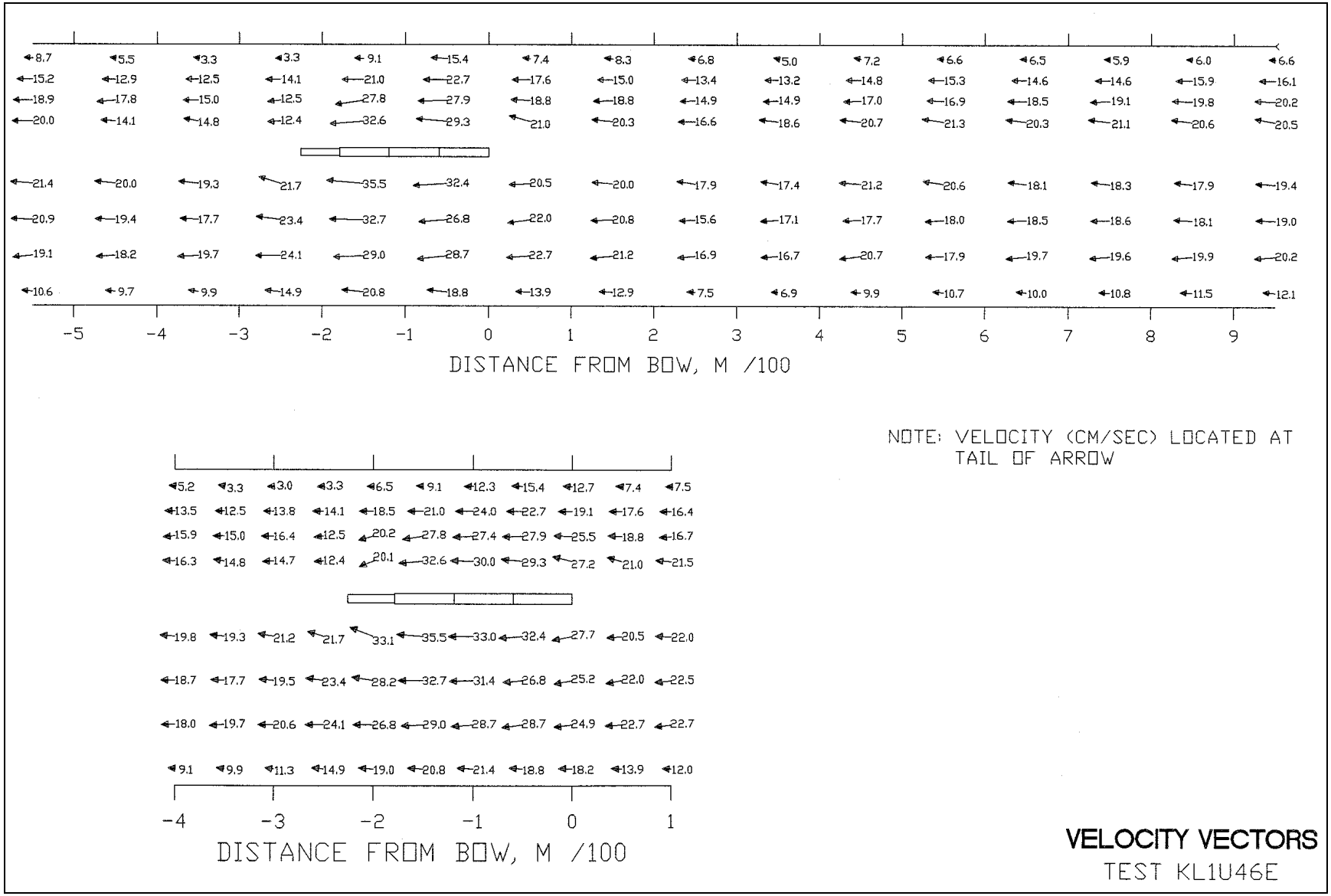

Figure 53. Velocity vectors, experiment KL1U46E

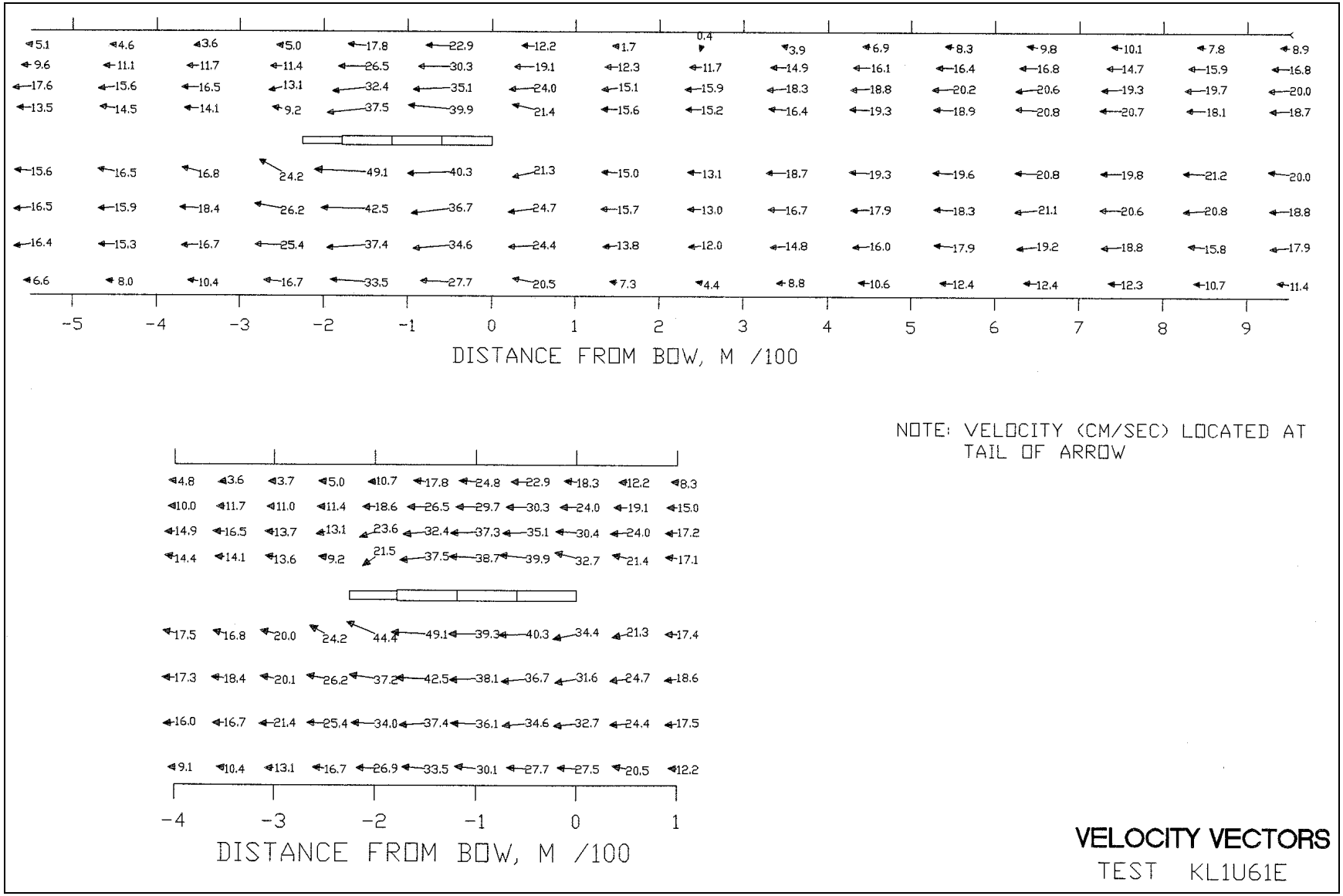

Figure 54. Velocity vectors, experiment KL1U61E

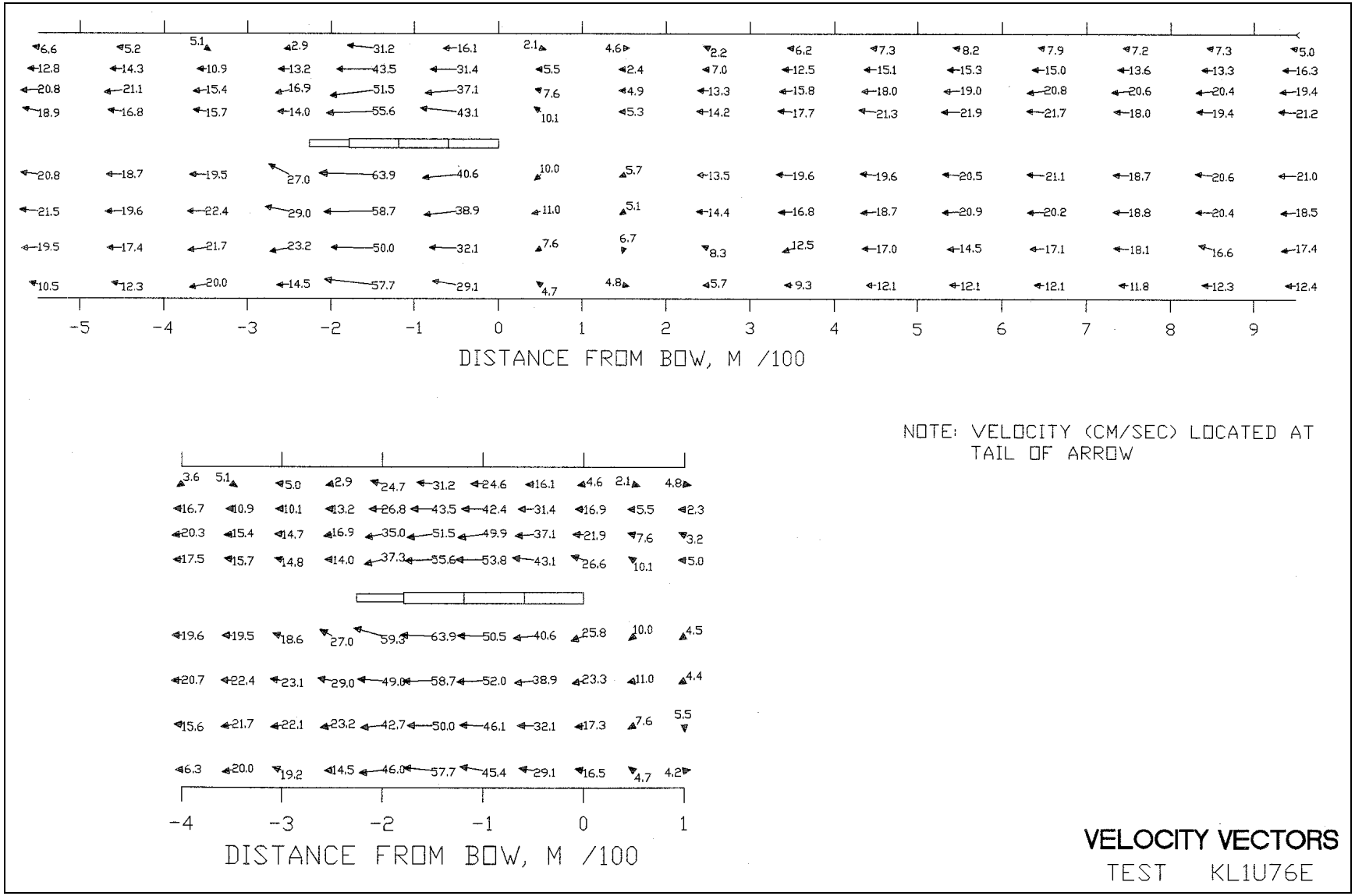

Figure 55. Velocity vectors, experiment KL1U76E

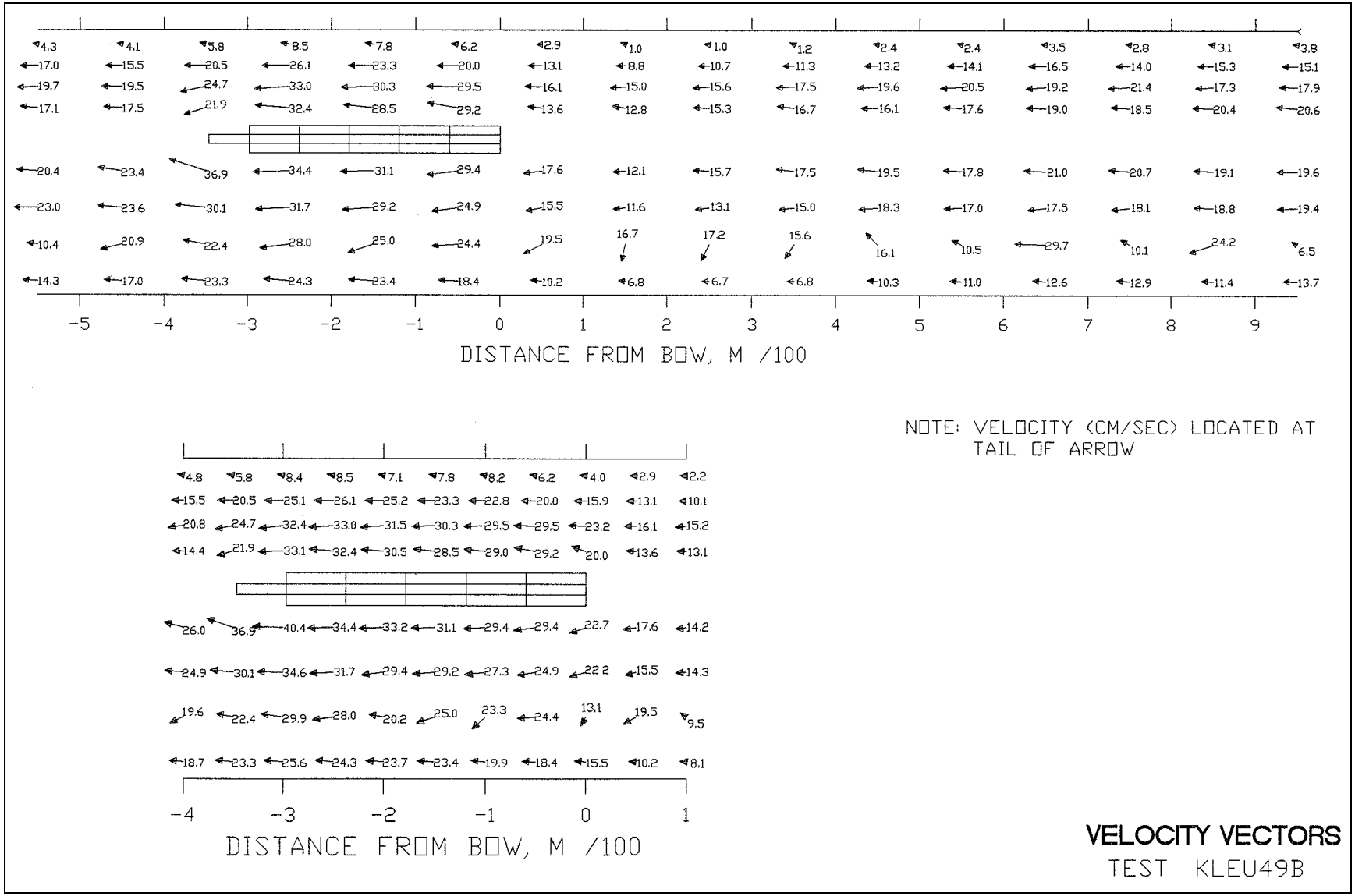

Figure 56. Velocity vectors, experiment KLEU49B

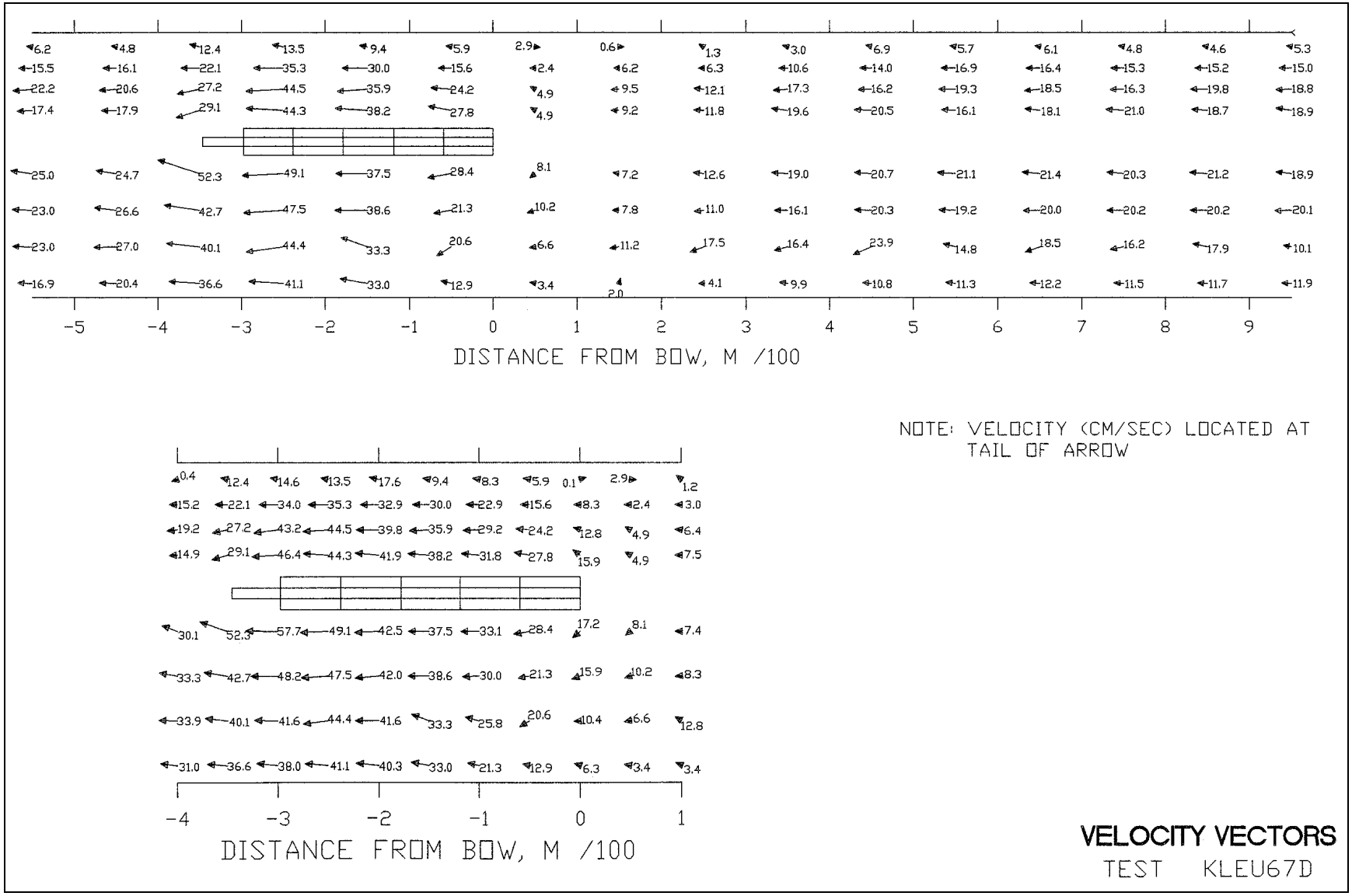

Figure 57. Velocity vectors, experiment KLEU67D

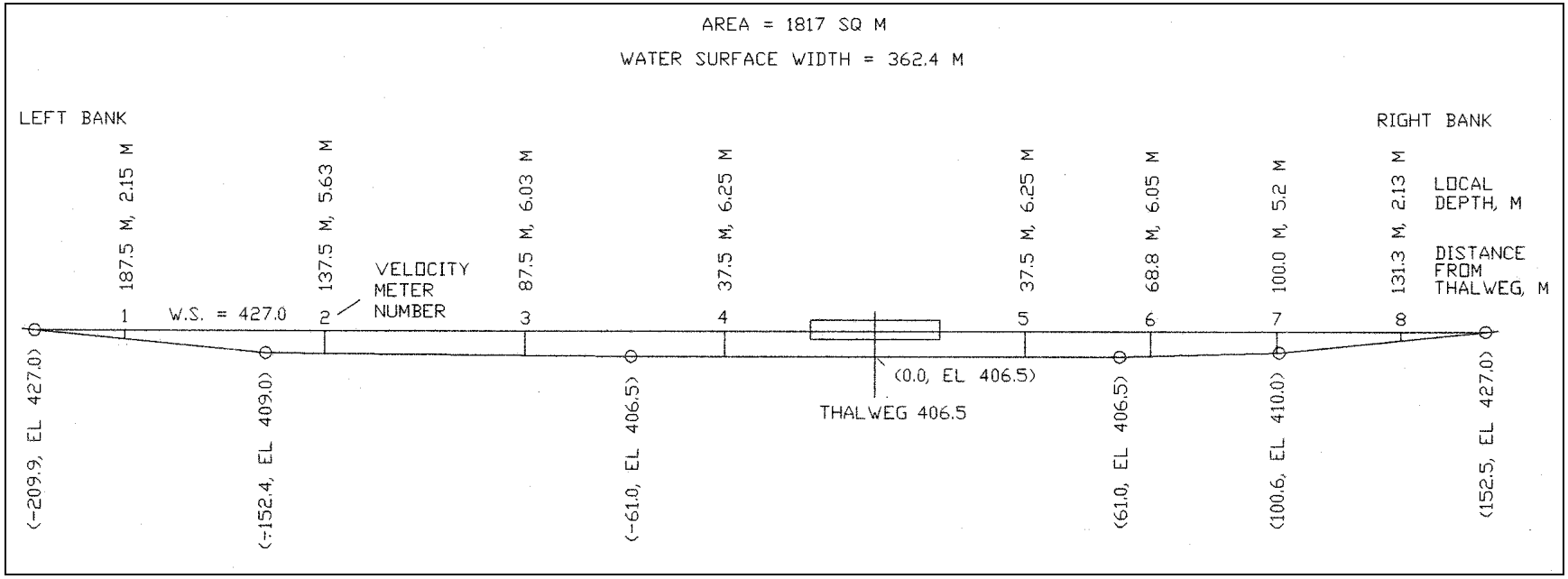

Figure 58. Cross section and meter locations for pool el 427.0 experiments

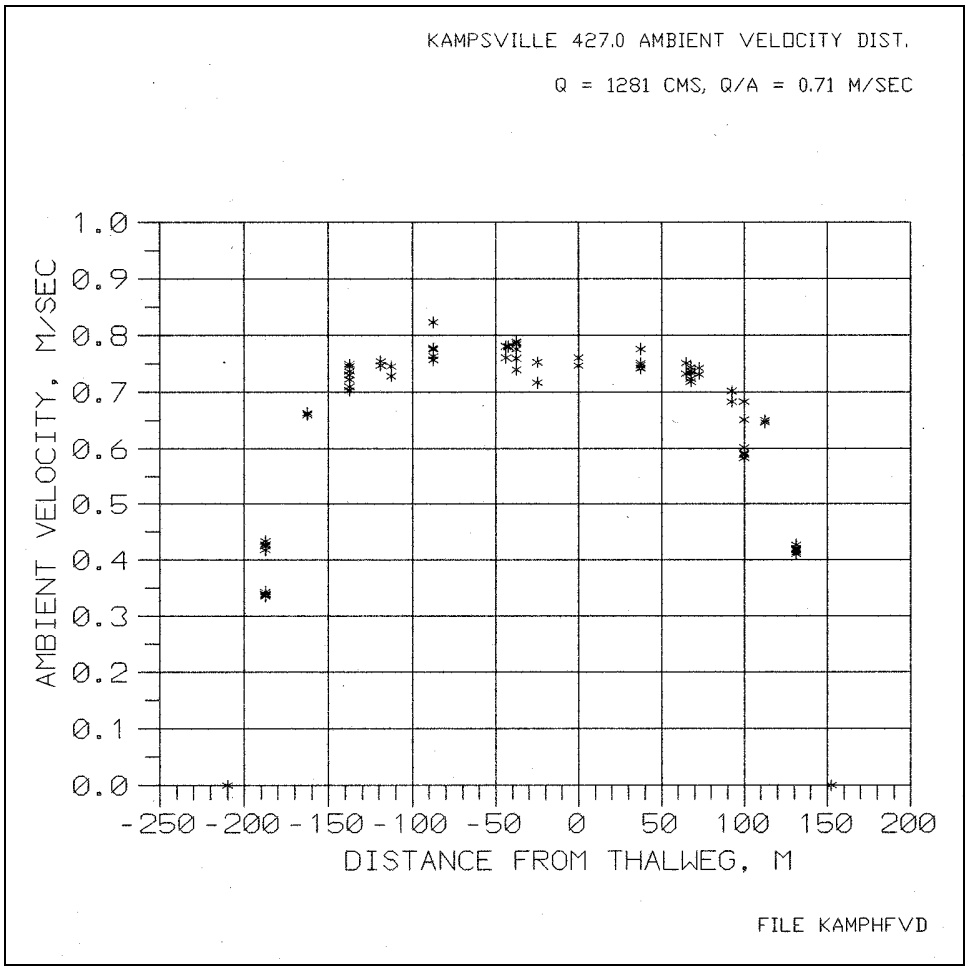

Figure 59. Ambient velocity distribution for pool el 427.0, disharge 1,281 cu m/sec, average channel velocity 0.71 m/sec

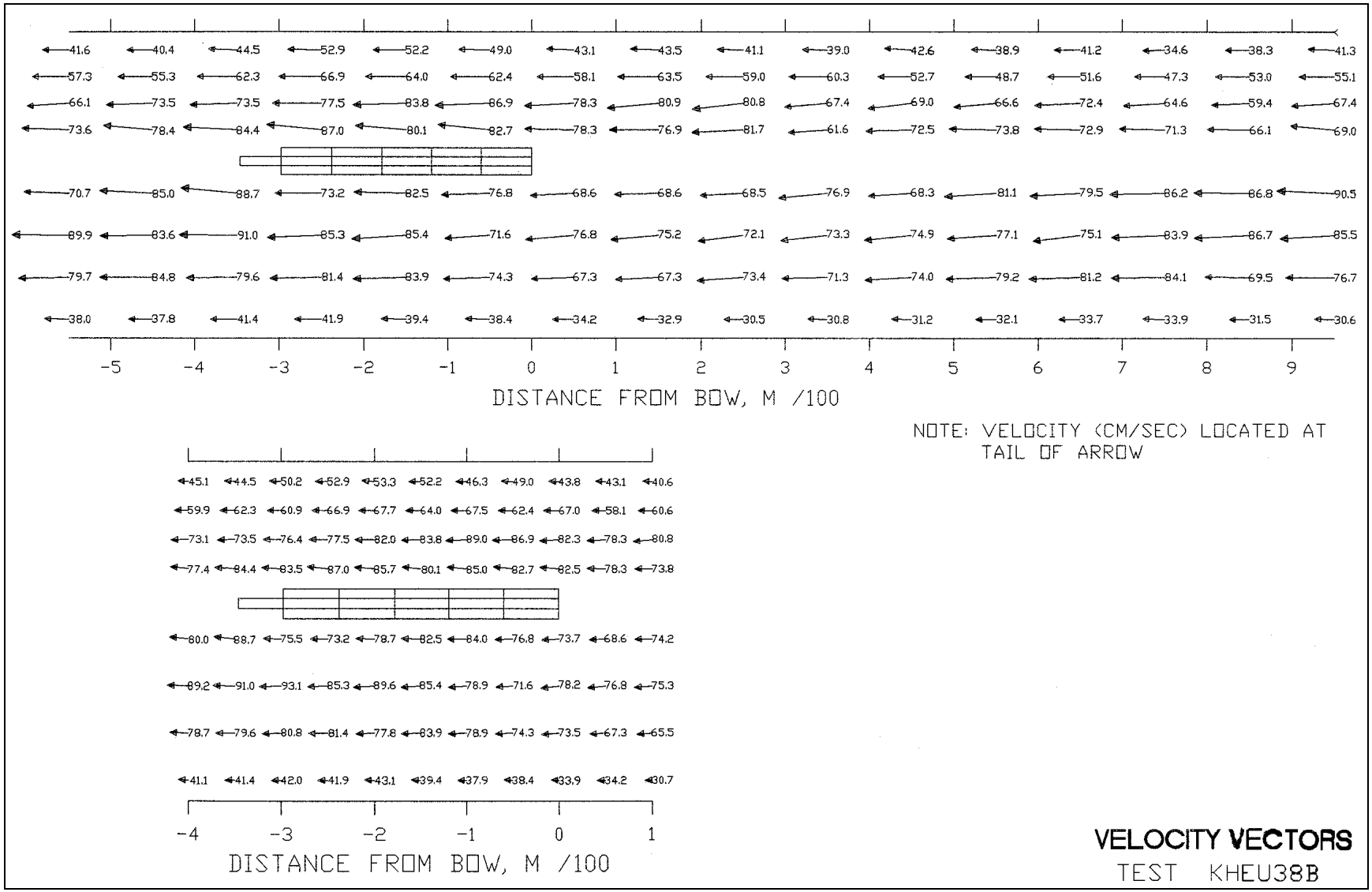

Figure 60. Velocity vectors, experiment KHEU38B

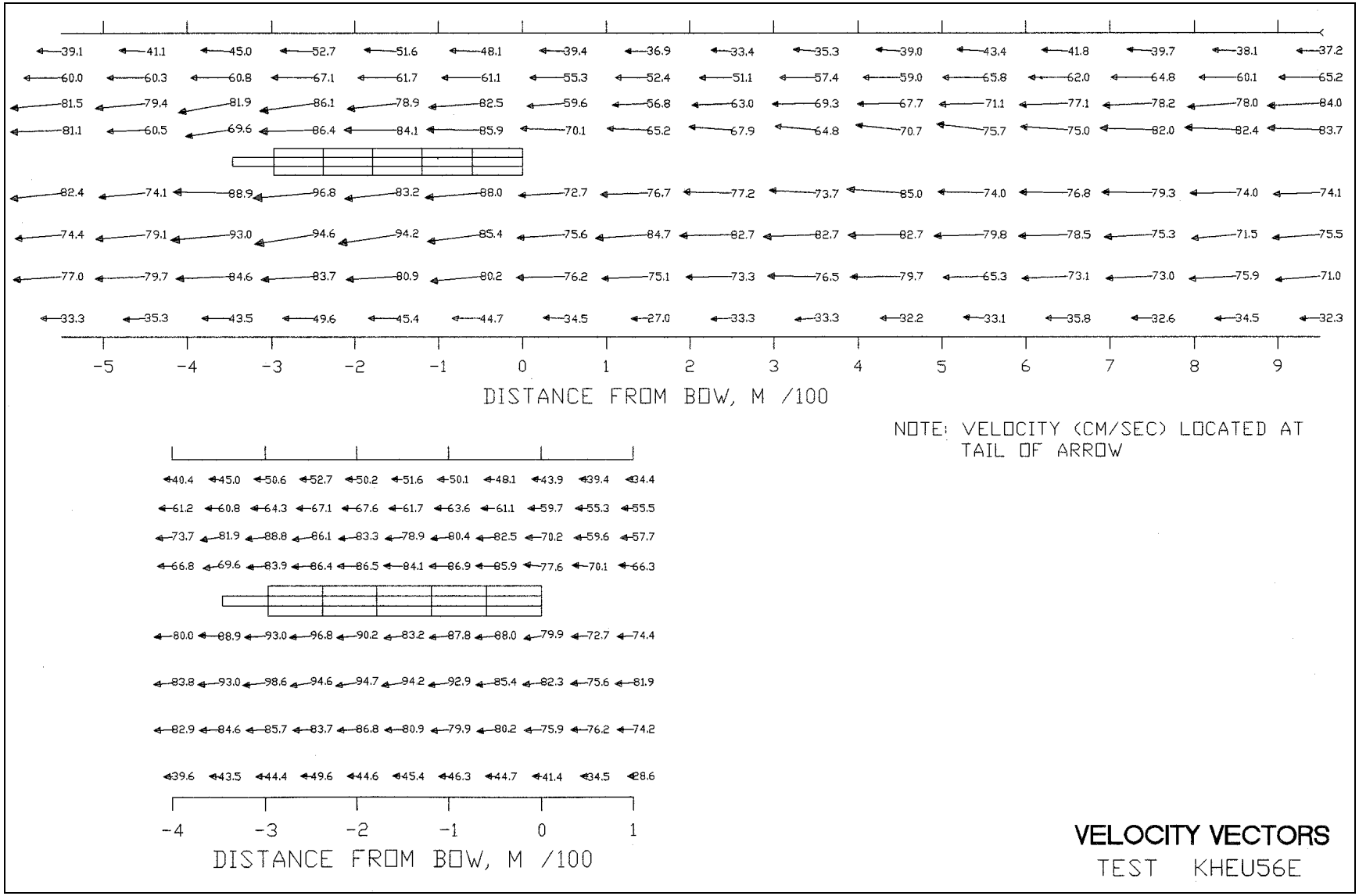

Figure 61. Velocity vectors, experiment KHEU56E

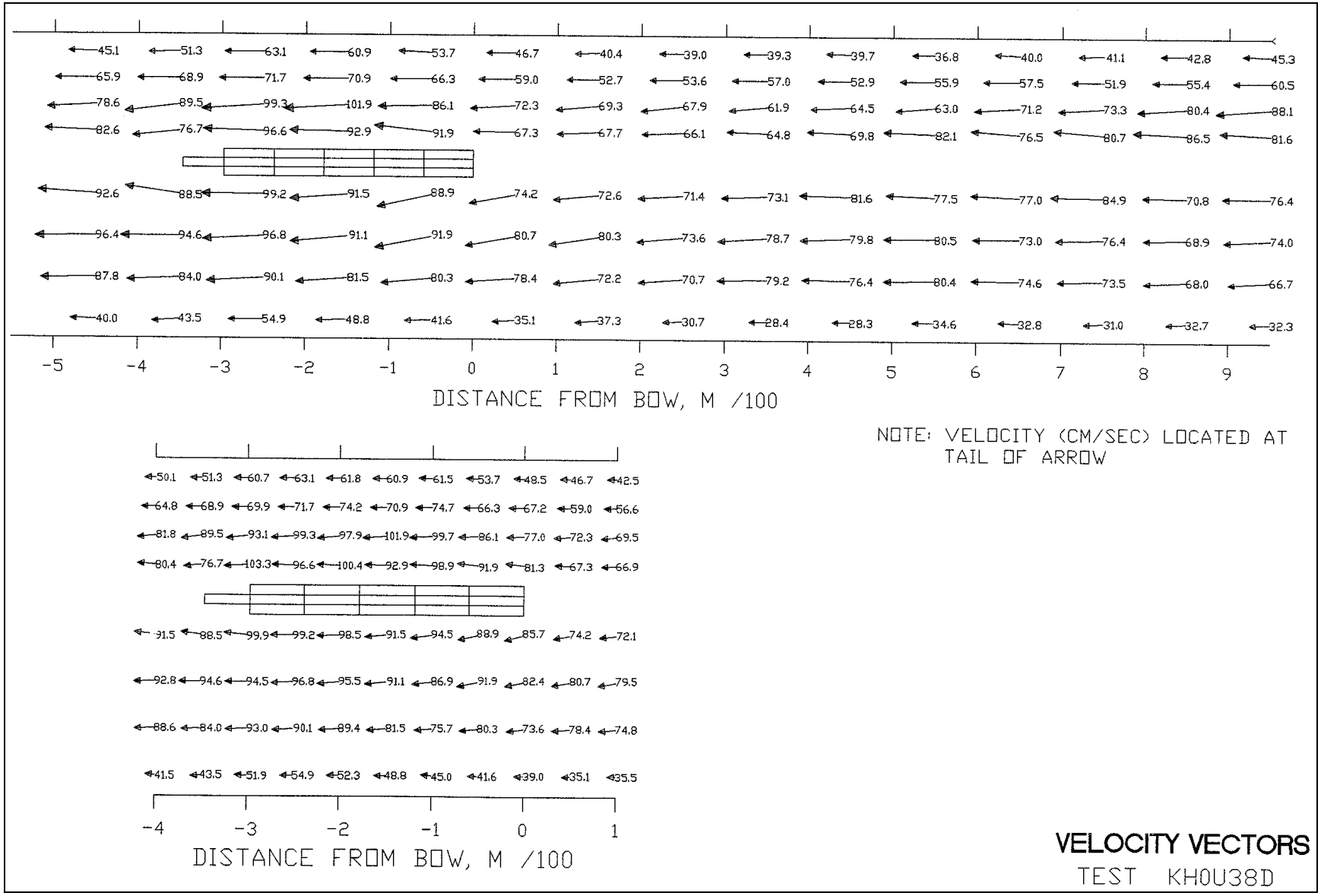

Figure 62. Velocity vectors, experimetn KHOU38D

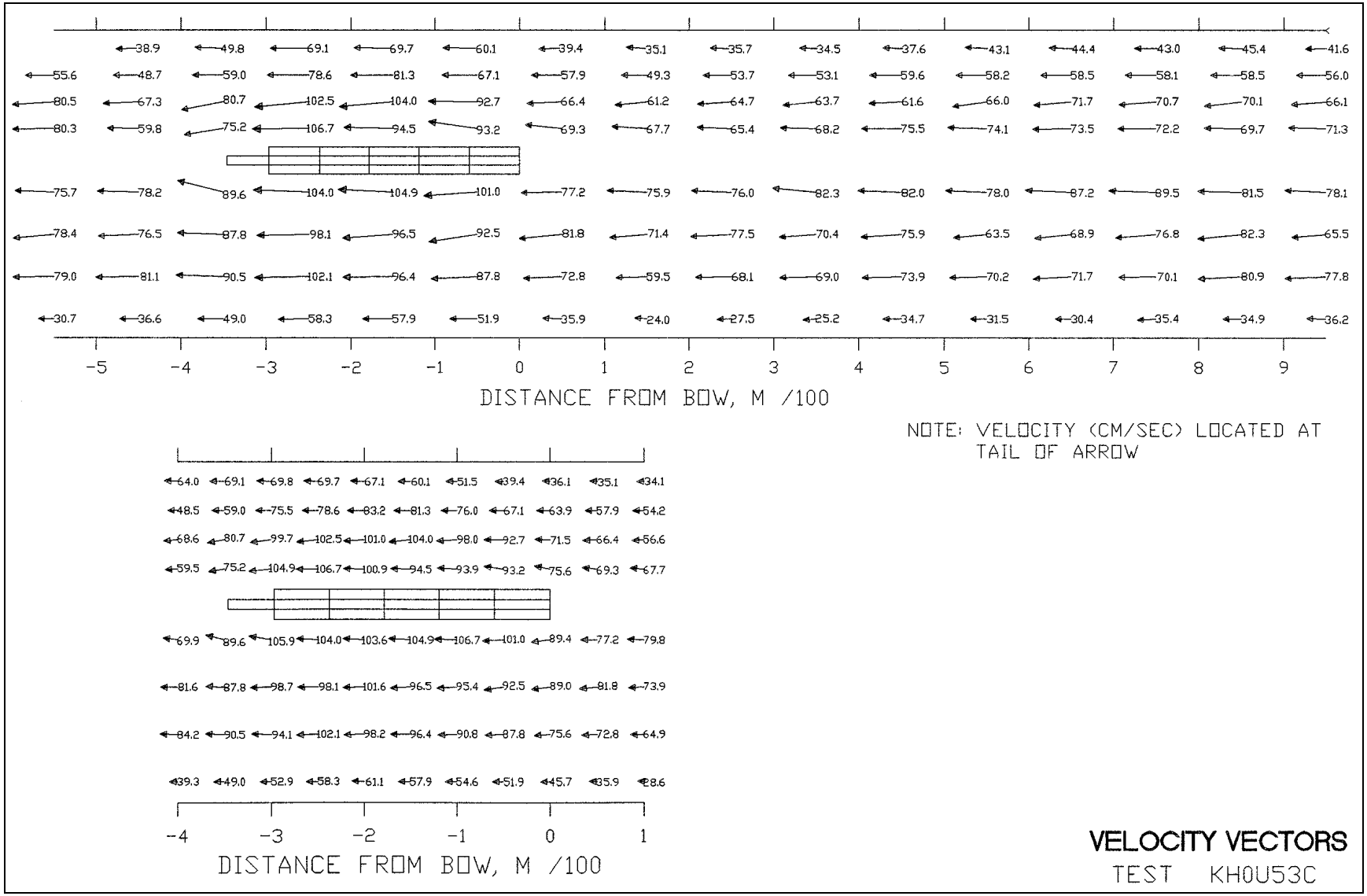

Figure 63. Velocity vectors, experiment KHOU53C

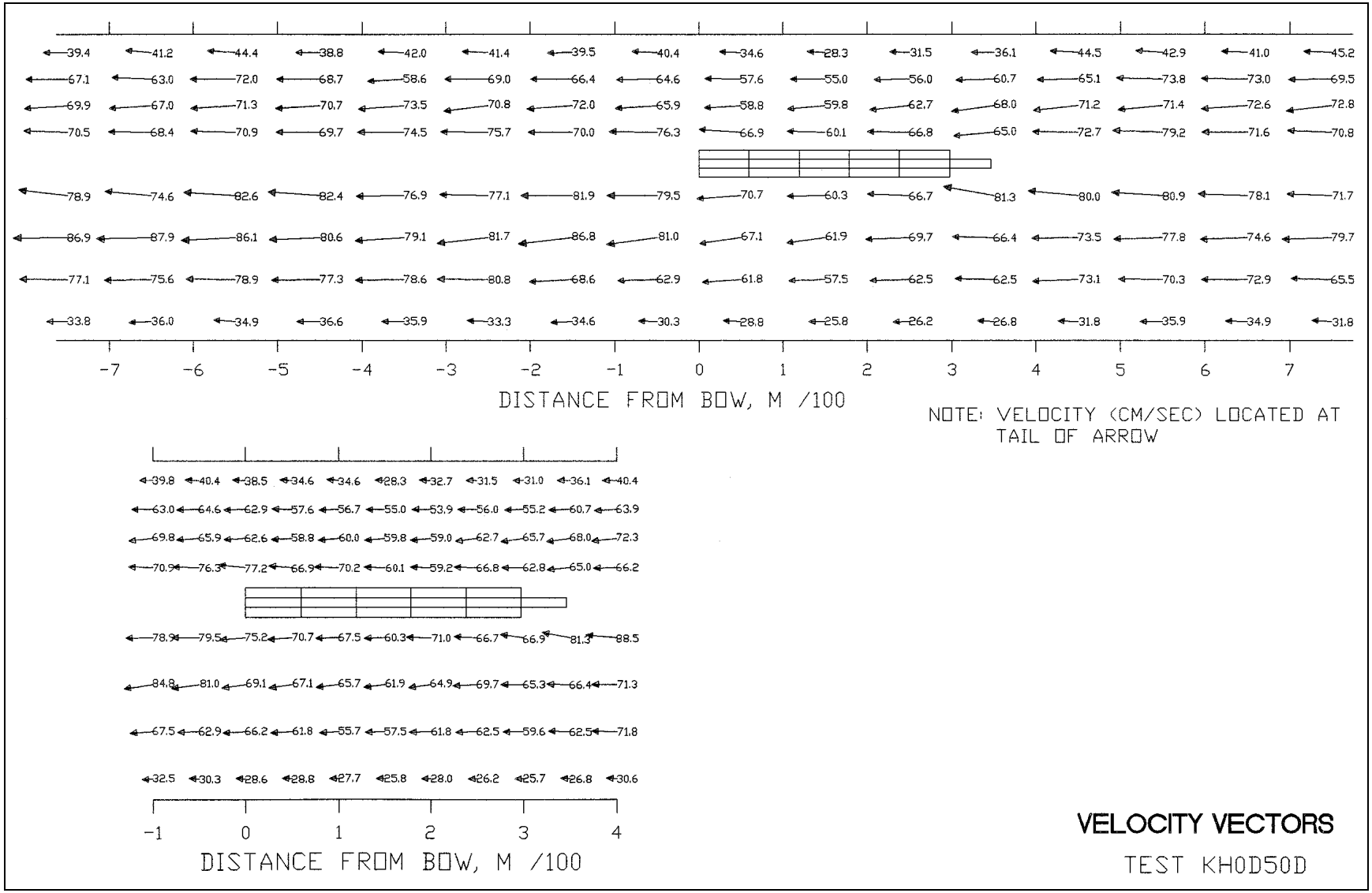

Figure 64. Velocity vectors, experiment KHOD50D

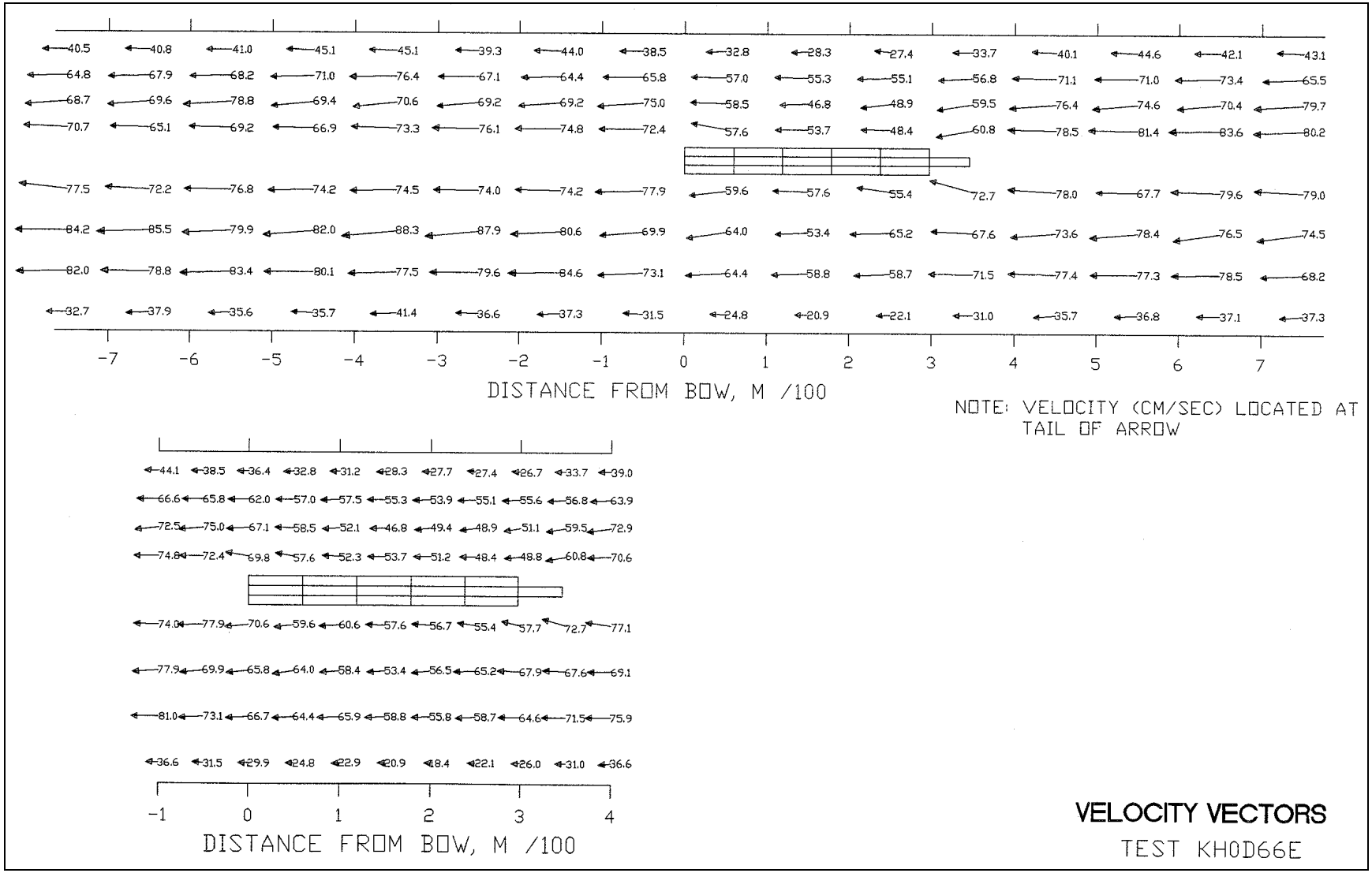

Figure 65. Velocity vectors, experimetn KHOD66E

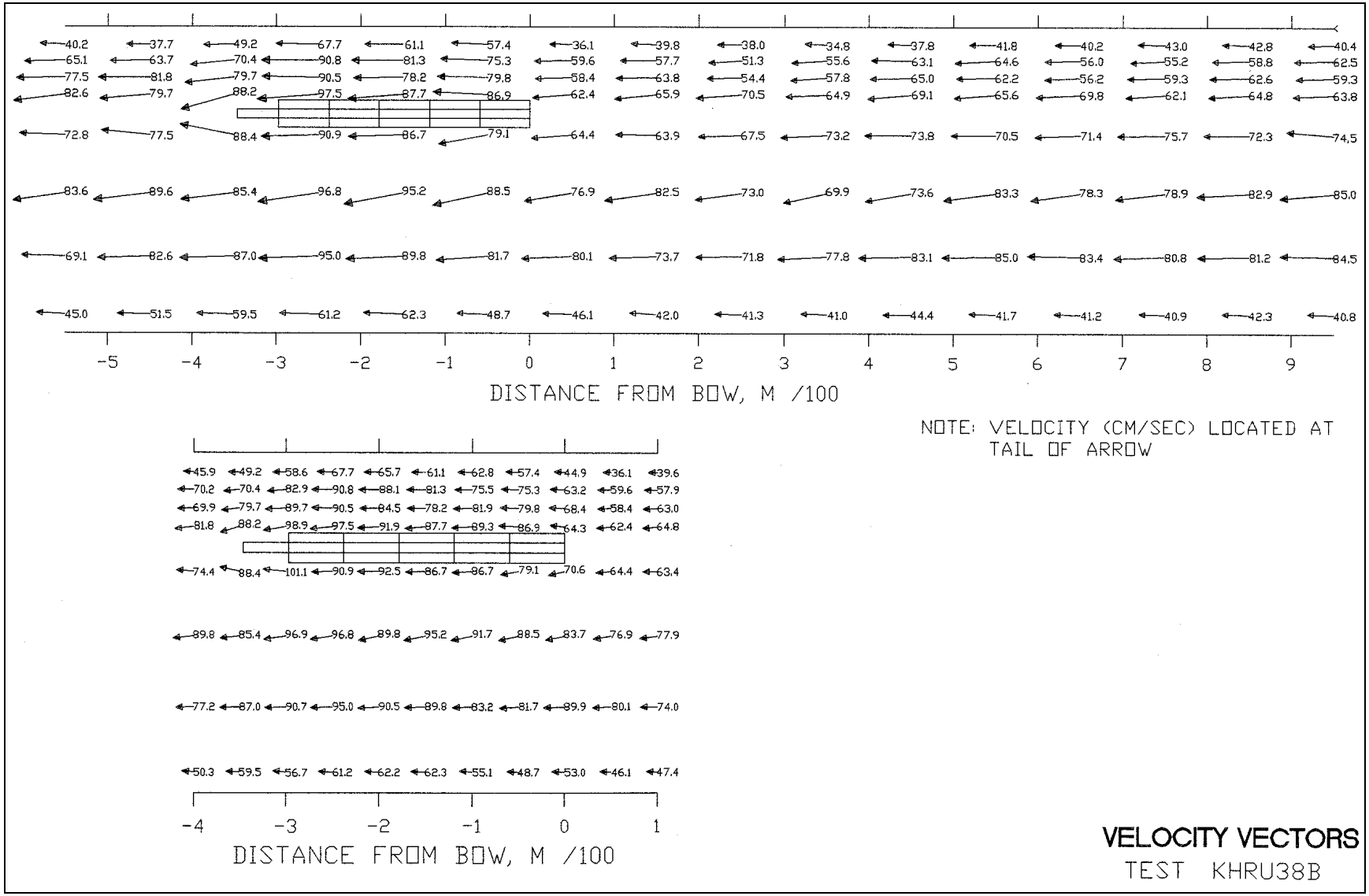

Figure 66. Velocity vectors, experiment KHRU38B

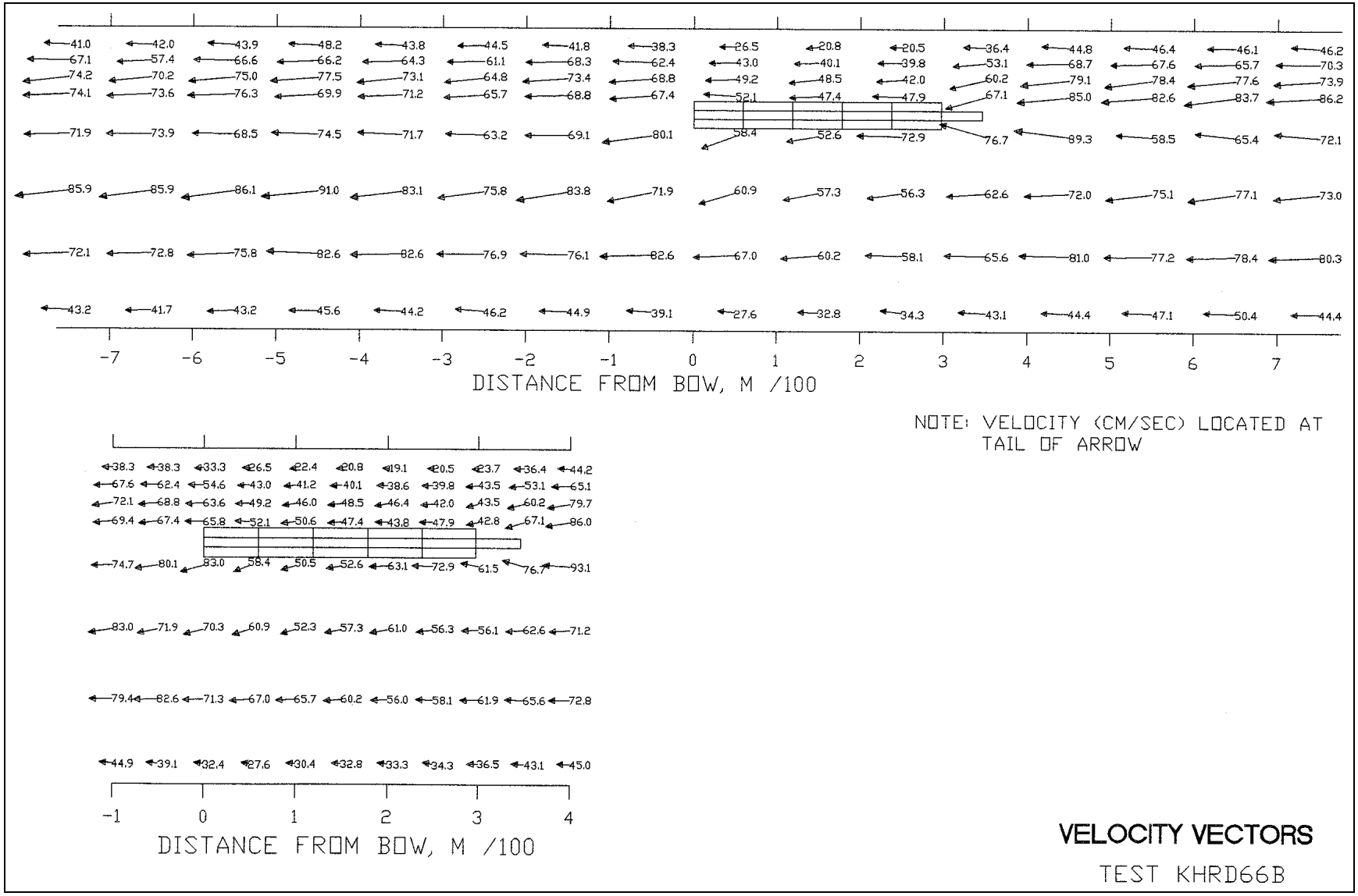

Figure 67. Velocity vectors, experiment KHRD66B

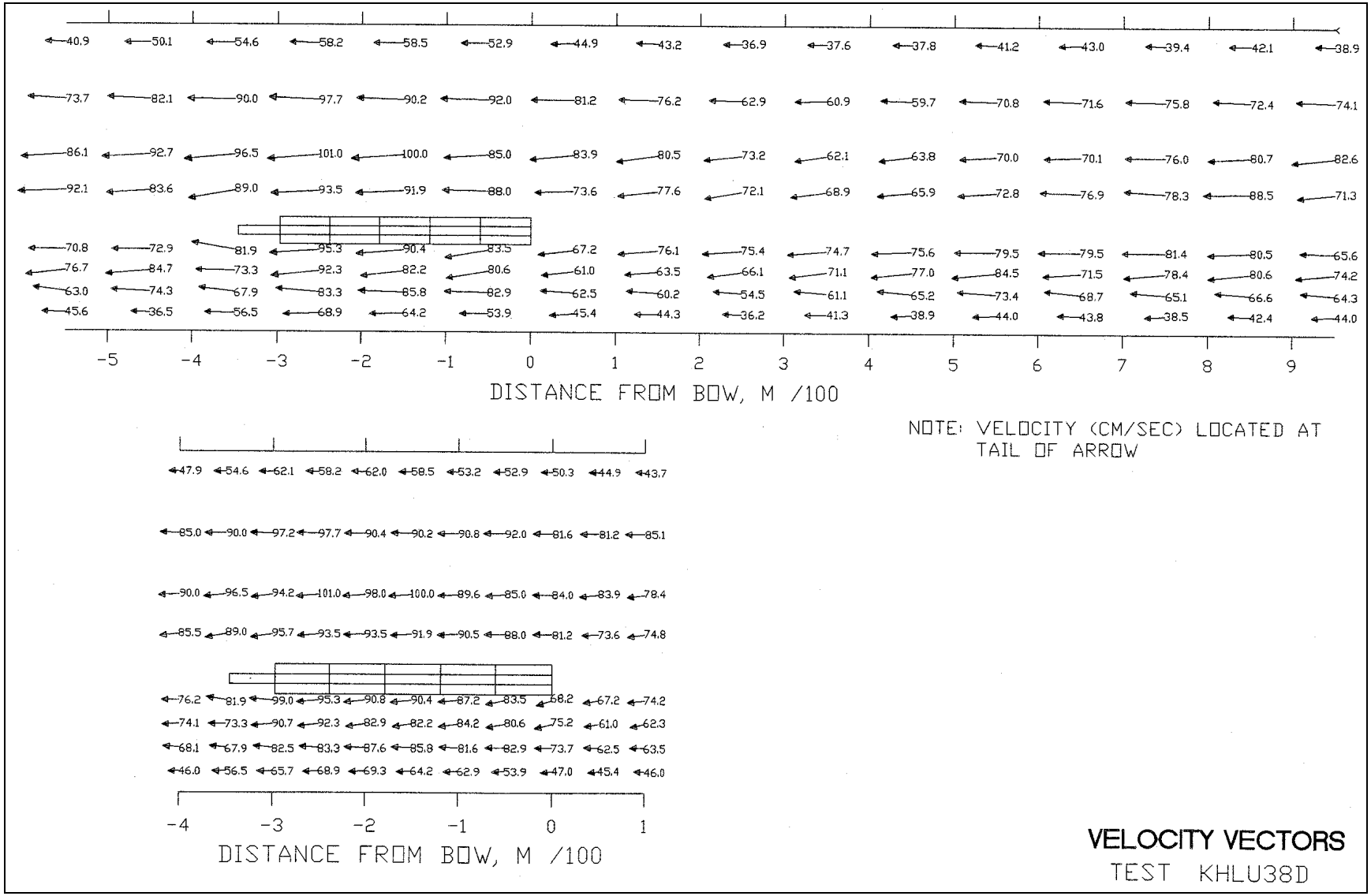

Figure 68. Velocity vectors, experiment KHLU38D

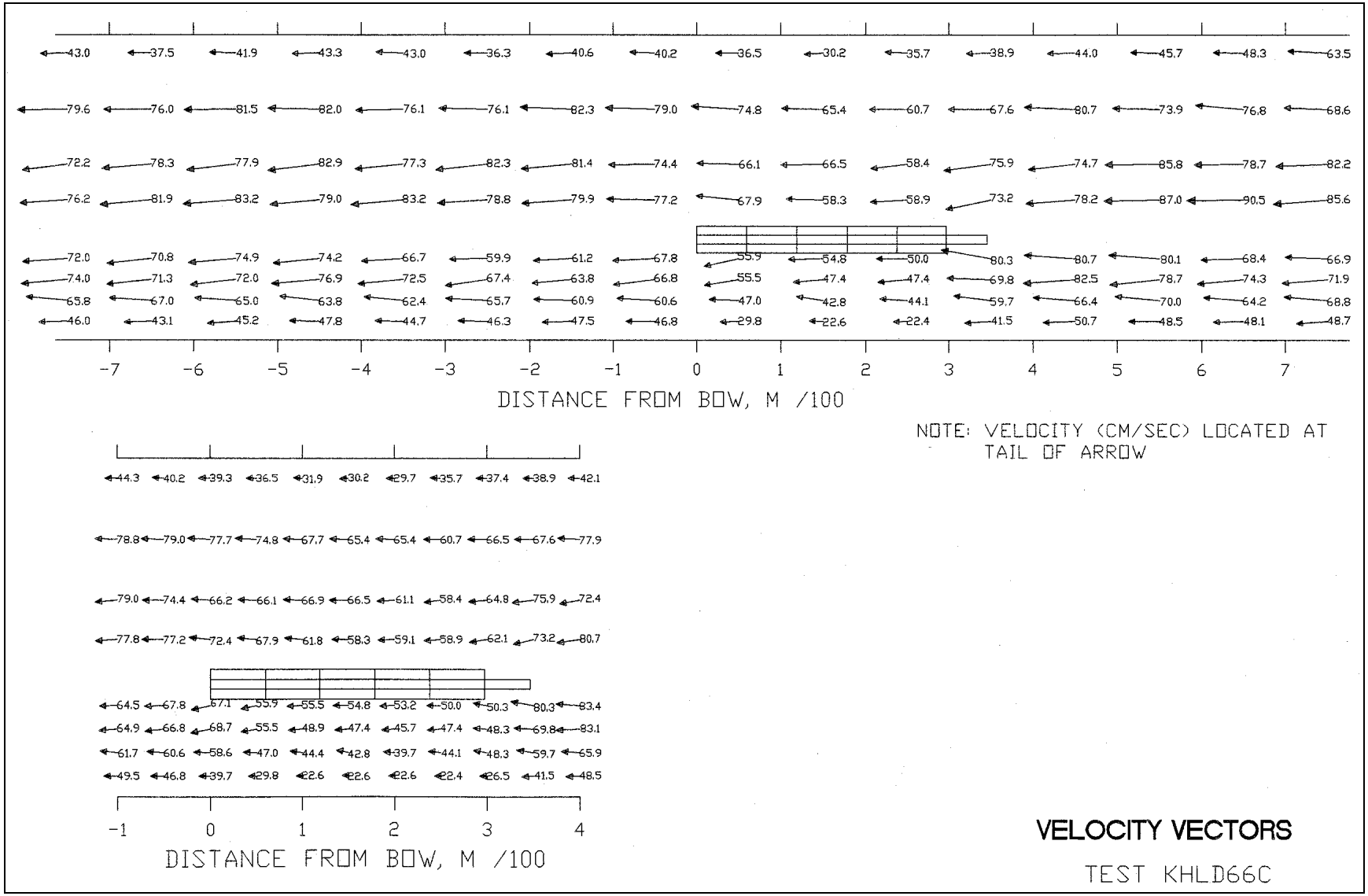

Figure 69. Velocity vectors, experimetn KHLD66C

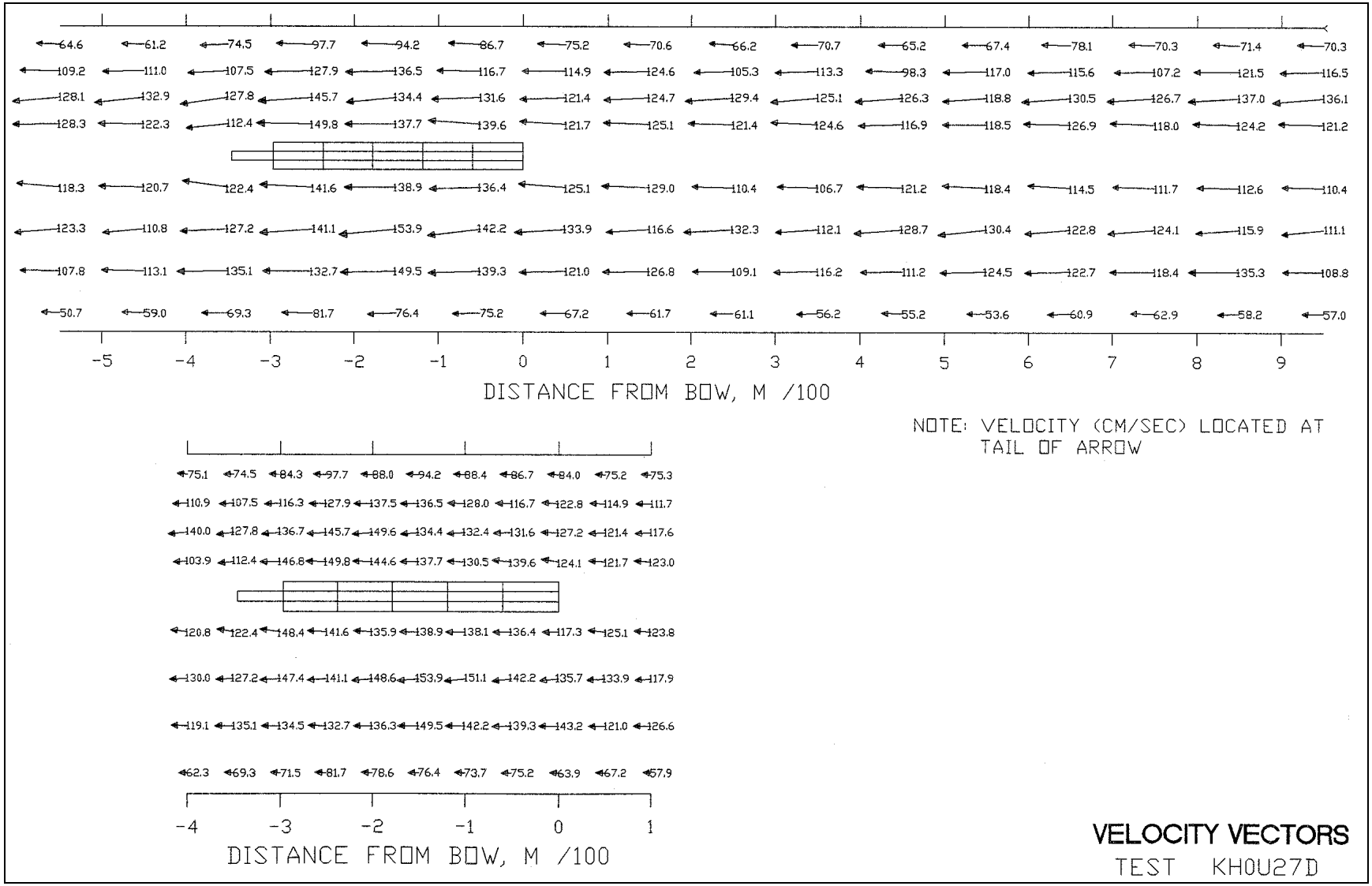

Figure 70. Velocity vectors, experiment KHOU27D

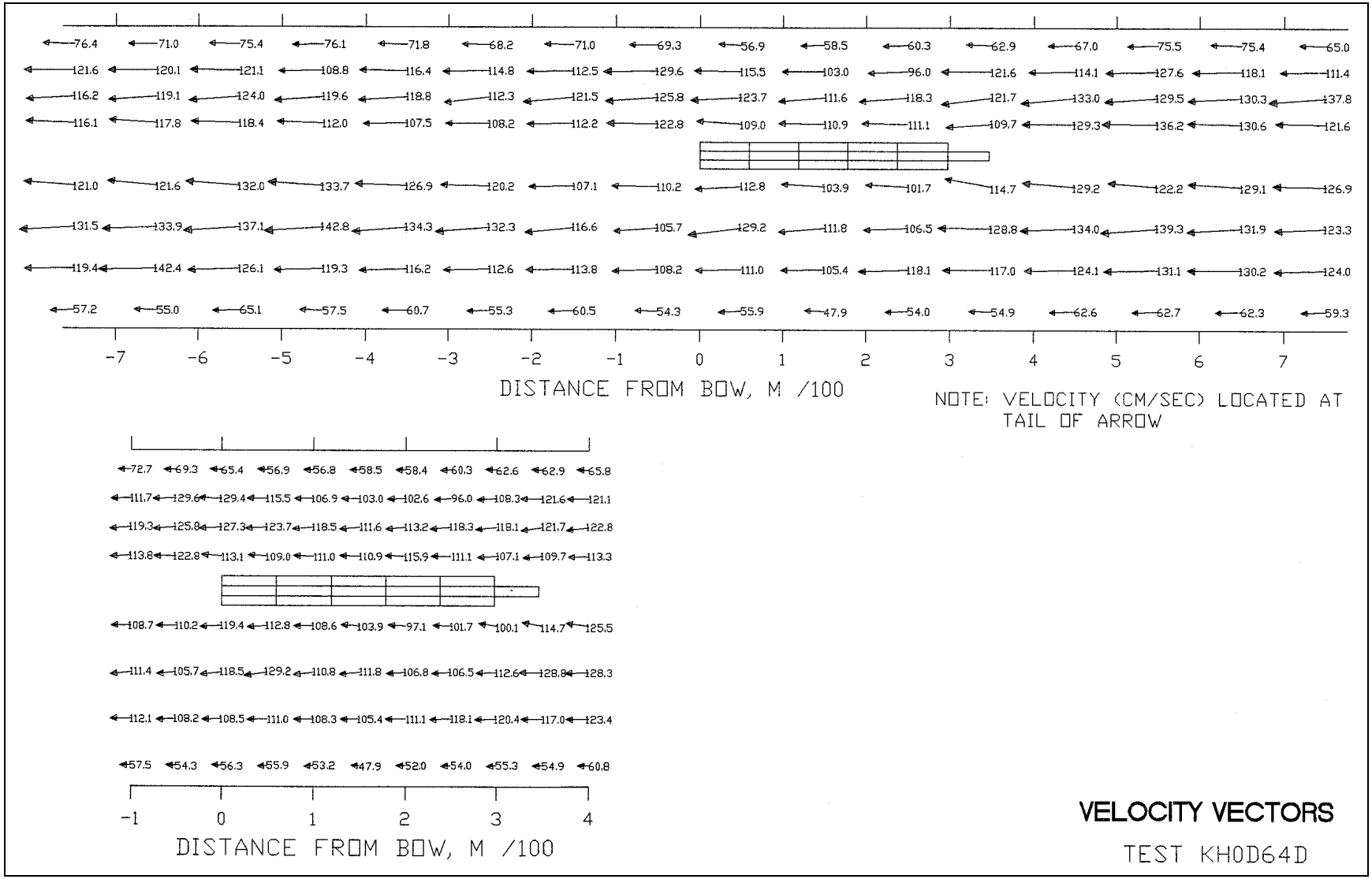

Figure 71. Velocity vectors, experiment KHOD64D

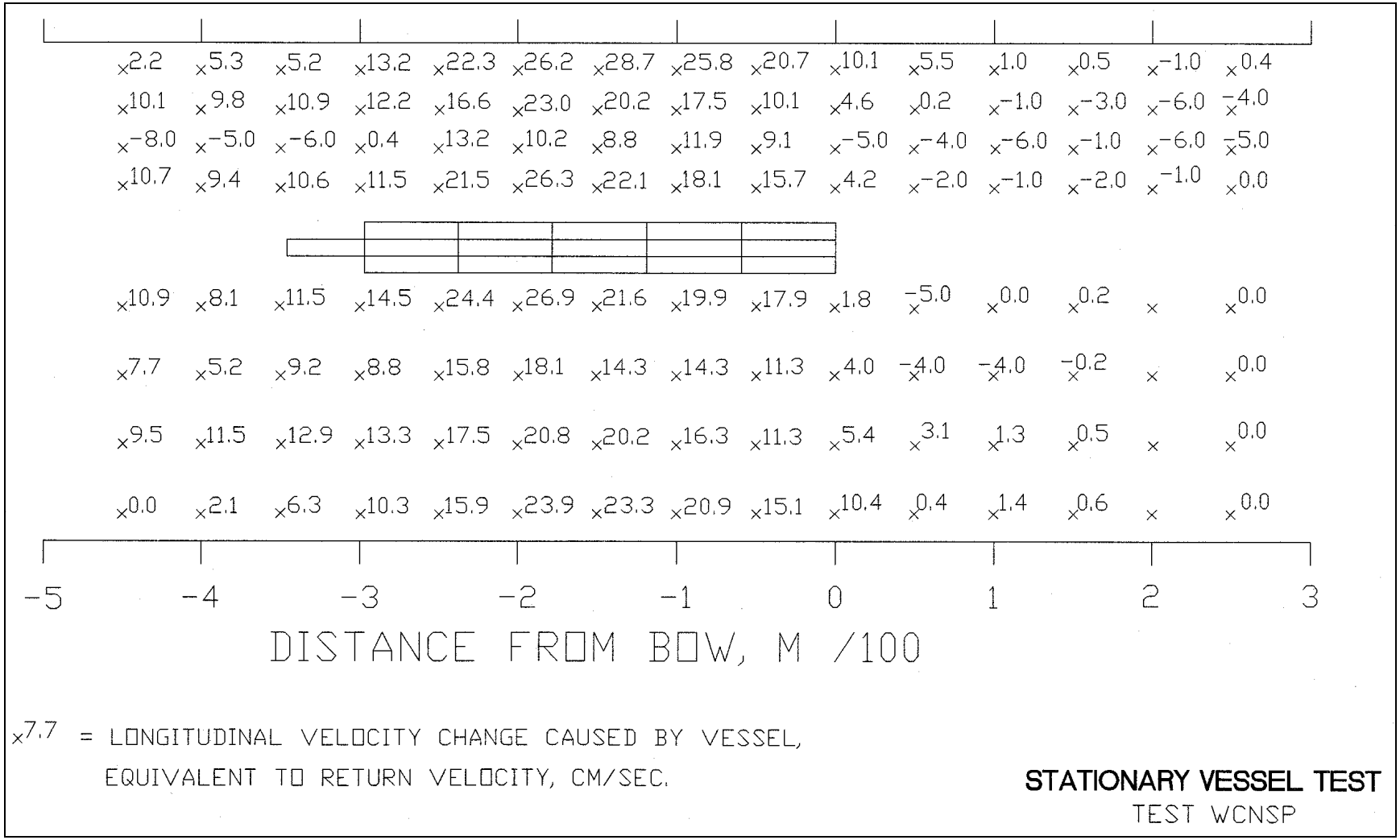

Figure 72. Stationary vessel test, experiment WCNSP

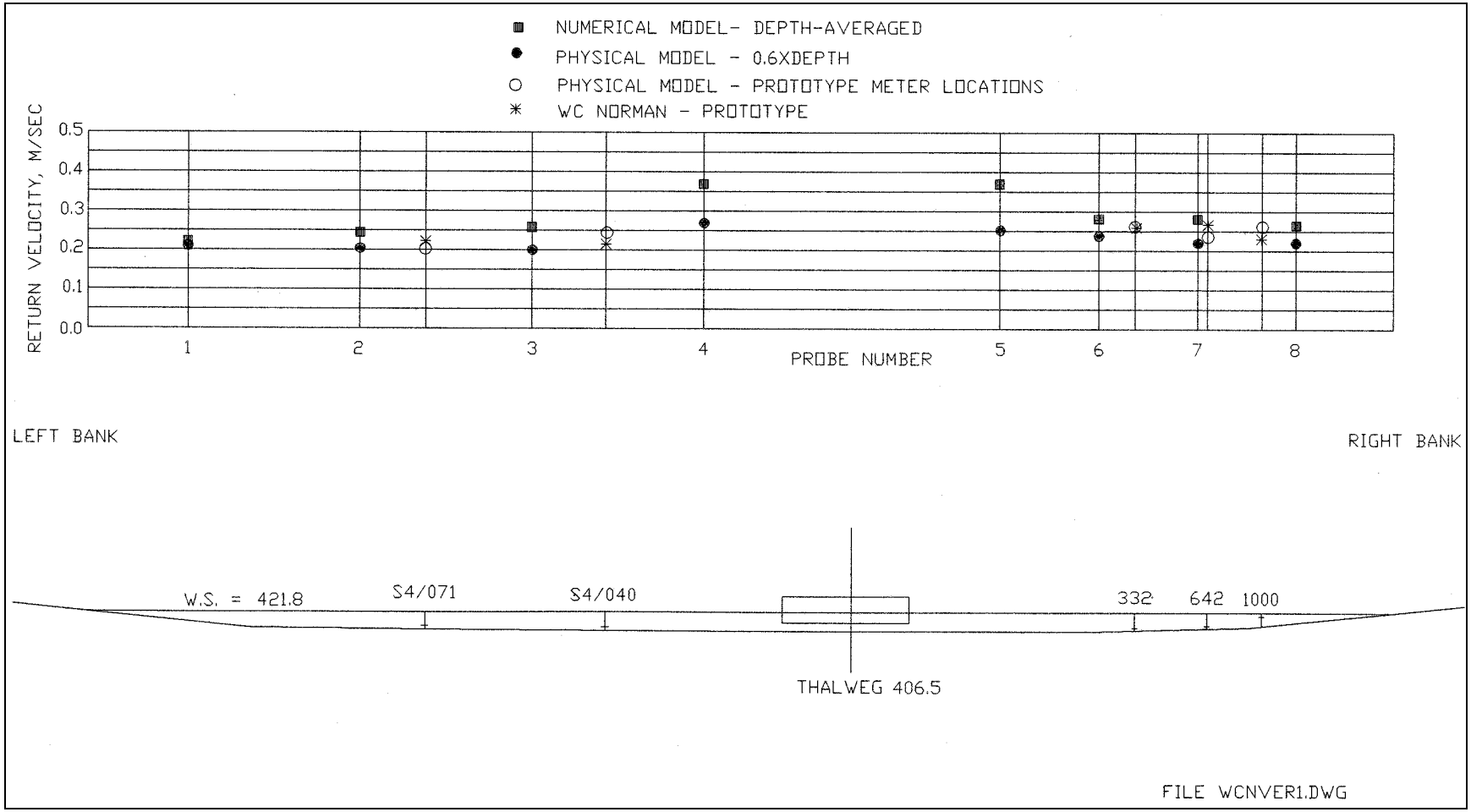

Figure 73. Return velocities for physical model, numerical model, and prototype for *William C. Norman*

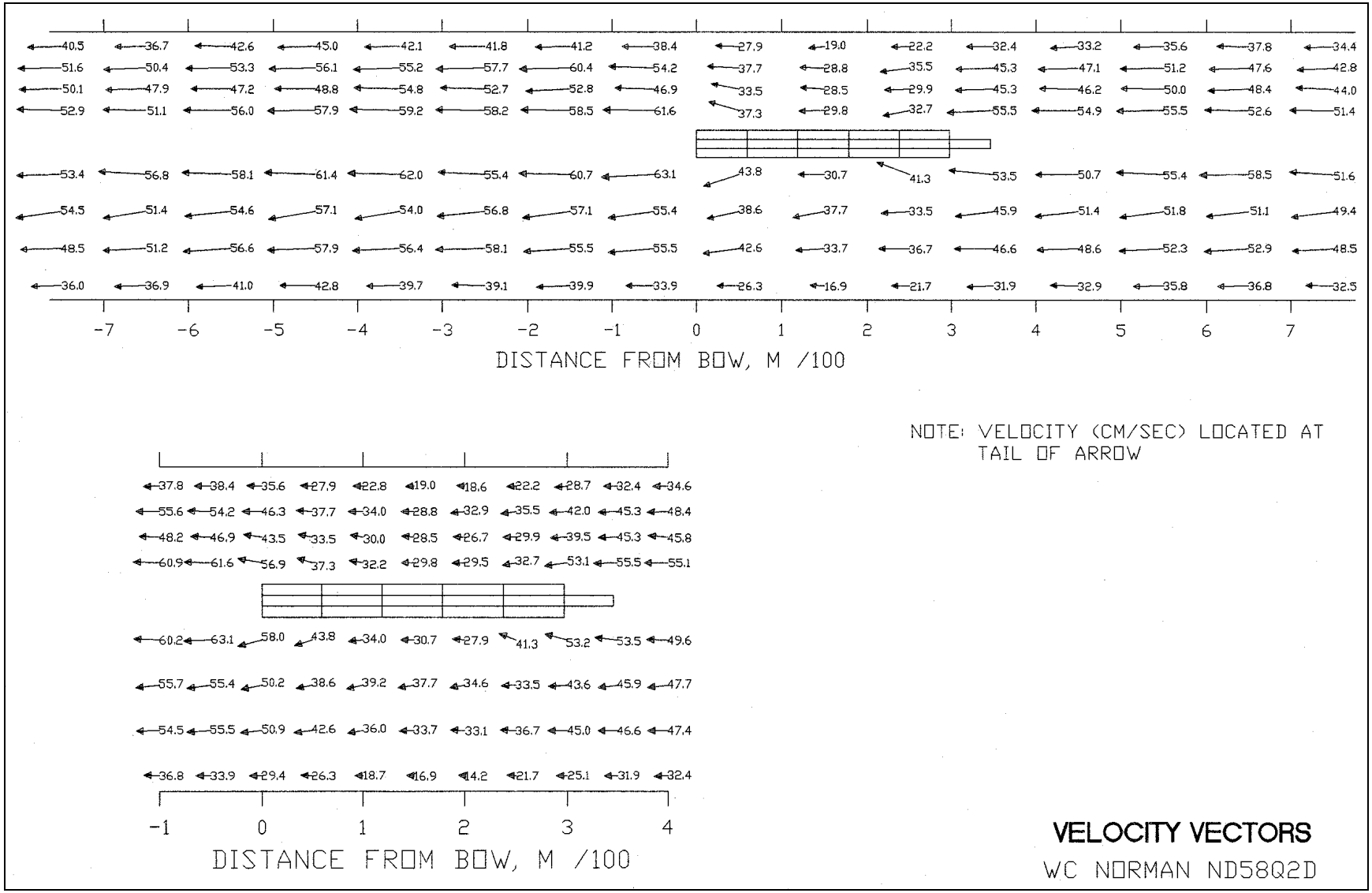

Figure 74. Velocity vectors, *William C. Norman* ND58Q2D

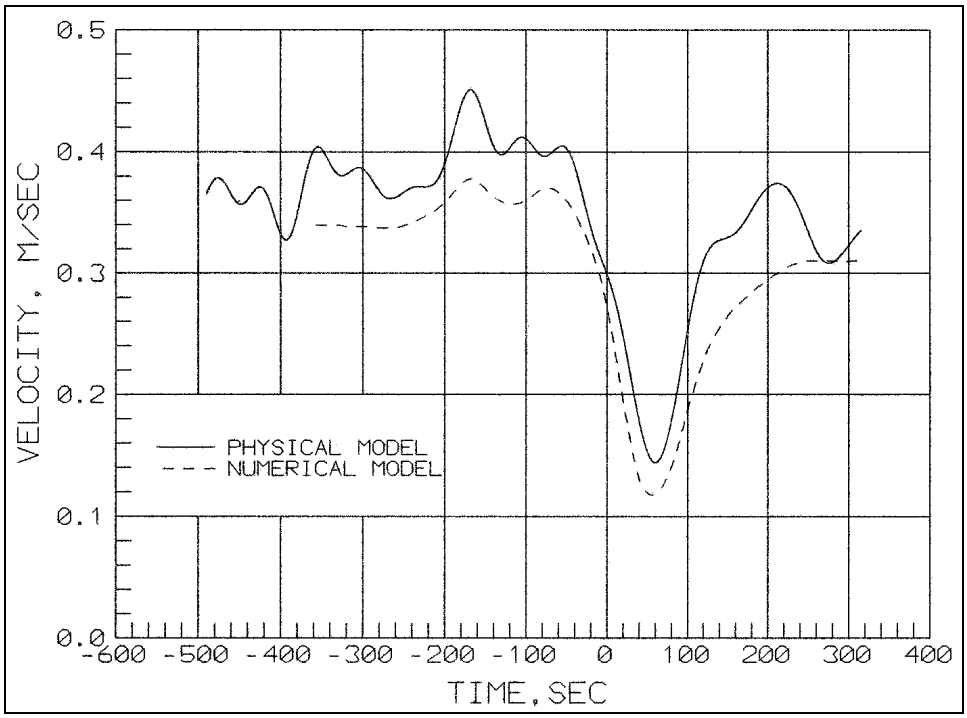

Figure 75. Physical model versus numerical model, probe 1, 168.8 m left of Thalweg

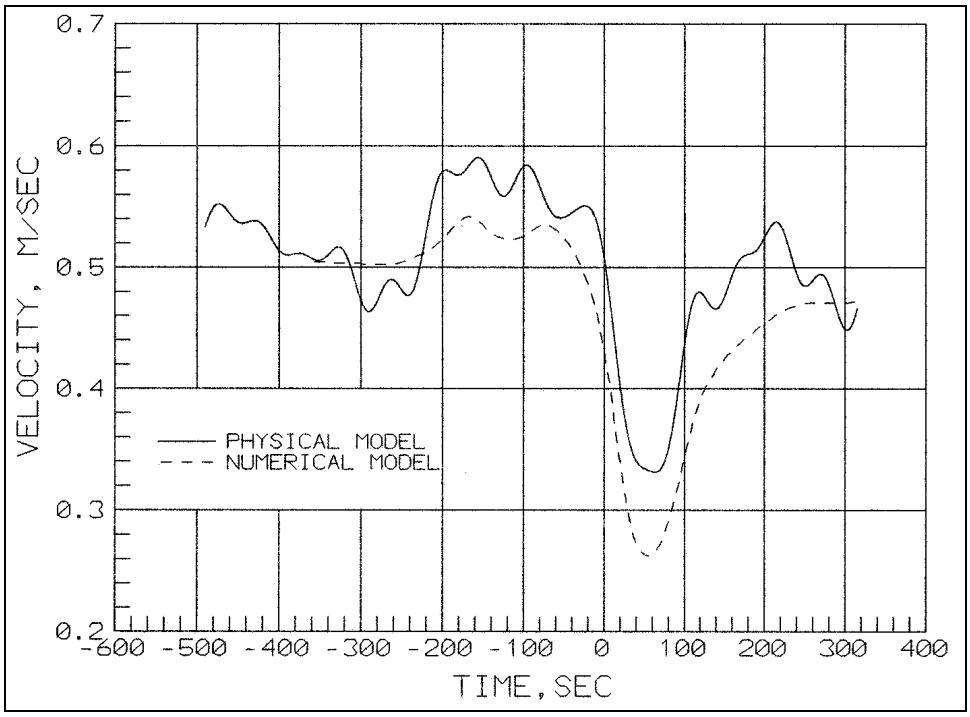

Figure 76. Physical model versus numerical model, probe 2, 125.0 m left of thalweg

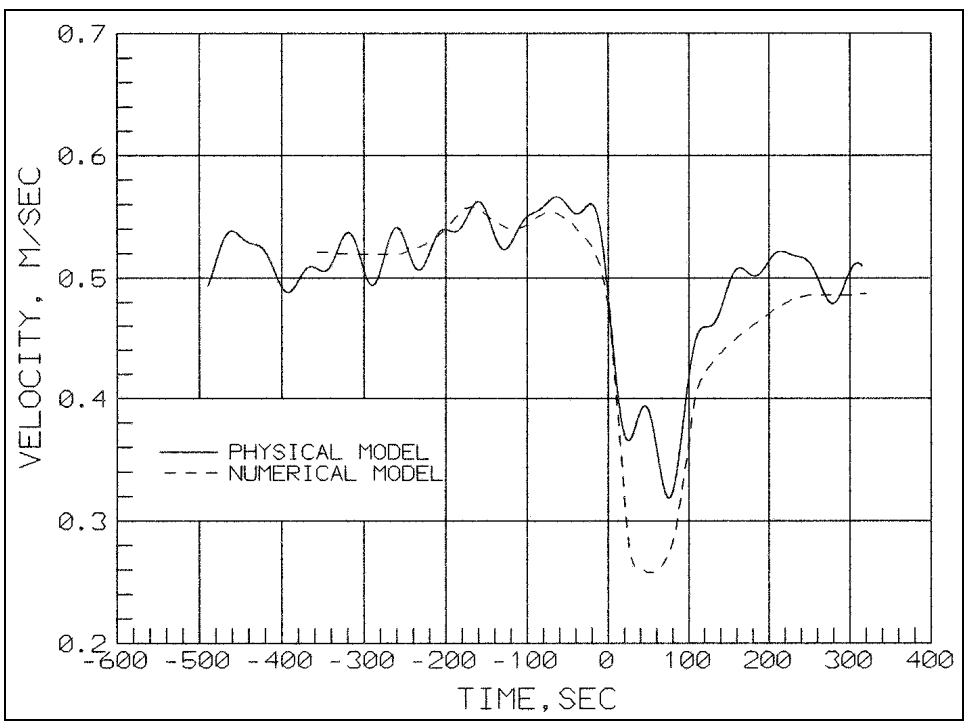

Figure 77. Physical model versus numerical model, probe 3, 81.3 m left of thalweg

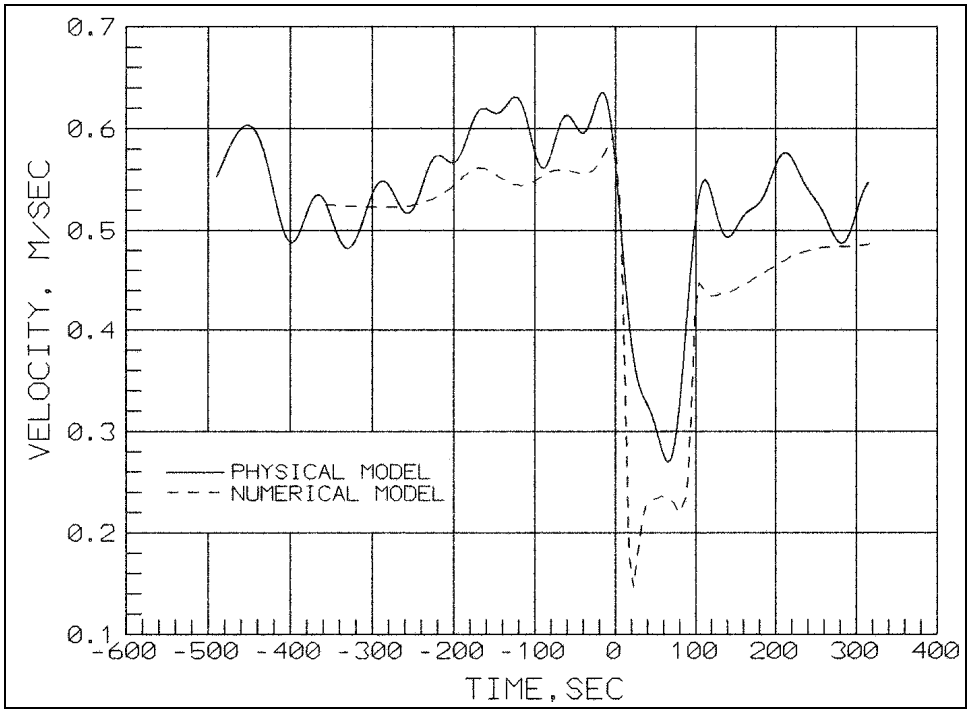

Figure 78. Physical model versus numerical model, probe 4, 37.5 m left of Thalweg

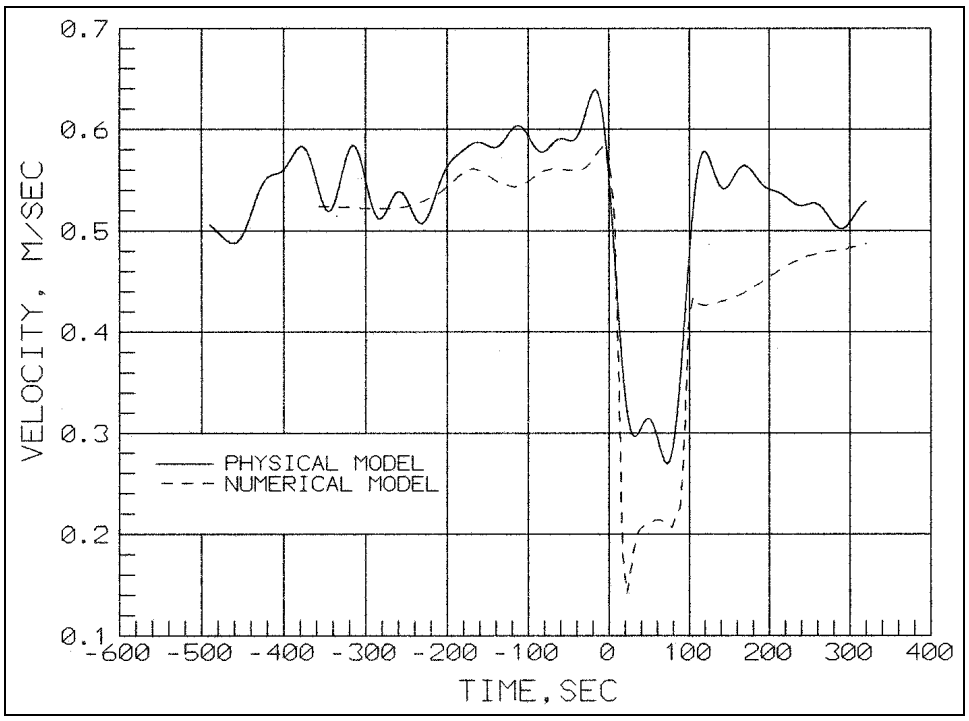

Figure 79. Physical model versus numerical model, probe 5, 37.5 m right of thalweg

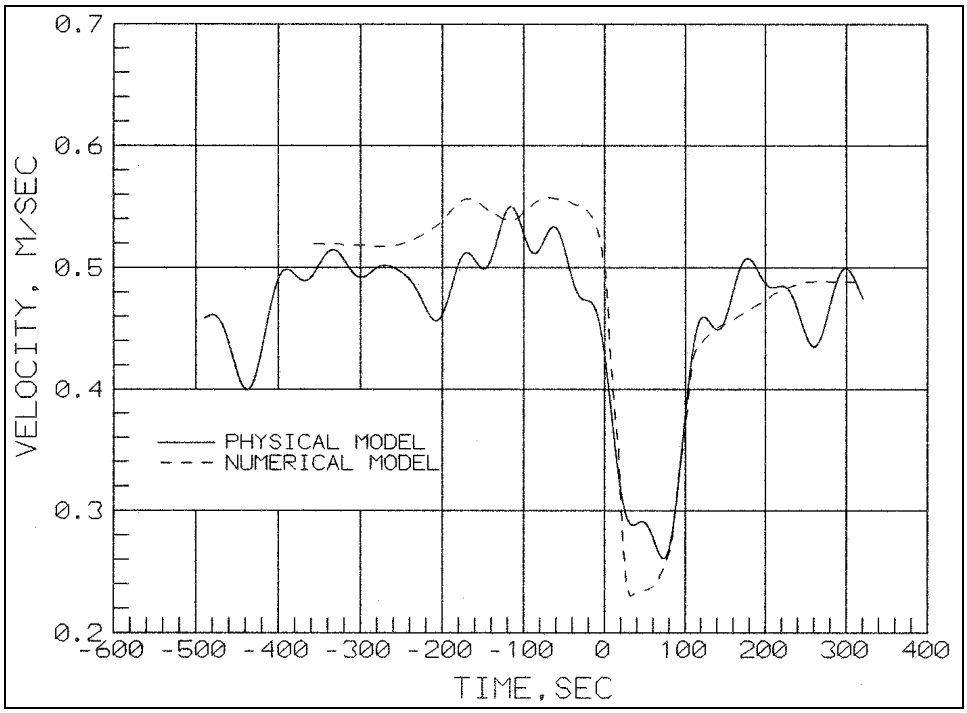

Figure 80. Physical model versus numerical model, probe 6, 62.5 m right of thalweg

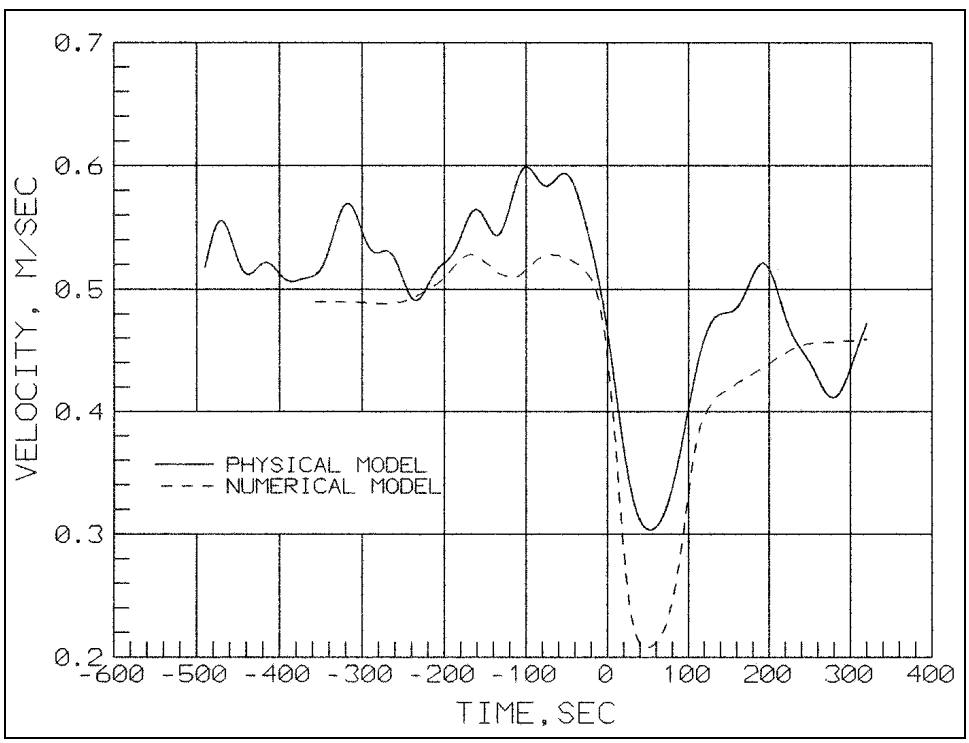

Figure 81. Physical model versus numerical model, probe 7, 87.5 m right of thalweg

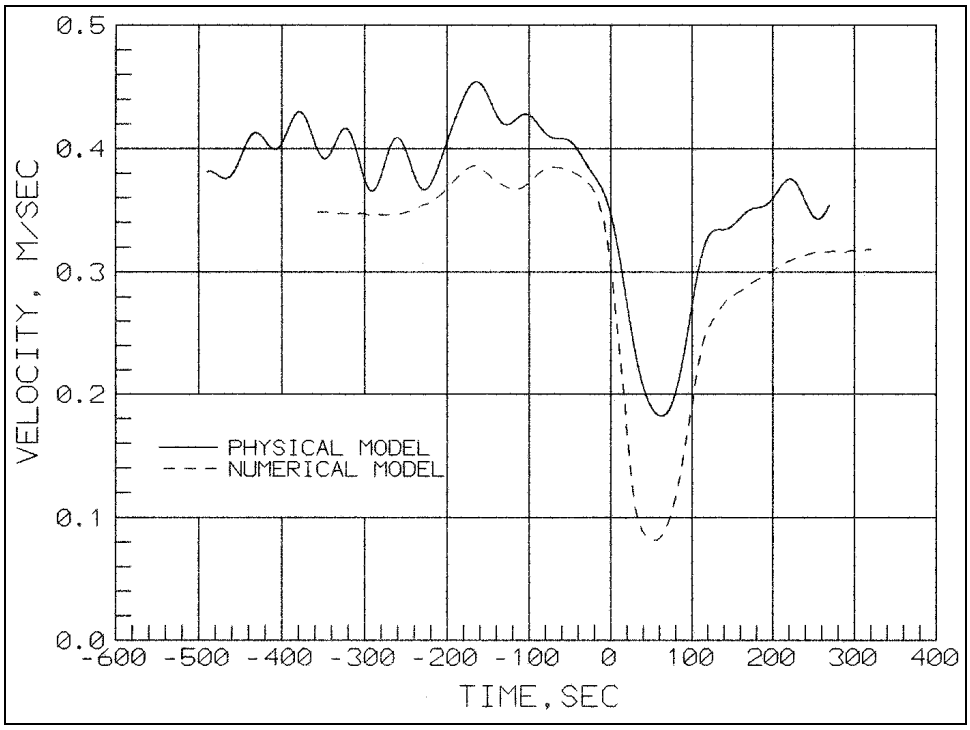

Figure 82. Physical model versus numerical model, probe 8, 112.5 m right of thalweg

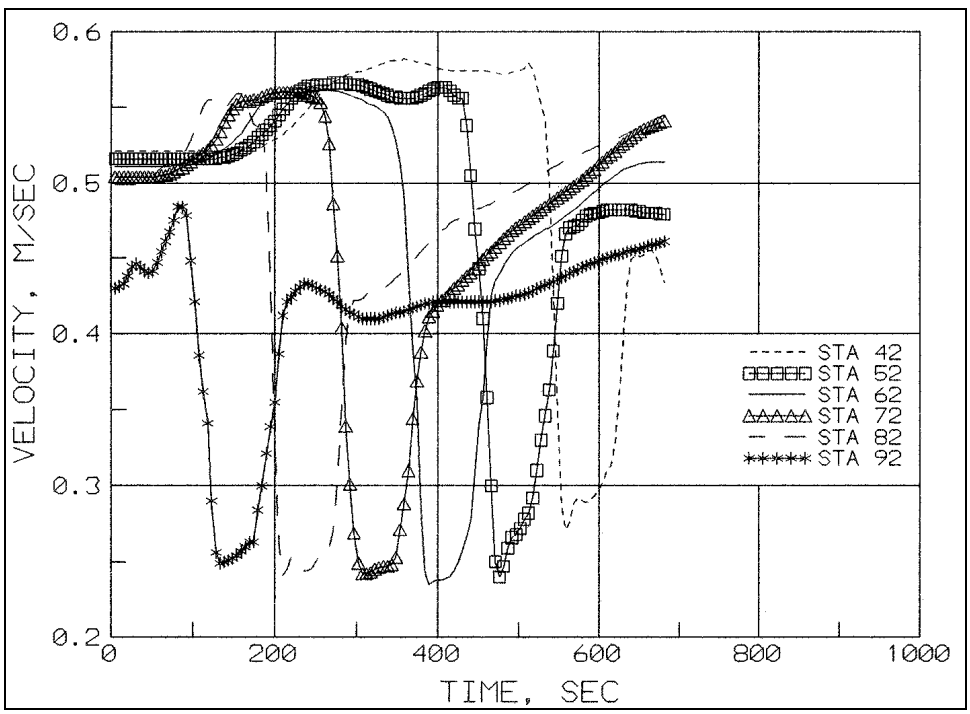

Figure 83. Variation of vessel effects along length of physical model, downbound tow, based on probe 6 of numerical model

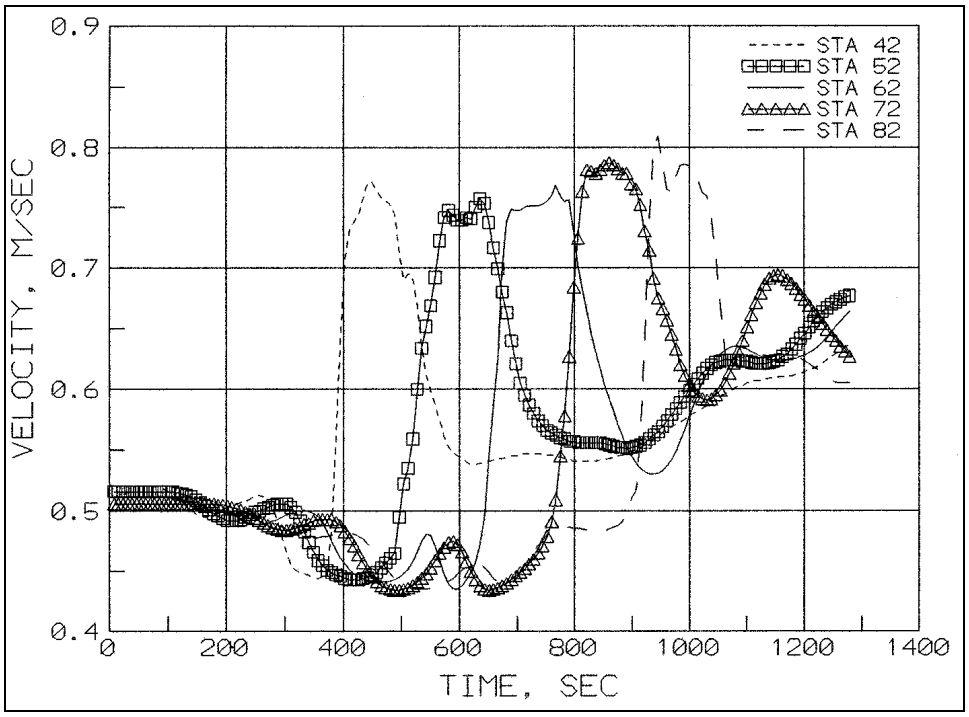

Figure 84. Variation of vessel effects along length of physical model, upbound tow, based on probe 6 of numerical model

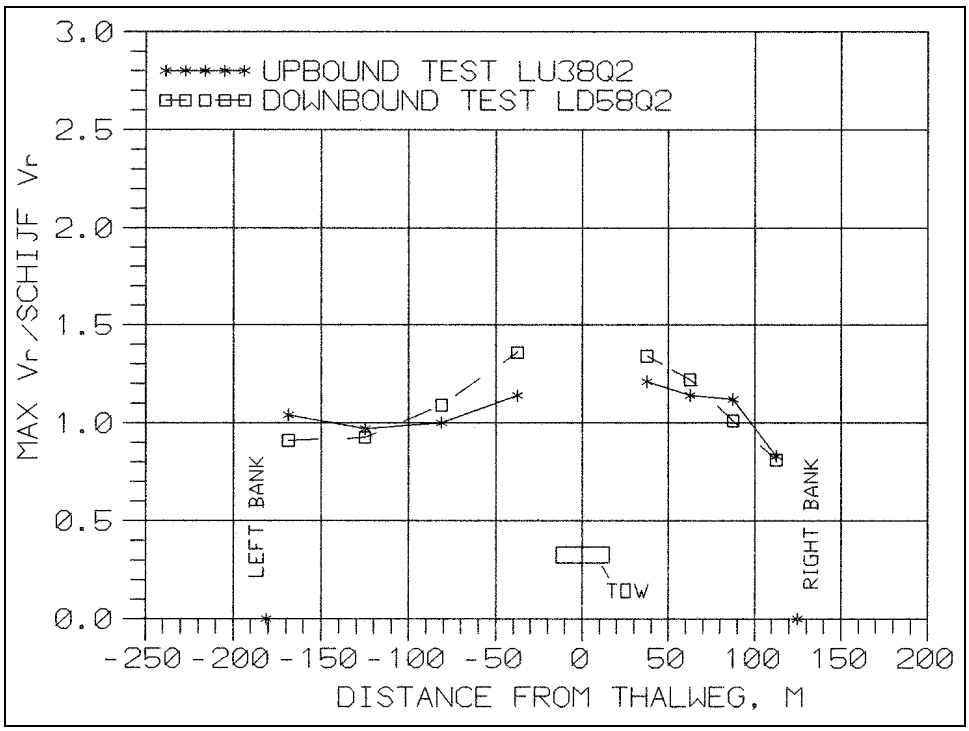

Figure 85. Dimensionless return velocity, experiments LU38Q2 and LD58Q2

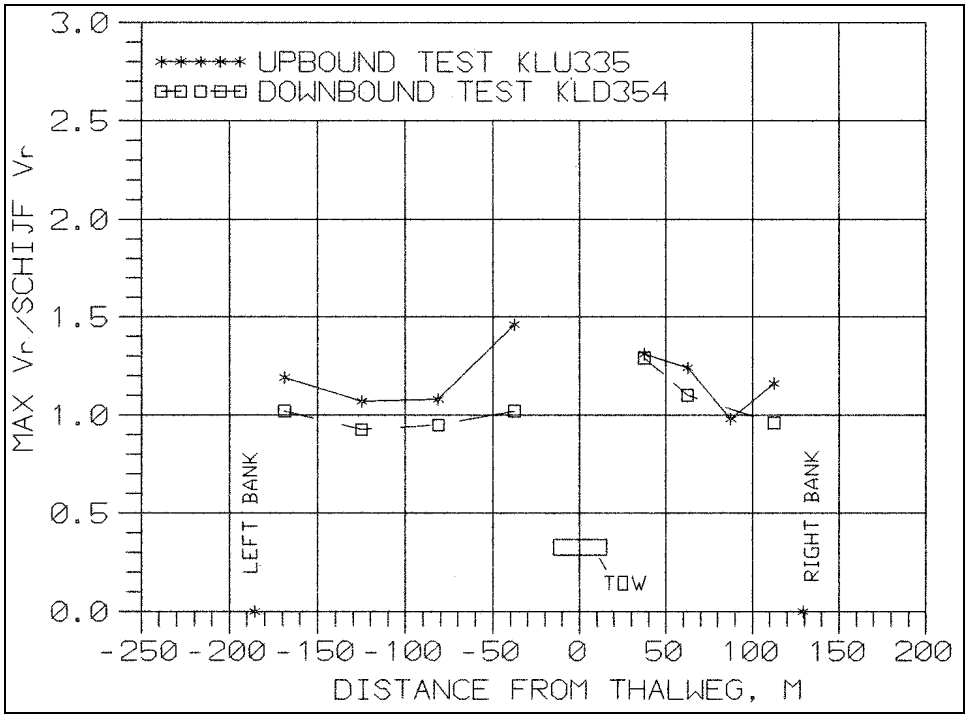

Figure 86. Dimensionless return velocity, experiments DKU335 and KLD354

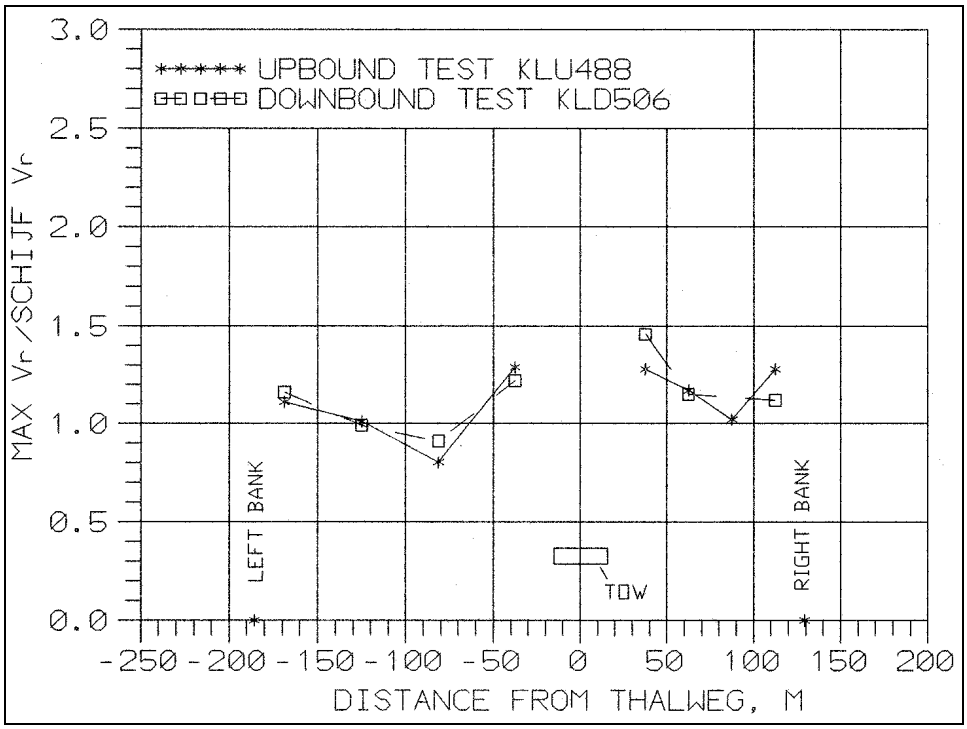

Figure 87. Dimensionless return velocity, experiments KLU488 and KLD506

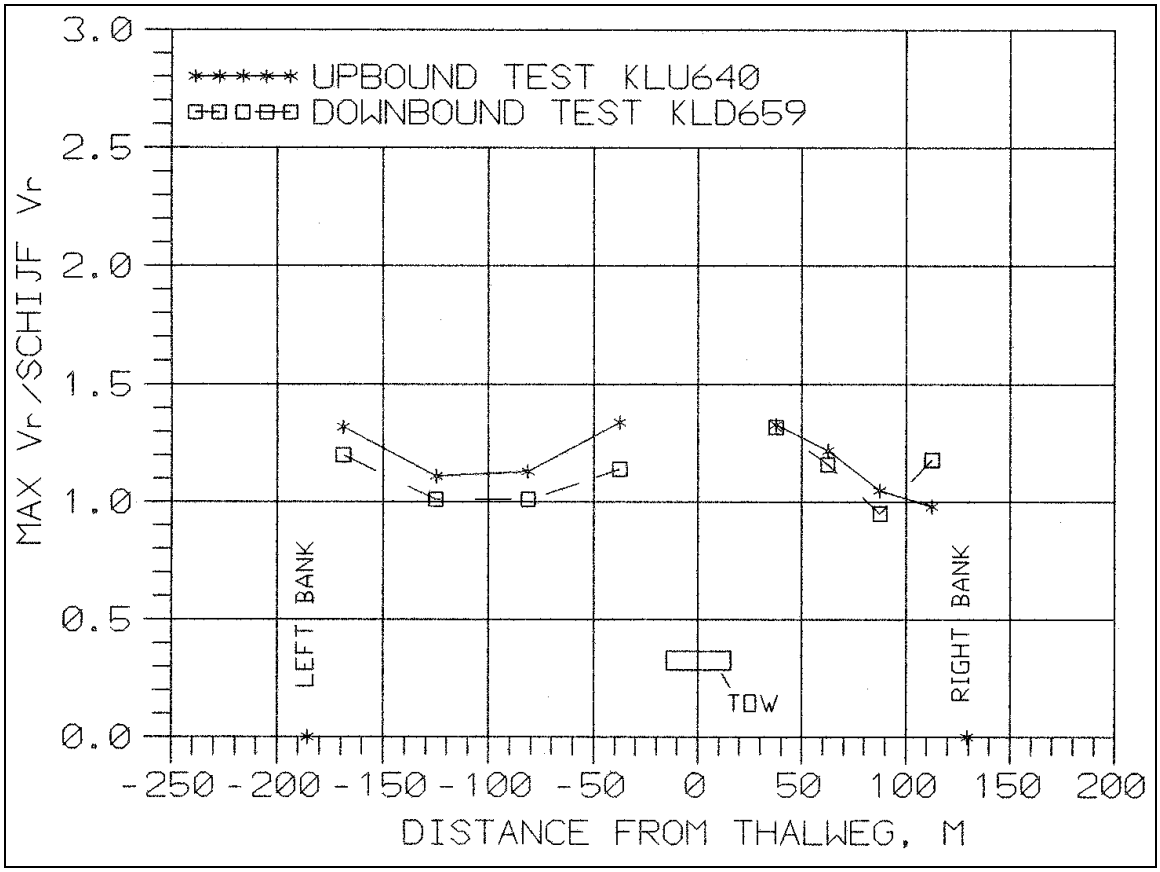

Figure 88. Dimensionless return velocity, experiments KLU640 and KLD659

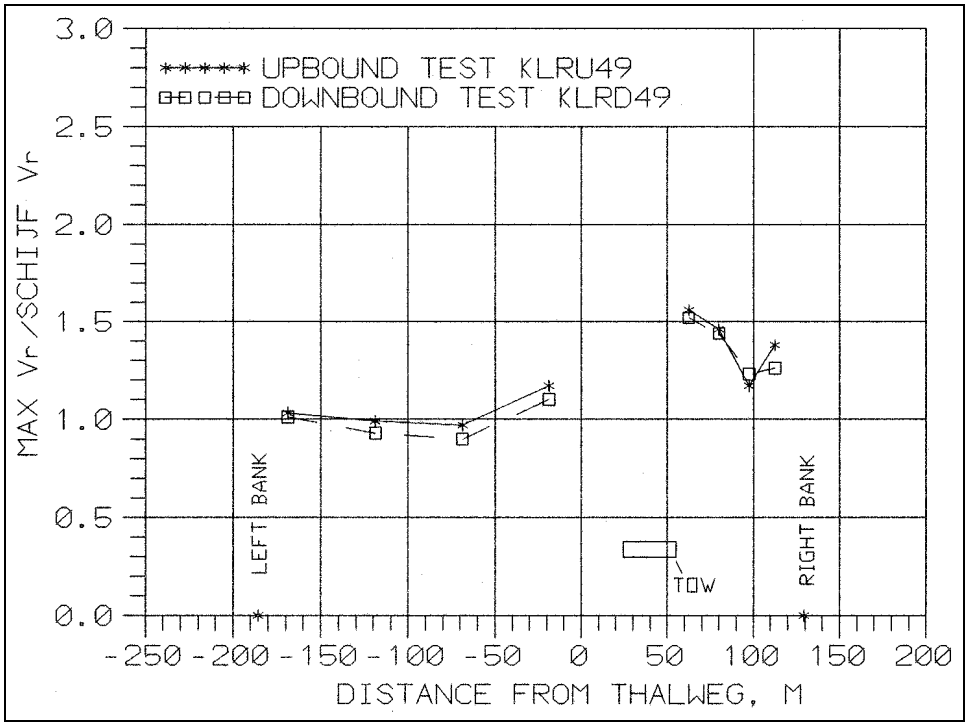

Figure 89. Dimensionless return velodity, experiments KLRU49 and KLRD49

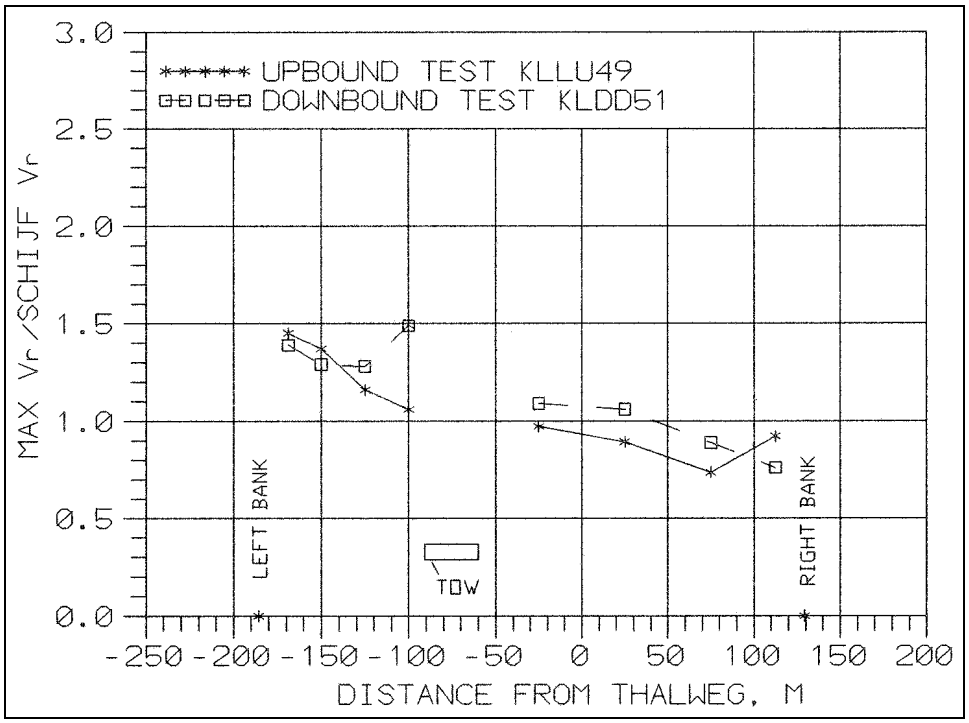

Figure 90. Dimensionless return velocity, experiments KLLU49 and KLDD51

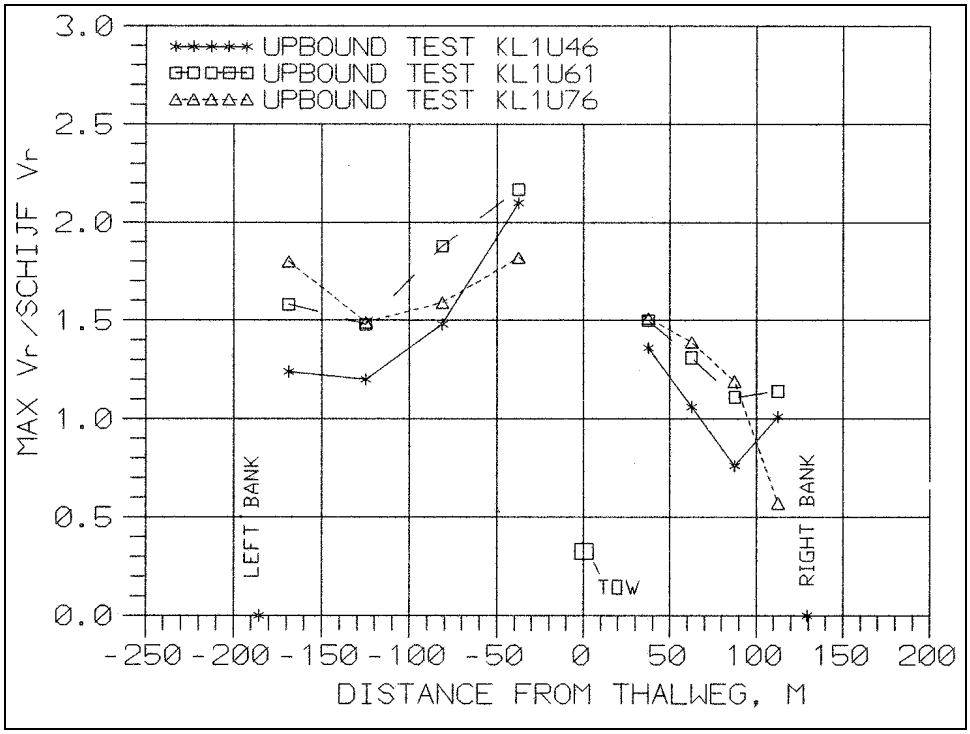

Figure 91. Dimensionless return velocity, experiments KL1U46, KL1U61, and KL1U76

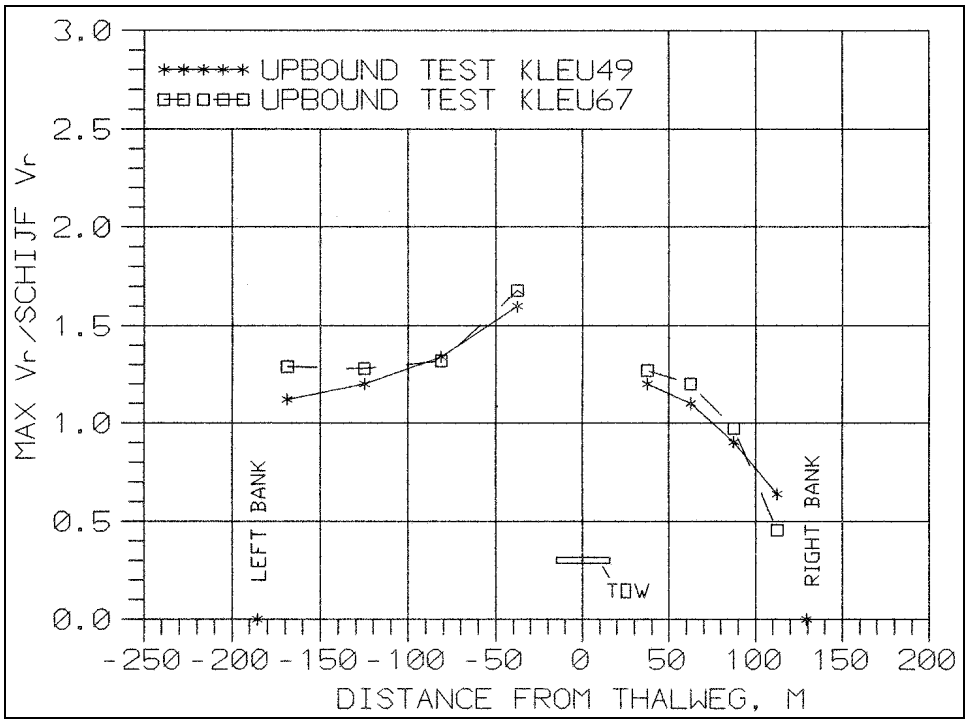

Figure 92. Dimensionless return velocity, experiments KLEU49 and KLEU67

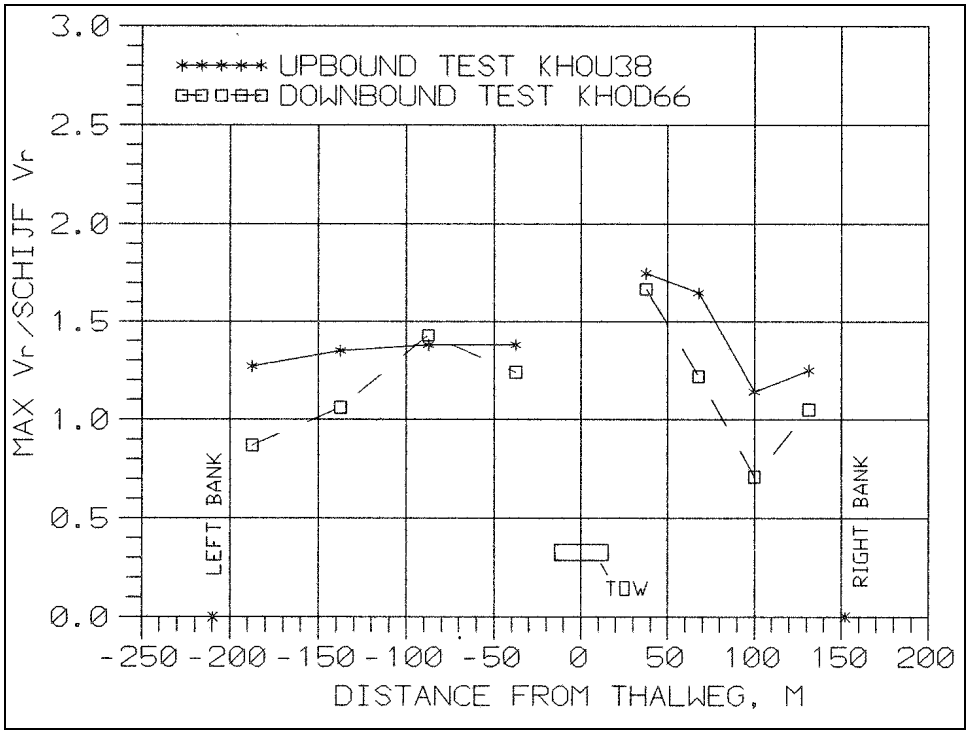

Figure 93. Dimensionless return velocity, experiments KHOU38 and KHOD66

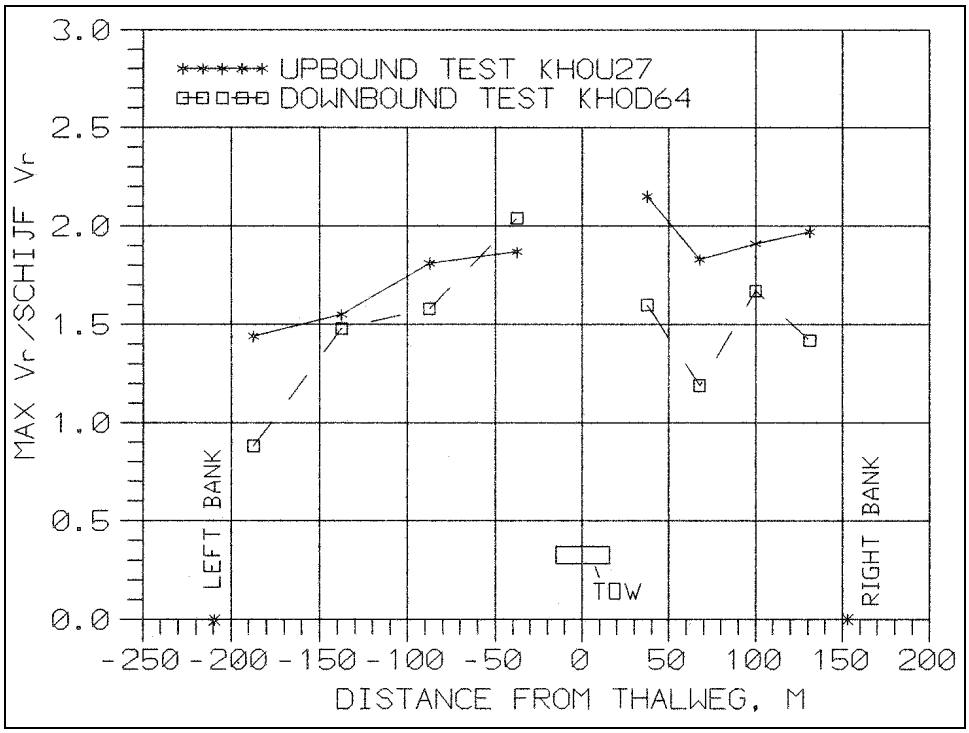

Figure 94. Dimensionless return velocity, experiments KHOU27 and KHOD64

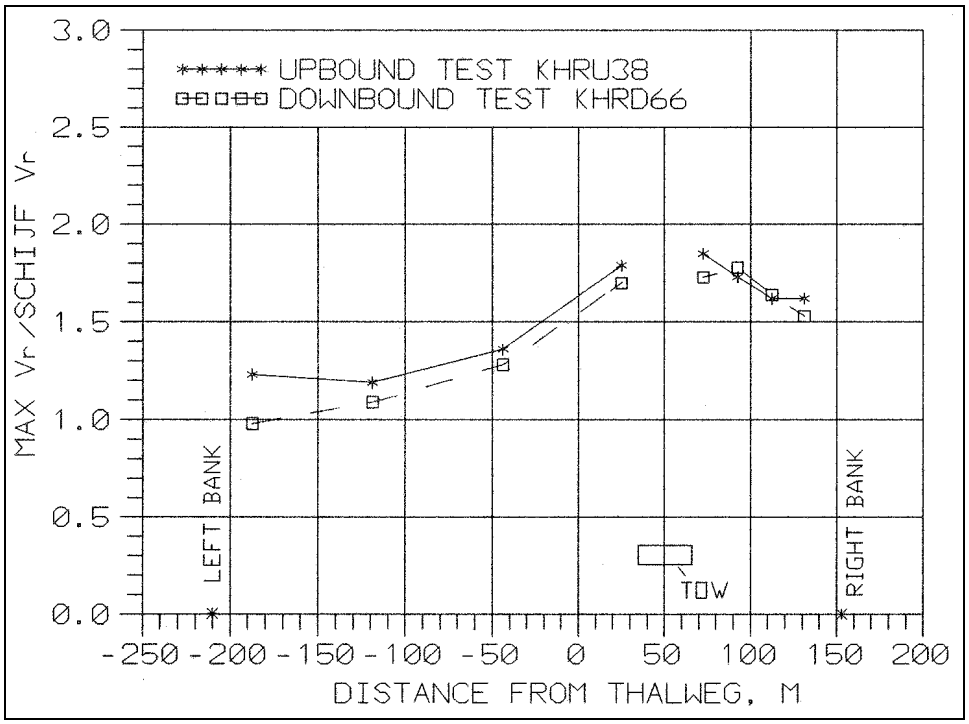

Figure 95. Dimensionless return velocity, experiments KHRU38 and KHRD66

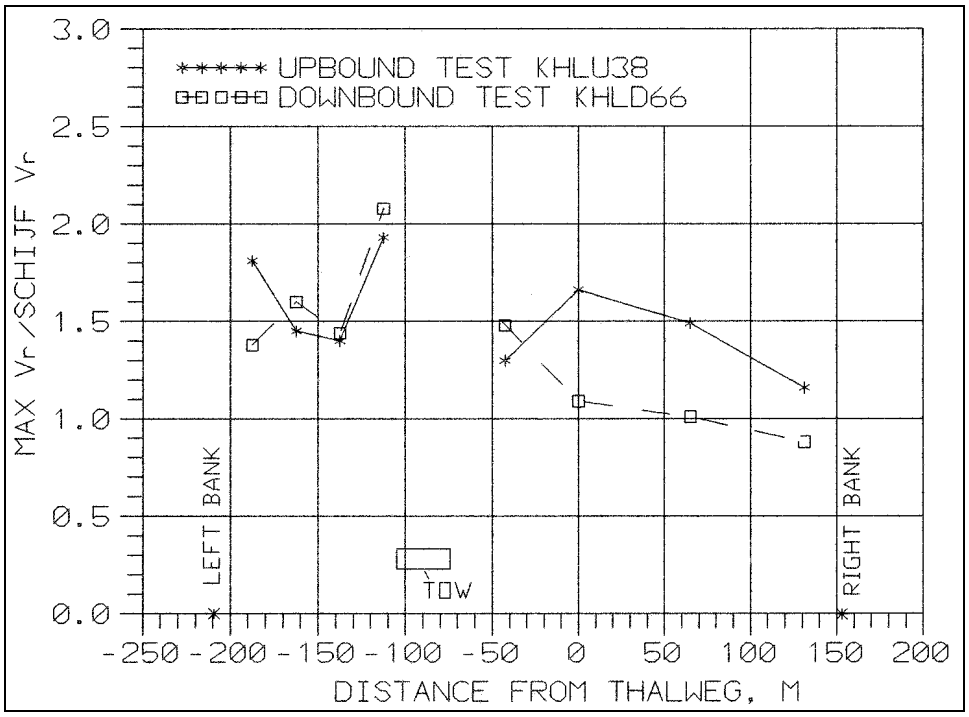

Figure 96. Dimensionless return velocity, experiments KHLU38 and KHLD66

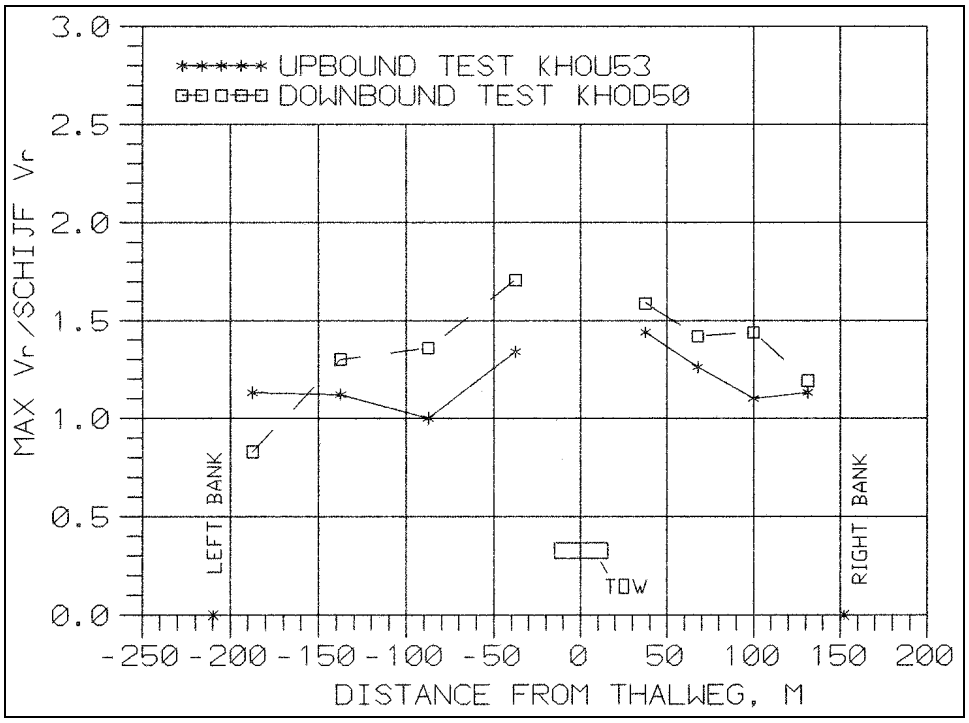

Figure 97. Dimensionless return velocity, experiments KHOU53 and KHOD50

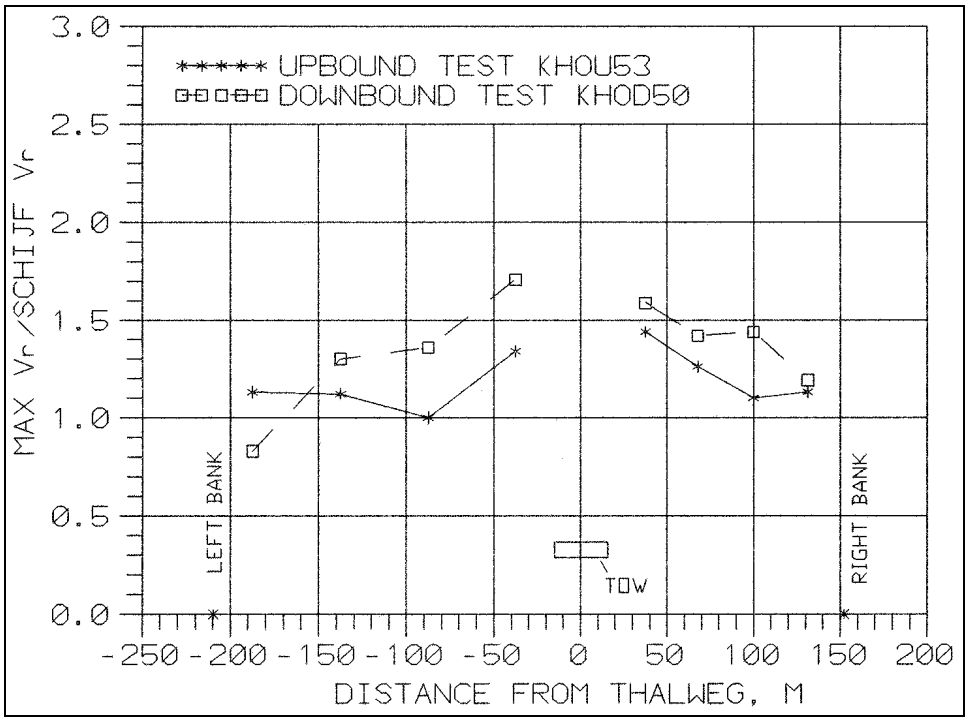

Figure 98. Dimensionless return velocity, experiments KHEU38 and KHEU56

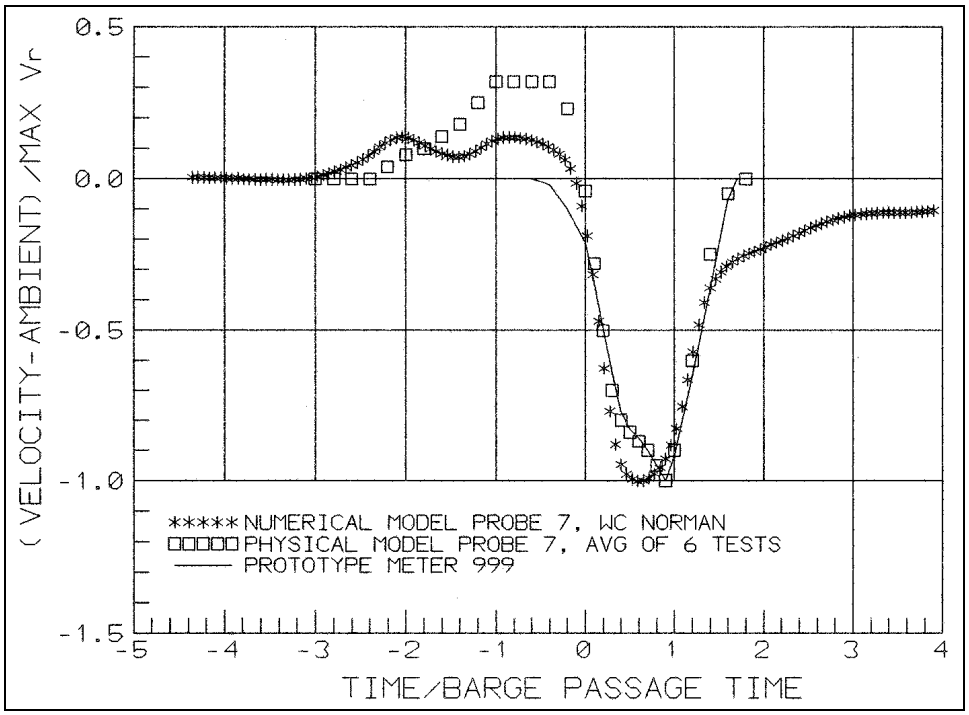

Figure 99. Dimensionless time-history of return velocity